Development of a Micro-total Analysis System for the detection of Biogenic Amines

Dissertation zur Erlangung des
Doktorgrades der Naturwissenschaften
(Dr. rer. nat.)
an der Fakultät Chemie und Pharmazie
der Universität Regensburg
Deutschland

Vorgelegt von
Sarah Nagy Ali Mobarez
aus Kairo
im Jahr 2020

Printed with the support of the German Academic Exchange Service

Die vorliegende Dissertation entstand in der Zeit von April 2017 bis September 2020 am Institut für Analytische Chemie, Chemo- und Biosensorik der Universität Regensburg.

Die Arbeit wurde angeleitet von PD. Dr. Axel Dürkop.

Promotionsgesuch eingereicht am: 23.07.2020
Voraussichtlicher Kolloquiumstermin: 02.09.2020

Prüfungsausschuss

Vorsitzender: Prof. Dr. Alkwin Slenczka

Erstgutachterin: PD Dr. Axel Dürkop

Zweitgutachter: Prof. Dr. Antje J. Bäumner

Drittprüfer: Prof. Dr. Alexander Breder

Acknowledgement

I would like to especially thank my supervisor PD Dr. Axel Dürkop for helping and supporting me through all. I would like to express my gratitude to him for guiding me through the whole work and being so friendly. I also thank him for the detailed discussions and patiently answering my questions.

I would like to thank my supervisor Prof. Dr. Antje Bäumner for the opportunity to work on this interesting topic, as well as for giving me the chance to be a part of her scientific research and supporting me during the entire doctorate.

I want to thank Dr. Nongnoot Wongkaew for useful discussions and sharing her experience in this field. I would also like to thank Prof. Dr. Alexander Breder and Prof. Dr. Alkwin Slenczka for taking on the roles of third-party reviewer and chair in my doctoral examination.

I would like to thank Marcel for taking the SEM images of the two types prepared of the nanofibers to characterize them. I want to thank my lab members Marcel Simsek and Antonia Teodora for their good, friendly company, and having a really good time. I would also like to thank my working group, and all of my colleagues for being nice and cooperative.

I want to thank Arne Behrent for being a good supportive friend. Special thanks to my best friends either here in Germany or in Egypt Nashwa Ibrahim, Hoda Mahmoud, Soha Hassan, and Marwa Eletreby for being there for me especially through the hard time.

Last but not least, my greatest thanks go to my parents Nahed Mohamed and Nagy Ali and my sister Rana Nagy for their support. I want to thank my mother again for believing in me and always supporting me.

Many thanks to all of you!

Declaration of Collaborations

This work was conducted in large degrees of experimental and theoretical work solely by the author. However, to a certain extent, collaborations with other researchers were conducted to generate results, which is stated in this chapter in accordance with §8 Abs. 1 Satz 2 Ziffer 7 of the "Ordnung zum Erwerb des akademischen Grades eines Doktors der Naturwissenschaften (Dr. rer. nat.) an der Universität Regensburg vom 18. Juni 2009".

Optical Sensors for Determination of Biogenic Amines in Food (Chapter 1)

Major parts of his chapter have been published as a review article. Alexandra Danchuk, Nadezhda S. Komova, Sarah Mobarez, Sergey Doronin and Axel Duerkop performed literature search and wrote the manuscript. The article was revised by Natalia A. Burmistrova, Alexey V. Markin and Axel Duerkop. Axel Duerkop is corresponding author.

Functional Electrospun Nanofibers for Multimodal Sensitive Quantitation of Biogenic Amines in Food via a Simple Dipstick Assay (Chapter 3)

This chapter has been published as a research article. Sarah Mobarez shared in the experimental work and revision of the manuscript. The experimental work was mainly done by Nadezhda S. Yurova and Alexandra Danchuk. Antje J. Baeumner and Nongnoot Wongkaew contributed with strategic discussions. Axel Duerkop is the corresponding author. Axel Duerkop was the leader of this project.

Dipsticks with Reflectometric Readout of an NIR Dye for Determination of Biogenic (Chapter 4)

This chapter is intended for submission in Chemosensors. The experimental work and writing the manuscript was carried out by Sarah Mobarez. The article was revised by the Sarah Mobarez and Axel Duerkop who is corresponding author and leader of this project. Antje J. Baeumner contributed with strategic discussions. Nongnoot Wongkaew and Marcel Simsek contributed with useful discussions and sharing skills and experience especially for data analysis.

Approaching a µ-TAS for the quantitation of Biogenic Amines in Food (Chapter 5)

The experimental work and writing of this chapter were carried out by Sarah Mobarez.

Table of Contents

1 Optical Sensors for Determination of Biogenic Amines in Food

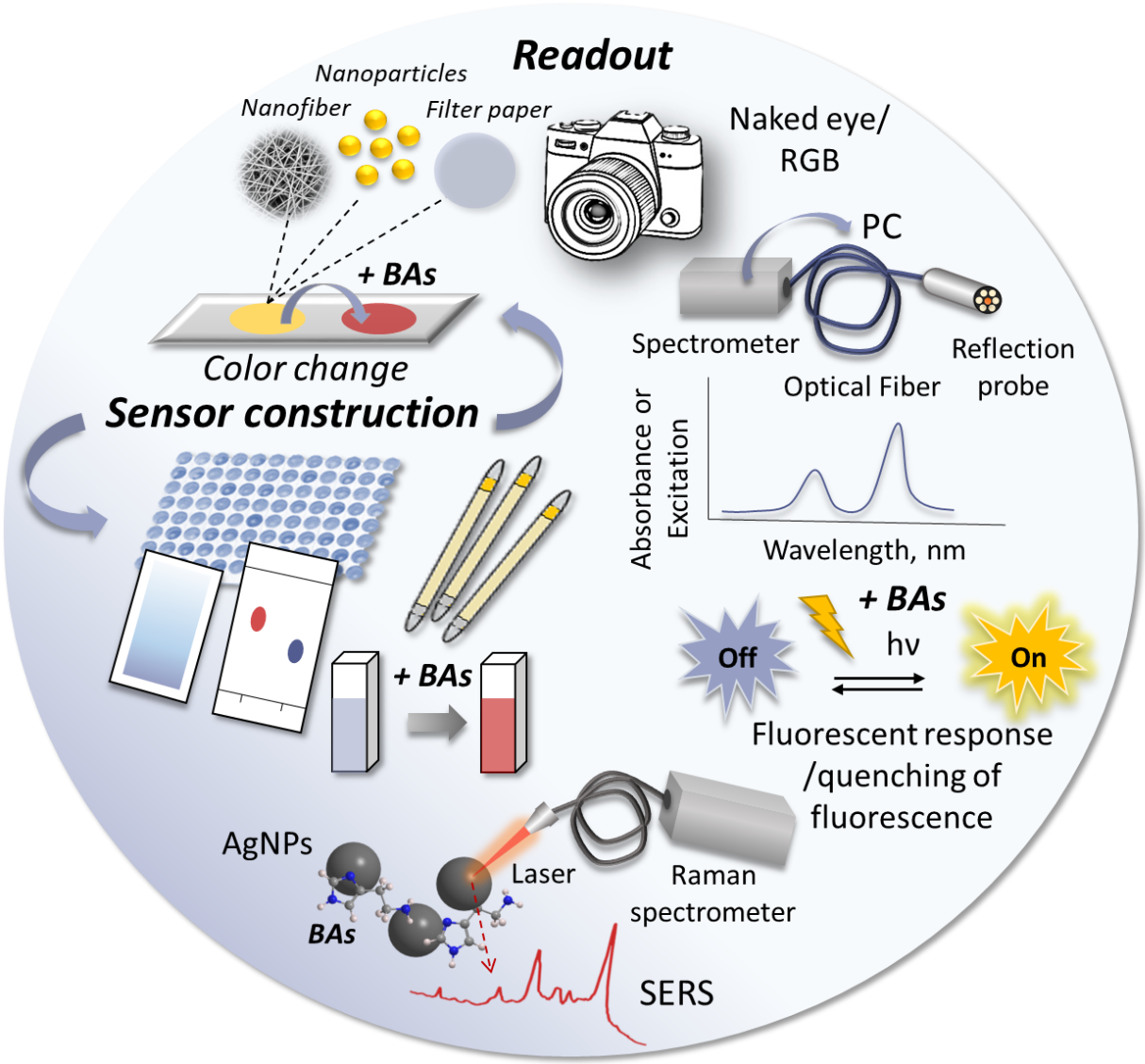

1.1 Abstract

This chapter presents the state-of-the-art of optical sensors for determination of biogenic amines (BAs) in food by publications covering about the last ten years. Interest in the development of rapid and preferably on-site methods for quantification of BAs is based on their important role in implementation and regulation of various physiological processes. At the same time, BAs can develop in different kinds of food by fermentation processes or microbial

activity or arise due to contamination, which induces toxicological risks, food poisoning, and cause serious health issues. Therefore, various optical chemosensor systems have been devised that are easy to assemble and fast responding and low-cost analytical tools. If amenable to on-site analysis, they are an attractive alternative to existing instrumental analytical methods used for BA determination in food. Hence, also portable sensor systems or dipstick sensors are described based on various probes that typically enable signal readouts such as photometry, reflectometry, luminescence, surface-enhanced Raman spectroscopy or ellipsometry. The quantification of BAs in real food samples as well as the design of the sensors are highlighted and the analytical figures of merit are compared. Future instrumental trends for BA sensing point to the use of cell-phone-based fully automated optical evaluation and devices that could even comprise microfluidic micro total analysis systems.

This chapter has been published:

Alexandra I. Danchuk, Nadezhda S. Komova, Sarah N. Mobarez, Sergey Yu. Doronin, Natalia A. Burmistrova, Alexey V. Markin, Axel Duerkop, Anal. Bioanal. Chem., 2020, DOI: 10.1007/s00216-020-02675-9

Author contributions:

Major parts of this chapter have been published as a review article. Alexandra Danchuk, Nadezhda S. Komova, Sarah Mobarez, Sergey Doronin and Axel Duerkop performed literature search and wrote the manuscript. The article was revised by Natalia A. Burmistrova, Alexey V. Markin and Axel Duerkop. Axel Duerkop is corresponding author.

1.2 Introduction

Biogenic amines (BAs) are small organic molecules, which show high biological activity. They mainly arise in tissues of living organisms as a result of enzymatic decarboxylation of amino acids or by amination and transamination of aldehydes and ketones. In fresh foods, they are mostly found in protein-rich samples but their concentrations in any food can quickly increase upon improper storage. The molecular structure of some main BAs which can occur in food and which are involved in food poisoning are shown in Fig. 1.

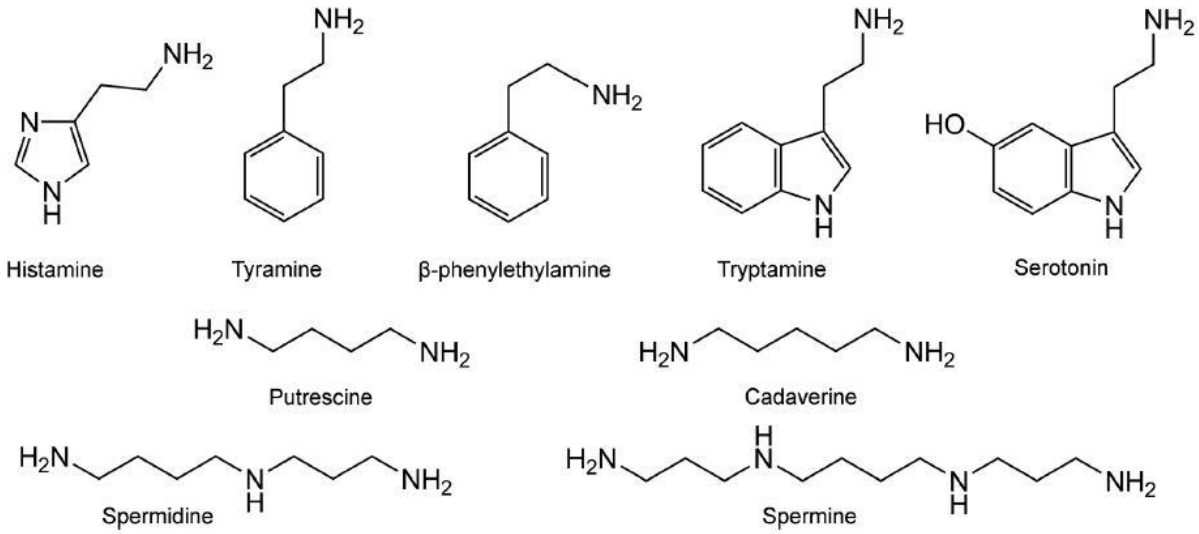

Fig. 1. Molecular structures of main biogenic amines present in food.

This chapter focuses in detail on optical chemosensor systems for BA determination in quality control of real food samples and particularly highlights the analytical aspects of the various optical detection methods. Commonly, different types of probes (organic dyes, metal-ligand complexes, nanomaterials, enzymes, etc.) and sensor designs as well as signal readouts find their way into BA sensors and hence those are classified here with respect to the various optical detection methods.

1.3 Biogenic amines as indicators of food spoilage

Fish, meat, cheese, vegetables, fruits, nuts and chocolate and various beverages like wine or beer are typical foodstuffs in which BAs are present at various concentration levels. The concentration of BAs in food depends on its nature and bacterial environment [1, 2]. For example, scromboid fish has a high free histidine content, which may produce (especially with increasing temperature) histamine . The levels of histamine, putrescine and cadaverine usually becomes higher during ageing of fish and meat whereas the levels of spermine and spermidine (exist at high concentrations from the beginning) will be reduced with food ageing [3]. Other amines, such as trimethylamine and dimethylamine are indicators of fish freshness [4]. In dry sausages especially the concentration of histamine and tyramine increases during ripening [5]. Several juices, nectars and lemonades made from oranges, raspberries, lemons, grapefruit, mandarins, strawberries, currants and grapes include various biogenic amines in different concentrations, among them putrescine is the most dominant one [6]. High amine concentrations are found in orange juice (noradrenaline, tryptamine), tomato (tyramine, tryptamine, histamine), banana (tyramine, noradrenaline, tryptamine, serotonin), plum (tyramine, noradrenaline) and spinach leaves (histamine) [7]. Cocoa and chocolate contain tyramine, serotonin, β phenylethylamine, and tryptamine [8]. Some types of mushrooms also include high content of phenylethylamine and pyrrolidine was found also in high concentrations in white and black pepper and soya sauce [9]. Fresh and processed pork meat contain high concentrations of adrenaline, spermidine and spermine but low concentrations of noradrenaline, putrescine, histamine, cadaverine and tyramine [7]. Spermine and spermidine in meat and meat products are within 6.4 - 62.1 mg/kg for spermine and 0.7 - 13.8 mg/kg for spermidine. There is a big difference in tyramine, histamine, putrescine, and cadaverine contents in meat especially in ripened products. In general, biogenic amines in cooked meat products are less than 10 mg/kg, while in 40% of

ripened products they may exceed 300 mg/kg [10]. Seven amines were found in beef: 1,2 diaminopropane, histamine, putrescine, cadaverine, permine, permidine and tyramine [11]. Low levels of polyamines were observed in full cream and semi-skimmed cow's milk [12]. During the fermentation process, food is stored over days, weeks, or months. At the first steps of the fermentation process all types of microorganisms can flourish so the biogenic amine concentration expected to increase. This is already validated by the analysis of some fermented products like cheese, sauerkraut, wine, and fermented sausages [13]. Regarding milk-based fermented foods, cheese is the most probable product to contain a potentially unsafe BAs, especially tyramine, histamine, and putrescine [14]. Comparing cheeses made from raw and pasteurized milk, BA concentrations were higher in cheeses made from raw milk than in those made from pasteurized milk. Blue cheeses made from raw milk contain the biggest BA content with tyramine being most predominant [15]. Putrescine has been detected in all the fruits and nuts, with the highest amounts in orange, orange juice, mandarin, grapefruit, grapefruit juice, banana, passion fruit, and pistachio. The range of the amine amount in citrus fruits and their juices is very wide varying from 0 - 200 mg/kg [16]. Although BAs can act as hormones and neurotransmitters their potential toxicity accounts for their significant role in food analysis [1, 2]. Papageorgiou and co-workers summarized different matrices (food and beverage products) in their review [2] that could contain biogenic amines in order to show which of them should be continuosly monitored for their toxicity. Moreover, the regulation policy and the toxicity of BAs are discussed.

Histamine is one of the most bioactive and toxic BAs, which can trigger an allergic reaction in humans and mammals. According to the European Food Safety Authority (EFSA), the U.S. Food and Drug Administration (FDA) as well as the World Health Organization (WHO) there are some ranges of BA concentration in foodstuff which point to various levels of food quality or food

degradation. A concentration of histamine of less than 50 mg/kg indicates good quality fresh food. Concentrations of histamine between 50 and 200 mg/kg may cause adverse health effects and levels above 200 mg/kg of histamine are reported to cause toxic effects in humans. Cadaverine and putrescine can potentiate the toxic effect of histamine. Poisoning of BAs on the one hand depends on the amount that has entered the body and on the other hand also on the individual human sensitivity to each BA. The permissible concentrations of other BAs are greater than for histamine. Therefore, e.g. doses of tyramine can vary from 600 mg up to 2000 mg, depending on the individual tolerance of each person [2]. Inappropriate storage temperature often is the reason for high concentrations of histamine in fish which have formed following decarboxylation under bacterial action from initial histidine [17]. Tyramine and β-phenylethylamine may initiate a hypertensive crisis in certain patients and dietary-induced migraine [18]. Polyamines (putrescine, spermine, spermidine and cadaverine) however, play essential functions in living cells and can be present in micro- or even millimolar concentrations. On the other hand, some polyamines can react with nitrite to form carcinogenic nitrosamines, and can also be food spoilage indicators [18]. Therefore, monitoring of BAs is a mandatory part of food analysis as a quality indicator for the sample under investigation.

BA detection in food is challenging because these analytes are very polar and better soluble in water than in organic solvents (Table 1, left column). Furthermore, BAs need to be detected at low concentrations in a complex matrix, in most cases. Hence sensitive detection methods are required. Furthermore, high selectivity should be provided to avoid that interfering components in food may give a similar response as the target BA. The presence of structurally similar BAs in the sample can further complicate the analysis as a result of competitive interactions with the sensing material [2]. Therefore, the application of a new sensor to a specific food sample should be validated by a

chromatographic method to warrant sufficient selectivity. BA detection by optical analytical methods is often complicated because of the weak capability of BAs to absorb light in the visible range. Therefore, derivatization of BAs with chromophores or fluorophores are employed to make them amenable for being optically analyzed. Further, a huge number of separation methods like GC, HPLC or capillary electrophoresis is hyphenated with optical, electrochemical or mass spectrometric detection as shown in recent reviews [18–22]. Finally, ELISAs [23] are applied for BA determination in foodstuff, as well. The main advantages of those methods are their high sensitivity and selectivity. However, they require highly qualified and trained staff, expensive high-quality reagents and time-consuming sample preparation (Table 1, left column). In order to overcome these limitations, the recent development of fast, low-cost and portable chemo and biosensors which can be used for on-site analysis of BAs in food is shown by recent publications covering about the last ten years, in this chapter. Kaur et al. [24] published a comprehensive review describing the existing probes and their recognition mechanisms (including e.g. aggregation-induced emission (AIE), ligand exchange mechanism, photo-induced electron transfer (PET)/internal charge transfer (ICT) mechanism and some others) used for detection of biothiols and biogenic amines. Unlike this earlier publication, the present one focuses on evaluating whole sensors (comprising of probes, transducer and detector), discussing on-site use capability and compares the merits and disadvantages of the various optical detections methods together with discussing the impact of sensor material design (in view of the materials used for embedding of the probe and exclusion of unwanted interferents) on sensor performance. From this wealth of perspectives on the topic, it is obvious that optical sensors for qualitative and quantitative analysis of BAs are an attractive alternative to existing analytical methods and some of them may be handled by non-trained staff or in-field.

Table 1. Challenges to be solved in the determination of BAs in real food samples and merits of optical sensors that promote their use.

Challenges of BA determination	**Advantages of optical sensors**
a. derivatization of BAs and compliance with green chemistry; *b.* strong polar character of BAs; *c.* low concentration ranges of BAs; *d.* presence of complex matrix with potentially interfering compounds *e.* occurrence of several BAs simultaneously; *f.* complexity of sample matrix; *g.* time for sampling, work-up and detection; *h.* requirement of trained personnel.	<u>General:</u> *a.* fast signal reading and processing; *b.* low-cost instrumentation; *c.* minimum amount of sample required; *d.* ease of operation; *e.* evaluation by public-domain software; *f.* acceptable for analysis by less-trained users; *g.* flexible size from μm^2 to cm^2 *h.* multiplexing/array sensing possible *i.* amenable to remote sensing *j.* no electrodes required. <u>Luminescence sensors:</u> general advantages as from *a - j*; *k.* high sensitivity. <u>Surface-enhanced Raman spectroscopy sensor:</u> general advantages as from *a, c, d, f-j;* *l.* high sensitivity.

1.4 Sensor design

Sensors can be described as technical sensing organs [25]. Sensors are devices which respond to a physical input and convert it into a signal, usually optical or electrical, that can be read by an observer or an instrument [26].The sensing process occurs over two steps: first to measure or detect a variety of physical, chemical, and biological quantities, including proteins, bacteria, chemicals, gases, light intensity, motion, position, sound and many others and the second is converting the physical quantity into a signal by the transducer. The sensors can be classified with respect to different aspects such as e.g. the receptor part, or the transduction mechanism, etc. The transducer converts one form of energy to another [26].

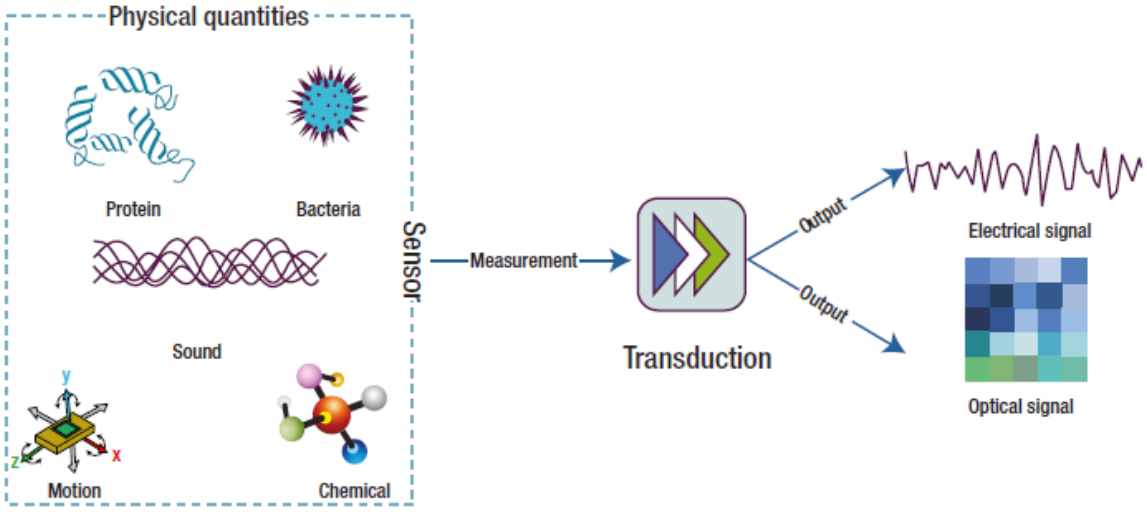

Fig. 2. The sensing process. Reprinted from [26].

The signal can be usually optical (fluorescence, absorption) or electrical (redox, capacitance, resistive) [27]. Sensors can be classified also according to the receptor element to chemical and biosensors. The main difference between chemical and bio- sensors is not the type of the analyte detected or the nature of the reaction taking place, it is according to the recognition element weather if it is a chemical or biological molecule [28]. Chemical sensors respond to stimuli caused by different chemicals or chemical reactions. These sensors are used for

qualitative and quantitative analysis of chemical species in liquid or gas phase [29]. Optical chemical sensors are of great advantage since they join the advantages from using optical fibers with the selectivity of the chemical transduction system [30]. Optical sensors are favorable over electrical sensors and other types since they are flexible, easily miniaturized, safe, selective, non-destructive, not subject to corrosion, of high resolution, allow remote sensing over several kilometers and offer a higher number of measurements over a small area using a single optical cable which leads to higher sensitivity [31]. Furthermore, the development in the quality of optical components, including light sources (lasers, light emitting diodes), photodetectors, amplifiers, etc. had a really high impact on the efficiency of the optical sensors [30]. Optical sensors depend on different optical principles such as absorbance, reflectance, luminescence, fluorescence that occur over different regions of the spectrum (UV, Visible, IR, NIR) and detection can be carried out not only by measuring the intensity of light, but also other related properties, such as lifetime, refractive index, scattering, diffraction and polarization [32]. Generally, optical sensors consist of molecular recognition elements and signal transducers. The molecular recognition elements interact with the analyte and give qualitative or quantitative information. As a result of this interaction, changes in the signal are produced by the sensor which are then transduced into easily evaluated and quantified optical signals [33]. The sensor quality relies on the overall components of the system, which are defined by the transduction, the sensitive layer, light source, data-acquisition electronics and evaluation software [34]. The optical detection depends on either a) direct sensing or b) indicator mediated sensing. The analyte can be directly detected by some intrinsic optical property such as, for example, absorption or luminescence. In an indicator mediated system, the determination of the analyte concentration is carried out based on the change in the optical response caused by an intermediate agent, usually an analyte-sensitive dye indicator [35].

Fluorescence has attracted special attention among the different optical sensing methods since it is sensitive, and has various variables that can serve as an analytical information [36]. Fluorescence is more sensitive than absorption detection because in absorbance it is about measuring the ratio of the intensity between the two light beams passing through the reference and the sample which are comparable to each other, while in fluorescence the emission intensity is measured against a black background [37]. Samples which show fluorescence emit light with a longer wavelength than the absorbed light used for sample excitation. Fluorescence sensors are usually characterized by their excellent detection limit [38]. The typical emission rates of fluorescence are around10^8 s^{-1}, so that a typical fluorescence lifetime is near 10 ns (10 x 10^{-9} s) [39].

Historically, the development of the (single use) test strips was mainly built on the principles of reflectometry [36]. Reflectance spectroscopy is a useful method of measuring the absorption spectra and other properties of solids. Reflectance based sensors are very useful for remote sensing since this kind of measurement can be done without contacting the sample [40]. Colorimetric sensors are an important category of optical sensors that show observable color change (often recognized by naked eye) upon reaction with the analyte. For more quantitative analysis, the change in intensity at certain wavelength within the visible range (400–800mm) of the spectrum can be determined using instruments. Colorimetric sensors are more popular because they are simple, inexpensive, easy to be used, selective and sensitive towards different analytes [41]. The comparison of the color change occurred in colorimetric strip tests with a color chart is useful for qualitative, or semiquantitative evaluation.

The use of a reflectometer to read the test strips has a great influence in increasing the reproducibility and accuracy of the measurements. The combination between indicator-based colorimetric strip tests with a

reflectometer to read them, is a practical alternative analyzing method to traditional laboratory methods [42]. Because of the increasing need for more sensitive sensors for many purposes such as global environmental monitoring, monitoring of food chains and medical diagnostics, there is rising interest in nanostructured materials such as nanofibers and nanowebs.

Electrospinning is a perfect technique for producing different forms of nanofiber sensor mats and achieving homogenous and highly uniform fibers at the same time. The electrospun nanomaterials are well known by their specific surface area and high porosity which promotes the sensor sensitivity [43].

Most of the optical sensors for BAs follow the classical sensor design where a probe for recognition is immobilized in a membrane and/or fixed on a suitable support which can be paper [44–46], glass [45, 47], TLC plates [48–50], microtiter plates [51] and test-tubes [52]. To deposit the recognition layer knife coating, spin coating or simple soaking may be used. The probe is mostly embedded into a polymer layer as a thin film [48, 53], or eventually allowed to settle on another film of e.g. gold or silicon [54], on polymer particles [51, 55, 56], a hydrogel [57] or inside nanofibers [58].

1.5 Detection methods

Various optical methods are applied for detection. Those will be discussed in the following sections together the individual sensor schemes and with their major merits towards quantitation of BAs in real samples. Only if these methods have shown to work in real food samples, they are presented in Table 2 (see page 16) together with an in-depth overview on sensor composition and individual sensor details like response times, analytical ranges and limits of detection.

The optical BA recognition is correlated to binding to the receptor molecules that create the analytical signal. Unfortunately, many BAs themselves do not carry structural features that promote their optical detection

(i.e. large conjugated π-systems which are necessary for reflectometric, photometric or fluorimetric readout), so they need to be transformed into corresponding derivatives with the desirable detection properties [59]. The derivatization reagents may be divided into several groups: they can be chromophores and fluorophores (to impart absorption of UV light or fluoresce emission into the derivatives, respectively); fluorogenic molecules (which show fluoresce upon formation of the fluorescent derivative with the analyte) and redox reagents (which reduce/oxidize analytes to enable detection). For instance, reagents such as o-phthalic aldehyde, 1-fluoro-2,4-dinitrobenzene (DNFB), 2,4,6-trinitrobenzenesulfonic acid (TNBS), 4-fluoro-3-dinitro-fluoromethylbenzene, ninhydrin, benzoyl chloride and many others were widely used for derivatization of primary, secondary amines or polyamines to form colored products, followed by their chromatographic determination with absorbance or a fluorescence detector. However, most of these methods require expensive instrumentation that cannot be used in the field and the related reagents cannot be used in optical sensors for BAs because they lack long-term storage stability inside the sensor membrane.

Optical sensors (so called pH opt(r)odes) have the merit not to require electrodes and hence to be electrically safe which made them increasingly attractive in the fields of gas sensing, ion sensing, bioanalysis and pH sensing. Optodes are based on changes of optical properties such as absorbance, fluorescence, luminescence, chemiluminescence, energy transfer or reflectance by measuring the intensity of light in various regions of the spectrum (UV, Visible, NIR, IR). Moreover, related properties such as light scattering, luminescence lifetime, refractive index (via surface plasmon resonance spectrometry), diffraction and polarization may be exploited analytically. Optodes are beneficial due to their flexibility in size and shape, low cost, fast response and light weight (Table 1, right column). They can be used in both aqueous or organic media and can deliver information with either highly local

resolution (using fiber-optical sensors down to µm), which additionally can reduce the sample volume down to nL. This is e.g. hardly available for electrical sensors. Also areas until tens of cm^2 can be read using in optical imaging. A further benefit is the potential to use multiplexed sensing, e.g. when various optical probes with different detection wavelengths are used for simultaneously probing a collection of analytes or to build up and read out a sensor array [48, 53, 60]. Arrays of multiple sensors with similar and low selectivity often require multivariate data analysis methods to introduce analyte-selectivity but also enable prediction of the freshness of food samples. Luminescence is the detection method of choice if high sensitivity is required because due to the absence of interfering excitation light it is more sensitive than reflectometry and photometry. Sensors based on surface enhanced Raman spectroscopy (SERS) present another modern highly sensitive alternative here because they are based on analyte-induced changes of the refractive index. For appropriate use in food sensing these sensors either may require labelling or derivatization procedures in or on the sensor membrane or a sample pretreatment that involves analyte separation from the matrix to warrant selectivity. Leaching or photobleaching of the optical probe may compromise long-term stability and therefore has to be carefully controlled, as well as selectivity. Optical sensors are suitable for remote sensing (even over distances of kilometers) and can be used for in-vivo measurements because of their immunity to electromagnetic interferences. This wide range of how optical sensors can be tailored makes them hot candidates for emerging into new fields like food chemistry that is dominated by more expensive separation methods (GC and HPLC) hyphenated to various optical, electrical or mass detection techniques. Here, optical sensors can operate on a much less expensive level by using e.g. digital cameras, smartphones or flatbed scanners for detection together with public domain software for evaluation. The use of these inexpensive components provides a much easier operation of the

sensors. This will further promote the use of optical sensors in food sensing as well as by less trained personnel.

Table 2. Selection of representative sensors with proven applicability to real food samples and their analytical figures of merit.

Composition of Sensor Layer / Response time	**Analyte**	**Detected Signal / Tool**	**Analytical Range; LOD; (LOQ)**	**BAs found in real sample, SD or RSD (%), n of samples**	**Object**	**Ref.**
1	**2**	**3**	**4**	**5**	**6**	**7**
Reflectometric readout						
Cellulose filter paper; Thiosemicarbazide–naphthalimide based chromophore / 10 min	Butylamine	Reflectance/absorbance conversion / Ocean Optics spectrometer (Oceanview software)	3 – 224 mg/kg; –	-	Fish meat (salmon) (vapors)	[46]
Multi-dye (8 pH indicators and 8 porphyrins or metalloporphyrins) array printed on a TiO_2 nanoporous film plate / 9 min	Trimethylamine	RGB / Permeater flatbed scanner model PD-1B-2 (Gastec Corporation, Japan)	3.7 – 10.1 mg/kg*; –	Trimethylamine < 5 mg/kg SD = 0.05 mg/kg, n = 5	Yao-meat (vapors)	[48]
TLC plate with Meldrum's acid activated furan (MAF) as an amine-selective stain-based synthetic sequence (< 1 min) Nylon	Dimethylamine	Visual detection, digital image / smartphone	0.3 – 2 mg/kg; 0.4 mg/kg	-	Fish meat (cod and tilapia)	[49]

filter membranes spotted with MAF / 5 min					(vapors)	
TLC plates pre-coated with silica gel G, diazonium reagent / 15 min	Histamine	Optical density / Mobile phone, ImageJ software	50-150 ng/spot 14.03 ppm; (39.15 ppm)	Histamine RSD = 1.07 % – 2.76 %, n = 6	Fish meat (mackerel) (vapors)	[50]
Array of pH indicators (methyl red, alizarin, bromophenol blue, thymol blue, chlorophenol red) cellulose acetate membranes / 10 min	Isobutylamine, triethylamine, isopentylamine	RGB / iPhone®	2-8 ppm 2-10 ppm 1-4 ppm (1 mg/kg)	-	Minced meat (vapors)	[53]
Inkjet paper with monolayers array of hollow AuNPs received by reversal nanoimprint lithography / 30 min	Putrescine	Shift of reflectance spectra	0.1 – 200 mg/kg; 13.8 mg/kg	-	Spiked fish meat (vapors)	[56]
Au NRs with Ag metallization / 30 min	Trimethylamine	RGB / smartphone, visual detection	0.011 – 0.200 μM; 8.6 nM = 0.51 μg/kg *	-	Fish (salmon), beef meat (vapors)	[57]
Combination of 2-fluoro-4-[4-(2-hydroxyethanesulfonyl)-phenylazo]-6-methoxyphenol and Remazol Brilliant Blue R, immobilized on cellulose microparticles / 1.5 h	Methylamine, dimethylamine, putrescine, cadaverine, histamine, tyramine and	CIE lab color space / color measurement device (Mathi, Germany)	0.3 – 30 mg/kg –	-	Chicken, pork meat (micro-biological spoilage) (vapors)	[60]

	tryptamine					
Silica gel 60 F_{254} plates, 16 chemo-sensitive dyes/24 h – several days	Trimethylamine, dimethylamine, cadaverine, putrescine	Gray scale / Corel Photo- Paint X3, flatbed scanner (Epson V750-M Pro Perfection scanner)	81.7 – 350 mg/kg* –	Volatile basic nitrogen (TVB-N) 81.7 mg/kg* (1 day), 350 mg/kg* (9 day), RSD < 9 %, n = 4	Fish meat (atlantic salmon) (vapors)	[63]
AuNPs (13.1 ± 0.7 nm) / 15 min	Histamine	Color change / visual detection or camera; Absorbance / TU-1901 spectrophotometer	0.1 – 2.1 μM; 1.81 μM; 38 nM	Histamine 1.81 μM SD = 0.3 – 0.7 μM, n = 3	Fish meat (salmon) (solution)	[66]
Photometric readout						
Polymeric film, Nitrated conjugated polythiophene (NPTh) / 2.5 – 37 min	Ethylenediamine, putrescine, cadaverine, spermidine, phenethylamine, histamine	Color change / visual detection or camera; Absorbance / UV–vis spectrophotometer	– 5.6 mg/kg; 0.92 mg/kg; 0.45 mg/kg; – –	-	Beef, pork, and salmon meat (vapors)	[68]

		(JASCO V-650)	–			
AuNPs (11–19 nm)	Histamine, histidine	Color change / eye-vision	2 – 16 μM; 0.6 μM	-	Poultry meat (solution)	[67]
o-phthalaldehyde (OPA) and thioglycolic acid (TGA) derivative of putrescine / 12 min	Putrescine	Absorbance / UV–vis spectrophotometer (Perkin Elmer Lambda 35, USA)	0.8 – 200 μM; 0.44 μM	Putrescine 41 – 180 mg/g RSD = 10 – 42 %, n = 3	Fish meat (10 commercial products) (solution)	[70]
Luminescence readout						
Cellulose acetate nanofibers embedded with Py-1 / 20 min	Tyramine	Fluorescence with RGB / Digital camera Canon EOS 550D	10 – 100 μM; 20 μM	Histamine (μmol/g) 14.1 ± 0.3 (day 0), 16.4 ± 1.5 (day 3), 38.8 ± 2.6 (day 6) RSD = 17 – 21 % n = 4	Shrimp meat (solution; TAC)	[58]
Microtiterplate with sensor film based on Py-1 embedded in Hypan HN 80 / 10 min	Histamine putrescine tyramine	Fluorescence / FLUOstar Optima microtiterplate reader	Histamine: 0.5 – 70.0 mg/kg; 0.165 mg/kg; (0.495 mg/kg)	Total content of BAs (TAC) 49.6 – 137.8 μg/mL (day 1), 97.6 – 397 μg/mL	10 samples of meat, cheese (solution; TAC)	[61]

				(day 5) SD = 0.23 – 2.19 μg/mL RSDs 3.71% (10.0 μg/mL), 4.08% (20.0 μg/mL), 3.73% (30.0 μg/mL) 5.03% (40.0 μg/mL) n = 5		
Tiss®-Link (NanoMyP®) support with immobilized tryptamine / 15 min	Tryptamine	Phosphorescence /Varian Cary-Eclipse luminescence spectrophotometer with flow-through cell	19 – 600 μg/kg; 6 μg/kg; (19 μg/kg)	Tryptamine 366.8 – 697.6 ng/mL RSD = 1.8 – 6.1 % n = 4	Beer (solution)	[74]
DAO immobilized on chitosan-coated magnetic microparticles (MCH) or SEPABEADS® EC-HA (MFS) deposited with Ru-bathophenanthroline on a lens connected to optical fiber	Putrescine	Home-made time-correlated single photon counting instrument	MCH, mM 0.1 – 1.000; 0.025 = 2.2 mg/kg*; (0.082) 0.1 – 1.000;	MFS, mM 0.1 – 0.750; 0.061 = 5.4 mg/kg*; (0.202) 0.1 – 1.000;	-	Beer (solution)	[76]

	Cadaverine		0.030 = 3.1 mg/kg*; (0.102)	0.052 = 5.1 mg/kg*; (0.175)			
	Spermidine		0.1 – 2.200; 0.271 = 39.6 mg/kg*; (0.905)	0.1 – 1.250; 0.093 = 13.5 mg/kg*; (0.309)			
	Histamine		0.1 – 2.200; 0.479 = 53.2 mg/kg*; (1.595)	0.1 – 1.250; 0.205 = 22.7 mg/kg*; (0.683)			
Chemiluminescence readout							
Glass support with hydroxyethyl cellulose membrane included luminol and covered with Co(II) and enzyme (putrescine oxidase or diamine oxidase) fixed on the photodiode	Putrescine	Chemiluminescence/ Anthos Labtec Instruments Microplate luminometer	Putrescine using putrescine oxidase: 1 – 2 mg/L; (0.8 mg/L); Putrescine using diamine oxidase: 1 – 2 mg/L;		Putrescine using putrescine oxidase 0.72 – 2.76 mg/L SD = 0.1 – 1 mg/L; Putrescine using	Beef, pork, chicken, turkey and fish meat (solution)	[51]

		Lucy1	(1.3 mg/L)	diamine oxidase 0.78 – 2.45 mg/L SD = 0.3 – 1.1 mg/L n = 15		
Bis(2,4,6-trichlor-ophenyl)oxalate(TCPO)–H_2O_2 system modified with Mg–Al–CO_3- LDH nanosheet colloids	Histamine	Ingibition of chemiluminescence/Hitachi, F-7000 fluorescence spectrophotometer	0.1 – 100 μM; (3.2 nM = 0.4 μg/kg*)	Histamine 14.6 – 14.7 μM SD = 0.2 – 0.4 μM (day 12) 30.8 – 31.2 μM SD = 0.2 – 0.4 μM (day 5) n = 3	Fish, pork meat (solution)	[80]
Surface-enhanced Raman spectroscopy						
AuNPs; preliminary solid phase extraction of the analyte by PVC film with incorporated MIP	Histamine	Raman spectrometer with 785 nm excitation wavelength	3–90 mg/kg –	-	Fish meat (canned tuna) (solution)	[82]
AgNPs; preliminary liquid-liquid extraction of the analyte		Raman spectrometer with 514 nm excitation wavelength	10–200 mg/kg –	-	Fresh fish meat (solution)	[83]

AgNPs; preliminary TLC separation of the analyte		Raman spectrometer with 633 nm excitation wavelength	15–100 mg/kg –	Histamine 1) 54.3 mg/kg, SD = 5.2 mg/kg RSD = 9.5 % 2) 69.5 mg/kg SD = 6.8 mg/kg RSD = 9.8 % n=4	Fresh fish meat (solution)	[84]
AgNPs; preliminary HPTLC separation of the analyte	Tyramine	Raman spectrometer with 633 nm excitation wavelength	30–80 mg/kg* –	Tyramine found 22.5 – 5.9 mg/kg SD = 0.7 – 2.1 RSD 6.7% n = 3	Cheese (solution)	[87]

* Calculated by the authors of the review based on data from referenced manuscripts.

1.5.1 Reflectometric readout

Frequently, colored or fluorescent dyes, such as acid-base indicators [48, 53, 60], porphyrins [47], phthalocyanines [54], chameleon dyes [44, 61], coumarin derivatives [45], azo dyes[62] or nanomaterials are used for optical BA determination. Among them, selectivity may be either introduced by a specific reaction, (co-)introduced by the material(s) the sensor is composed of, or is the result of chemometric evaluation of data from a sensor array. Such arrays may either be composed of several highly selective sensors to provide multi-analyte sensing or contain many sensors of low specificity [48, 53, 63] that may also be evaluated by pattern recognition. In general, reflectometric sensors require a light source, a wavelength-dispersive element to select the detection wavelength(s) and a detector. In modern setups, only one or few inexpensive LEDs (for array illumination) may be used as light source. Considering the narrow spectral bandwidth of those, selection of the light reflected from the sensor can be accomplished either by optical filters which are low-cost devices, or by the detector itself if CCDs or CMOS-sensors are used. These sensors typically deliver an RGB (red-green-blue) readout of a sensor array, as shown in several publications [48, 53, 58, 63] which can open a gate for multi-wavelength detection if the reflected light or different sensors matches the red, green and blue spectral window of the array detector. The widespread use of those detectors in digital cameras and cell phones opens many new options for the use of these inexpensive devices for the readout of reflectometric sensors in food analysis and point-of-care diagnostics. The rapid sensor readout and simple evaluation by public-domain or OEM software are further advantages of the reflectometric readout. Hence, the major advantages of reflectometric optical sensors are their instrumental simplicity, the option to arrange (multi-)sensor arrays with reasonable demand and rapid evaluation with commercial detection equipment. Hence, a complete sensor (array) can be produced for a few hundred US-$ or less. The major drawback of reflectometric sensors is their

comparatively low sensitivity and accurate positioning of the sensor (spot) with respect to light source and detector is required.

In one study, an array of five pH-indicators (methyl red, alizarin, bromophenol blue, thymol blue, chlorophenol red) in cellulose acetate membranes with Tween as plasticizer [53] was read in short time (10 min) to discriminate between isobutylamine, triethylamine, isopentylamine in ppm concentrations through RGB readout via a cellphone. The mechanism of the color change is based on BA solubility and acidity constants. RGB analysis data of the color difference map of the membranes prior and after reaction with BAs was fed into chemometric analysis (principal component analysis and hierarchical cluster analysis) for non-supervised pattern recognition evaluation. This can help the readout of the array for users that are color blind because the three BAs could then be discriminated without misclassification. The membranes could be reused up to 14 times and were shown to work with meat samples.

In another sensor array, eight pH-indicators (gentian violet, leucomalachite green; thymol; methyl yellow; bromophenol blue; congo red; methyl orange; methyl orange) were used to detect trimethylamine in meat in the range of 60 ppb – 10 ppm [48]. TiO_2 nanoporous films were found to be superior as a support compared to C_2 reverse silica gel plates on which colorimetric arrays of dyes were printed using microcapillary pipettes. Chemometric analysis was again required after trimethylamine (TMA) vapor was detected using reflectometric RGB color-difference maps recorded by a flatbed scanner. The data from the color difference maps was analyzed with principal component analysis and multiple regression analysis and the use of partial least square models allowed the prediction of the TMA content in meat samples and their freshness. The nanoporous structure significantly improved homogeneity, sensitivity and stability of the sensor arrays and lowered the response time minimally (9 min). A colorimetric sensor array for fish spoilage monitoring was

evaluated [63] which included sixteen chemosensing compounds incorporated to silica gel 60 F_{254} plates using a micromilled polymethyl metacrylate mask. The sensor response was evaluated based on the overall contribution of all compounds estimated as color change of each spot before and after the exposure to the analyte. It was shown that the arrays including Bromophenol Blue, Cresol Red, Bromocresol Green (Group 3) and Methyl Red, Xylenol Blue, Crystal Violet Lactone (Group 4) provided the highest response during fish (salmon) ageing at r.t. and 4°C. These arrays can be used as non-invasive, low-cost devices for monitoring food spoilage over time.

Cellulose-based microparticles were covalently conjugated with a pH-indicator [60] and a blue reference dye and embedded into silicone. This yields slow (1.5 h) traffic light color-changes of the sensor layer. The responses to BAs were reflectometrically acquired by a low-cost digital camera and evaluated in the lab color space of the CIE system for quantification of various amines and ammonia developed upon food ageing in food packages. Paper-based plasmonic reflectometric sensors were fabricated using reversal nanoimprint lithography [56], which is a robust and rapid method for embedding of metal NPs in a substrate and subsequent transfer onto paper. Gas-phase analysis of BAs was carried out using a digital camera. Six types of paper were tested and a commercial inkjet paper showed the best result to sense putrescine in spiked fish at ppm levels in 30 min time.

Activated furans (MAF and BAF) were investigated as versatile probes for selective detection of amines in solution, on TLC sheets and in the vapor phase [49] yielding a donor–acceptor Stenhouse adduct. Primary and secondary amines form a pink-colored (532 nm) product with MAF at a different rate which allows for their selective discrimination on solid phase resins for peptide synthesis. Further, dipsticks for BA vapor detection from various fish samples were created by deposition of MAF on nylon membranes that were read with a smartphone and free software.

In other publication [50] histamine recognition in mackerel samples was carried out by visualization with ninhydrin and diazonium reagents with high specificity and sensitivity of latter for histamine using TLC plates (LOD 14 ppm).

A thiosemicarbazide–naphthalimide based chromophore was also investigated [46] as a highly sensitive probe for visual and colorimetric determination of different amines including BAs with a color change from yellow to blue. The advantage of such a sensor is the regeneration capability of the chromophore (by trifluoroacetic acid) and hence the potential for a repeated colorimetric response. It was determined that the deprotonation and protonation processes can be repeated for at least six cycles.

Moreover, a sensor film containing a pyrylium salt [2,6-diphenyl-4(p-methacryloyloxy)-phenylpyryliumtetrafluoroborate] incorporated into a methacrylic polymeric membrane could be reused in presence of HCl vapors for at least 10 times. It selectively recognized trimethylamine with changing its color from yellow to pink [64] and LODs of 3.37 ppm and 4.42 ppm were found for colorimetric and photometric readout, respectively.

Inorganic nanoparticles (NPs) have been widely used in optical sensing due to their stability, good solubility, and favorable luminescence properties [24, 65]. The aggregation-induced change of the surface plasmon resonance of stabilized gold nanoparticles (AuNPs) after interaction with histamine allows to create a colorimetric approach for on-site monitoring (LOD 38 nM) based on the electrostatic interaction of citrate-modified AuNPs with the ammonium group of the BAs [66]. Histamine was also detected visually down to 1.81 μM in fish samples from a red-to-blue color change. Similarly, diamine recognition of AuNPs modified by cucurbiturils or cyclodextrins were used for visual and spectrophotometric detection of cadaverine in aqueous solutions (LOD 3.9 μM) [55]. The aggregation-based assay has good selectivity but requires up to 150 min incubation time for high reproducibility. Au nanorods (obtained by a seed-

mediated growth method) [57] were allowed to perform a hydrolysis-induced silver metallization that was used for colorimetric detection of BAs (LOD 8.6 nM) by the multiple color change and blue shift of the localized surface plasmon resonance (LSPR) of the gold nanorods.

1.5.2 Photometric readout

Photometric sensing schemes have the merit that they are available in most labs, are essentially not more complex than reflectometric setups and can be easily operated with little training. They share most of the advantages of reflectometry such as the requirement of only one or few (for reading arrays) inexpensive and simple light sources. Devices for the selection of the detection wavelength (e.g. filters) are only required if broadband light sources or multi-wavelength arrays are used. Hence, photometry can even be simpler than reflectometry. Similarly to the reflectometric readout, detection may be done with photodiodes, CCDs or CMOS sensors. The latter two became more and more popular with the common use of digital cameras and cell phones. Those are most frequently employed, if sensor arrays are to be read out. The sensitivity of photometry is modest alike reflectometry and for lower analyte concentrations luminescence sensing is recommended.

In an alternative strategy to the reflectometric readout e.g. the spectral shift of the absorption maximum of porphyrins or metalloporphyrins is used. Those probes are spun as films on glass slides and respond photometrically to volatile amines in the ppm range within 1 min (t_{50}) at around 440 nm [47]. If deposited on a flexible transparent support a use in food packaging seems feasible. Another team used AuNPs for detection of histamine (LOD 0.6 μM) as biomarker for poultry meat freshness [67] either by photometry or luminescence.

A nitrated conjugated polymer (NPTh) was employed for the photometric sensing of amines [68]. The polymer is a functional active material for

optoelectronic devices and chemical sensors. It was synthesized from parent polythiophene, adsorbed into silica gel and its response was compared with non-BAs and non-amine compounds. BAs with a lone electron pair on the central nitrogen have electron-donating properties in contrast to NPTh because of the powerful electron-withdrawing character of its nitro group. After exposing of the polymer film to BA vapors (ethylenediamine, putrescine, cadaverine, spermidine, phenethylamine, and histamine) its color darkens and this induces a broad absorption band in a wide wavelength range of 300 – 700 nm. A wavelength of 450 nm shows the most pronounced response to BAs.

Determination of primary BAs (isopentylamine, propylamine and putrescine) with the indicator dye ETH4001 immobilized in ormosil sensor layers formed by sol-gel technology was performed [69]. The sensing layers were read continuously by photometry at 520 nm in a flow-through cell and showed good reproducibility and high efficiency at mM concentrations with 5–15 min response times. The sensor foils were resistant against photobleaching and long-term stable for 9 months. This sensor has a good continuous on-site monitoring capability because it was used with appropriate miniaturized instrumentation.

A more long-wave photometric detection wavelength is achieved by the nucleophilic attack of 1-propylamine at an azo dye to irreversibly convert its tricyanovinyl group into a 1-propylamino-2,2-dicyanovinyl group. A sensor membrane with this dye embedded in plasticized poly(vinylchloride) on glass responded to BAs after modest 15–30 min with an absorbance decrease at 630 nm in a home-made flow-through cell in a UV–VIS spectrometer [62]. The response of the sensor is less linear at higher concentrations and the sensor layer is stable up six months. The linear quantitation range is from hundreds of μM to 4.0 mM of 1-propylamine.

A coumarin derivative yields covalent enamine adducts with BAs and enables not only ratiometric photometric (377/403 nm) but also fluorescence

sensing (470 nm) [45] in the micromolar range both, in solution and in the gas phase. The selectivity towards BAs is more pronounced at 403 nm with the exception of histamine, which is preferably detected at 377 nm. Upon drop-coating of a layer of a mixture of 5 mol% of dye with polymethyl methacrylate on glass slides putrescine and n-butylamine responded within 2 h to the gaseous BAs by decolorization whereas ammonia and secondary amines show no response.

A method of putrescine derivatization was established [70] using *o*-phthalaldehyde (and thioglycolic acid as a reductant) to generate red Schiff base derivatives (PUT-RD) which could be detected by the bare eye and spectrophotometrically at λ_{max} of 490 nm. The concentration of putrescine detected in 10 fish products was varying from 11 to 190 mg/kg with an apparent recovery in the 94 – 106% range.

1.5.3 Luminescence readout

Luminescence readout commonly is more sensitive by some orders of magnitude compared to photometry or reflectometry but formerly seemed to be complicated from an instrumental point of view and its evaluation was not easy for the layman. The requirement of an excitation light source and optical devices for selection of excitation and emission light together with blocking excitation light off the detector show that luminescence setups are more demanding and expensive than photometric and reflectometric schemes. Aside from the classical rectangular arrangement of excitation and emission light to read planar sensor membranes, fiber-optic setups became very popular over the last decades. Those share the advantages that the excitation light can be brought closely even to remote samples and be read out even through transparent polymers (e.g. detection through the wall of a plastic vessel or food package with a sensor layer fixed at the inside wall). Moreover, if the excitation light is guided to an array of sensors or fed into an several optical fibers (with different

sensors attached), multi-analyte sensing becomes feasible. Nevertheless, the use of simple tools like LEDs or handheld UV lamps for excitation and digital camera-based luminescence readout, enabled in-field setups for less than 1000 US-$, that can be operated by non-trained personnel [44]. Digital cameras and smart phones became very popular devices for luminescence detection, as well, but the demands for rejection of scattered excitation or ambient light are more demanding than in reflectometry or photometry.

A recent example uses an indicator dye (Py-1) comprising pyrylium groups [44] that responds only to primary but not to secondary and tertiary amines on dipsticks. The BA nucleophile converts the pyrylium moiety of Py-1 into the respective pyridinium salt which can visually be seen by a color change from blue (λ_{max}^{abs}= 605 nm) to red (λ_{max}^{abs}= 503 nm). Concomitantly, fluorescence appears at 602 nm with a quantum yield up to 0.5. Filter paper, indium tin oxide (ITO) and a microtiter plate were shown to be useful solid supports for quantitative analysis of the total content of BAs (TAC) [44, 58, 61] in real samples. A poly(acrylonitrile)-based hydrogel (Hypan) or cellulose acetate were chosen as polymer matrices to embed the Py-1 dye either in a sensor film or in electrospun nanofibers. Depending on whether in-field readout or quantitation in high-throughput is desired, the sensor cocktail can either be dip-coated on filter paper to yield dipsticks or be deposited in the wells of a microtiter plate. A standard fluorescence microtiter plate reader was then used to monitor the ageing of meat and cheese over time reliably and reproducibly which was confirmed by GC-MS [61]. Signal acquisition from dipsticks was performed upon excitation either in a black box with LEDs (λ_{exc}= 505 nm) [44] or with a UV-lamp [58] (at 254 nm) and subsequent fluorescence readout with a digital camera from RGB images taken in RAW format. Extraction and calculation of the fluorescence intensity ratio by free Image J software delivers the concentrations of all biogenic amines in a sample no matter if meat, seafood or cheese is investigated. Electrospun nanofibers on ITO dipsticks delivered a

higher sensitivity [58] due to their high porosity and surface area. Here, the anionic CA fibers are counter-charged with respect to the BAs and additionally serve for pre-concentration. Importantly, the dipsticks additionally deliver a visual no/yes (blue→red) answer to evaluate if the BA concentrations exceed the permitted level or not.

An aminodiacetic acid-modified Nile Red–Ni^{2+} complex and calcein blue complexed with Fe^{2+} ions served as luminescent probes for histamine [71] and dopamine [72]. Metal-induced luminescence quenching was switched off here upon ligand exchange with BAs. This also could be used in assays with a shortwave detection wavelength (440 nm) at µM concentrations of dopamine. A new optical sensor for histamine based on a zinc(II) salphen complex immobilized on silica microparticles was developed. The fluorescence emission of the complex increased upon the binding of histamine [73].

A commercial electrospun nanofiber mat (Tiss®-Link) was used as a support material for the direct highly selective and sensitive determination of tryptamine (LOD 6 ng/mL, LOQ 19 ng/mL) in beer [74]. Activated vinyl groups on the surface of the mat permit a fast covalent immobilization of tryptamine by means of a Michael type reaction so to form the transduction system. The intensity of Solid Surface-Room Temperature Phosphorescence (SS-RTP) is measured at 443 nm (λ_{exc} = 290 nm) after spotting with KI solution and total removal of oxygen from the measurement cell. The selective detection of putrescine and cadaverine based on quenching of a luminescent anthracene-Fe^{3+} chelate due to decomplexation in aqueous DMSO enabled sensing in ppb levels in both, vapor phase and solution using the chelate coated on alumina or inexpensive paper strips, respectively [75].

A fiber-optic enzymatic biosensor uses the oxidation of amines under oxygen consumption for determination of putrescine, cadaverine, spermidine and histamine [76]. Diamine oxidase (DAO) was immobilized on two types of magnetic particles based on either magnetite covered with chitosan or on

commercial SEPABEADS® EC-HA 403 with a ferrofluid. Embedding of the DAO magnetic particles and the Ru-bathophenanthroline complex into an inorganic–organic hybrid polymer ORMOCER® KSK 1238 yielded a cocktail that was deposited on a PMMA lens. The lens was fixed at the tip of an optical fiber in a gas-tight steel tube. The increase of the fluorescence lifetime (and decrease of oxygen quenching) of the ruthenium complex was proportional to the concentration the BAs at micromolar levels. Lifetime measurements need slightly more complex instrumentation but have the benefit of being independent of fluorophore ageing, leaching and ageing of the excitation light source. Even though, the instrumentation employed is small enough to make the sensor system amenable to on-site analyses.

New classes of materials also find their way into food sensing with a lanthanide metal–organic framework (EuMOF) comprising an organic dye (methyl red, MR) [77]. This sensing material was used for determination of histamine using an advanced analytical device based on a one-to-two logic gate. After exposition to histamine vapor the fluorescence intensity of Eu^{3+} at 613 nm decreased (3-fold) and the maximum emission of MR increased (44-fold) and a color transition under a UV lamp from red to blue occurred with a response time of 25 min.

A novel sensor chip based on a graphene oxide (GO) aerogel and photonic crystals (PCs) was fabricated. Its setup mimics the human nose with olfactory cilia and olfactory glomeruli for analyte binding and fluorescence signal processing, respectively [78]. It has the potential to discriminate ten biogenic amines and seven drug amines. Three fluorophores (Acridine orange, Rhodamine 6G and Rhodamine B) were chosen for multiple fluorescent sensing of BAs with various structures. For this purpose, PCs were prepared from poly(styrene/methyl methacrylate/acrylic acid) latex particles with three different diameters, which matched the emissions of 3 fluorescence dyes. The competitive interactions of fluorophores and amines to GO modulate the

fluorescence emission. The analyte discrimination is achieved chemometrically by additional linear discriminant analysis and hierarchical clustering analysis.

Histamine fluorescence sensing was also established using CdSe/ZnS quantum dots which were modified by a 1-vinyl-3-butyl-imidazolium hexafluorophosphate ionic liquid (QDs@IL@MIP) [79]. The surface of the QDs was covered with poly-methacrylic acid into which histamine was embedded as molecular imprint. The fluorescence of QDs@IL@MIP at 605 nm (λ_{exc} = 400 nm) was enhanced by histamine in a concentration range of 0.449–2.249 mM with a LOD of 0.11 mM.

1.5.4 Chemiluminescence readout

Chemiluminescence (CL) can be detected after a product of a chemical reaction is generated in an electronically excited state and returns to its ground state under emission of light. The underlying kinetic of the reaction imposes a transient signal, which often is amplified by coupling with an enzymatic reaction and/or an enhancer molecule for analytical purposes. Most importantly, as no excitation light is required, much less background signal and scatter from the matrix of real samples can be expected to occur when using CL detection as compared to reflectometry, photometry or luminescence detection. This yields very low detection limits in many cases provided that no cross reactions of enhancer and analyte molecule occurs. Further, the absence of an excitation source makes instrumentation for these methods considerably simpler because just a light-tight detection cell, sample holder, light-collecting lens and a sensitive photodiode are required. This way, CL detection is even more simple than reflectometry or photometry and hence, CL sensors have the potential for miniaturization and on-site analysis. These advantages hold true, if CL is coupled e.g. with enzymatic signal enhancement and luminol but also impose restrictions in the selection of analytes via the choice of the enzyme. Further, there are much less CL reactions (and with it potential analytes a sensor can

respond to) than other chemosensors which limits the use of this detection method.

Enzymatic biosensor membranes based on hydroxyethylcellulose [51] provide an indirect determination of BAs via the H_2O_2 formed from putrescine with under the action of putrescine oxidase or diamine oxidase, respectively. Here, the Co(II)-catalyzed reaction with luminol produces chemiluminescence that is proportional to both the concentration of the hydrogen peroxide as well as the concentration of putrescine. Such biosensors were used for determination of BAs in meat and fish samples (LOD at 1 mg/L level) and showed comparable results to HPLC with precolumn derivatization. A potential in-field use can be envisioned if minimized instrumentation would be used.

Mg–Al–CO_3 double layered hydroxide (LDHs) nanosheets show strong blue photoluminescence (λ_{exc}=365 nm) which is decreased by BAs through a displacement of the O–H···O bonds by O–H···N between BAs and sheets. The decreased catalytic effect of these LDHs on the chemiluminescence of the bis(2,4,6-trichlorophenyl) oxalate (TCPO)–H_2O_2 system successfully enabled histamine determination in spoiled fish and pork meat samples [80].

1.5.5 Total internal reflection ellipsometry

Thin hybrid films consisting of copper phthalocyanines on single walled carbon nanotubes (SWCNTs) were applied for sensing amine vapors [54] by total internal reflection ellipsometry. Those films were produced by spin-casting the solutions onto gold-coated slides and onto silicon substrates. Ellipsometry determines the change of the polarization state of light upon its reflection at a sample when irradiated with linearly or circularly polarized light. In spectroscopic ellipsometry the parameters Ψ and Δ are monitored in the respective wavelength range (400 - 1000 nm in [54]) with an ellipsometer. The tan Ψ is the modulus of the complex ratio of the reflection coefficients. In the present publication, shifts of Δ are induced on the hybrid films within 1–2 min

response time by adsorption of amine vapors (methylamine, dimethylamine, trimethylamine). Those phase shifts are due to the phase shift between the p- and s-components of polarized light and increase with the concentration of the BAs. Methylamine was detected with an LOD of 3.6 ppm while the steric hindrance of diethylamine and trimethylamine reduces their response. As ellipsometry more and more finds its way into sensing, there is the hope that the miniaturization of the bulky instrumentation and the simplification of the demanding data evaluation of this detection method will open a window for its in-field use for food analysis.

1.5.6 Surface-enhanced Raman spectroscopy

SERS uses the massive increase of a Raman signal which can occur once an analyte interacts with a surface that has a nanostructured metallic surface. Here, an electromagnetic and a chemical fraction contribute to the overall signal enhancement. The chemical enhancement originates from the greater polarizability of the molecule that is adsorbed onto the SERS substrate. Additionally, the incident light excites localized surface plasmons on the metallic surface which create an electromagnetic field that can be enhanced strongly (the electromagnetic enhancement). Enhancement factors up to 10^{14} have moved detection limits of this method to the single molecule level, albeit this concentration level cannot be expected in real samples but is obtained with research-level instrumentation, only. The main limitations of SERS-based BA detection in food analysis are the relatively high price of a portable Raman spectrometers (10000 – 30000 Euro) and the requirement for noble metal nanoparticles in the sample or a nanopatterned surface for quantitation. Moreover, temperature has to stabilized very carefully to eliminate potential interferences on the measurement. On the other hand, SERS does not require labeling of the target analytes and provides on-line sensing capability in flow cells.

Although SERS nowadays becomes more widely used for food analysis [81] with chromatographic separation techniques, the first report on its application for BAs detection in food was published in 2015 [82]. As histamine is one of the most popular BAs for monitoring of fish spoiling, this BA is also most widely used in new SERS-based methods. For example, Gao et al. [82] detected histamine in artificially spiked canned tuna meat. In order to separate the analyte from the complex matrix and to minimize the background signal, the authors performed solid phase extraction of the analyte from tuna extract by a polyvinyl chloride film with immobilized molecularly imprinted polymers (MIP). Then, a SERS substrate (a solution of AuNPs) was used for both analyte elution and detection of histamine. Liquid-liquid extraction [83] and TLC [84, 85] were also used as sample pretreatment techniques prior SERS-based histamine detection in fish meat. Most notably, SERS detection was performed directly on the developed TLC plate which additionally shortens analysis time. With this method, Tan et al. could not only detect ageing of artificially spiked meat, but also monitor fish spoiling over 48 h at room temperature. All reports allow for reliable quantification of histamine in real samples within the ranges of concentrations required for detection of the spoiling process (>100 mg/kg) (see table 2). A chemometric analysis (e.g., principal component analysis) was also widely used in order to improve the analysis performance [82, 83, 85]. The comparison of results obtained by SERS and HPLC [84] shows that the TLC-SERS protocol with simple partial least square regression analysis also has acceptable precision (RSD <10%). Additionally, the effect of TLC sample pretreatment on the reduction of the RSD is significantly larger than that of the chemometric treatment making a sample pretreatment step mandatory for reliable analysis [85]. This is in accordance with the general rule that sampling and sample pretreatment have more impact on precision of an analysis that the detection method itself, if real samples are studied. Finally, an advantage of all listed protocols [83–85] is the use of simple AuNPs solutions as SERS

substrates with appropriate reliability and efficiency in the sample pretreatment process.

Besides of detection of histamine (e.g. in seafood and fermented foodstuff), SERS can be successfully used for monitoring the decomposition (spoiling) of non-fermented foods, as well. For example, Wu et al. [86] proposed MIP coated silver nanoparticles (AgNPs) for direct SERS detection of histamine in solution down to 0.1 mg/L. The assay for histamine detection in spiked samples showed an appropriate accuracy with apparent recovery in the ranges 85 – 117% (canned tuna) and 93–108% (red and rice wines).

Besides of histamine, there are also some reports on detection of tyramine. Wang et al. [87] combined SERS with high performance TLC for tyramine detection in cheese. The authors successfully detected tyramine at 30–80 mg/kg in cheese (not spiked) with an apparent recovery within the 84 – 108% range.

As a conclusion, SERS expects a bright future as an on-site sensing method in food control if the prices for instruments will decrease with an increasing number of purchased devices and if further miniaturized instruments will be available. It has all the merits to become a viable on-site detection method provided that suitable selectivity can be obtained with a simple sample pretreatment.

1.6 Conclusion and Outlook

This chapter shows that a wide variety of optical sensors and methods for BA quantification in food exist that have the potential for future commercialization due to simplification of the sampling and detection schemes and proven applicability to real food samples. Presumably, the most widely used detection methods will comprise either photometry, reflectance or chemiluminescence using cell phone analysis due to the simplicity of the required instrumentation. However, also digital photographic sensor schemes seem promising because they can acquire photometric, reflectometric or even fluorescence responses of a

chemosensor with good reproducibility in-field at low costs. A fully automated software evaluation of the optical sensors is not available, yet although highly essential for on-site use with less educated staff, which should comprise chemometric data treatment because it has proven to enhance selectivity and reliability of food sensors. Chemometric data treatment is a further step companies could implement to bring food sensing schemes closer to home-users and which could be applied to dipstick sensors provided that a simple sample preparation exists. SERS expects a bright future as an on-site sensing method in food control, if the prices for instruments and nanopatterned detection cells will decrease with an increasing number of purchased devices and if further miniaturized instruments will be available. It has all the merits to become a viable on-site detection method provided that suitable selectivity can be obtained with a simple sample pretreatment.

Optical food sensing is also a chance for scientists working with microfluidics to get involved into a new inspiring field of sensor science because miniaturized microfluidic systems could also include automated sample pretreatment steps and combine them with detection inside a micro-total-analysis system. Hence, there are many access points and techniques to create new optical food sensor schemes and to adapt them to the wealth of analytes in real samples that may be analyzed by home users, the food industry and within food chains all over the world.

1.7 References

1. Silla Santos MH (1996) Biogenic amines: Their importance in foods. Int J Food Microbiol 29:213–231 . https://doi.org/10.1016/0168-1605(95)00032-1
2. Papageorgiou M, Lambropoulou D, Morrison C, Kłodzińska E, Namieśnik J, Płotka-Wasylka J (2018) Literature update of analytical methods for biogenic amines determination in food and beverages. Trends Anal Chem 98:128–142 . https://doi.org/10.1016/j.trac.2017.11.001
3. ten Brink B, Damink C, Joosten HMLJ, Huis in 't Veld JHJ (1990) Occurrence and formation of biologically active amines in foods. Int J Food Microbiol 11:73–84 . https://doi.org/10.1016/0168-1605(90)90040-C
4. Hotchkiss JH (1989) Preformed N-nitroso compounds in foods and beverages. Cancer Surv 8:295–321
5. Eerola S, Hinkkanen R, Lindfors E, Hirvi T (1993) Liquid chromatographic determination of biogenic amines in dry sausages. J AOAC Int 76:575–577 . https://doi.org/10.1093/jaoac/76.3.575
6. Maxa E, Brandes W (1993) Biogene Amine in Fruchtsaeften. Mitteilungen Klosterneubg 43:101–106
7. Halász A, Baráth Á, Simon-Sarkadi L, Holzapfel W (1994) Biogenic amines and their production by microorganisms in food. Trends Food Sci Technol 5:42–49 . https://doi.org/10.1016/0924-2244(94)90070-1
8. Treptow H, Askar A (1987) Biogenic amines in cocoa and chocolate. Gordian 87:223–224
9. Tricker AR, Pfundstein B, Theobald E, Preussmann R, Spiegelhalder B (1991) Mean daily intake of volatile N-nitrosamines from foods and beverages in West Germany in 1989-1990. Food Chem Toxicol 29:729–732 . https://doi.org/10.1016/0278-6915(91)90180-F
10. Hernández-Jover T, Izquierdo-Pulido M, Veciana-Nogués MT, Mariné-

Font A, Vidal-Carou MC (1997) Biogenic Amine and Polyamine Contents in Meat and Meat Products. J Agric Food Chem 45:2098–2102 . https://doi.org/10.1021/jf960790p

11. Sayem-el-Daher N, Simard RE, Fillion J (1984) Changes in the amine content of ground beef during storage and processing. Food Sci + Technol + Technol 17:319–323
12. Bardócz S, Grant G, Brown DS, Ralph A, Pusztai A (1993) Polyamines in food-implications for growth and health. J Nutr Biochem 4:66–71 . https://doi.org/10.1016/0955-2863(93)90001-D
13. Kielwein G, Treptow H, Askar A, Dross A, Wittkowski R (1988) Biogene Amine in Lebensmitteln. In: Molecular Nutrition food research. pp 420–423
14. Linares DM, Del Río B, Ladero V, Martínez N, Fernández M, Martín MC, Álvarez MA (2012) Factors influencing biogenic amines accumulation in dairy products. Front Microbiol 3:1–10 https://doi.org/10.3389/fmicb.2012.00180
15. Fernández M, Linares DM, Del Río B, Ladero V, Alvarez MA (2007) HPLC quantification of biogenic amines in cheeses: Correlation with PCR-detection of tyramine-producing microorganisms. J Dairy Res 74:276–282 . https://doi.org/10.1017/S0022029907002488
16. Sánchez-Pérez S, Comas-Basté O, Rabell-González J, Veciana-Nogués MT, Latorre-Moratalla ML, Vidal-Carou MC (2018) Biogenic amines in plant-origin foods: Are they frequently underestimated in low-histamine diets? Foods 7:1–17 . https://doi.org/10.3390/foods7120205
17. Stratton JE, Hutkins RW, Taylor SL (1991) Biogenic amines in cheese and other fermented foods: A review. J. Food Prot. 54:460-470. https://doi.org/10.4315/0362-028X-54.6.460
18. Önal A (2007) A review: Current analytical methods for the determination of biogenic amines in foods. Food Chem 103:1475–1486 .

https://doi.org/10.1016/j.foodchem.2006.08.028

19. Mohammed GI, Bashammakh AS, Alsibaai AA, Alwael H, El-Shahawi MS (2016) A critical overview on the chemistry, clean-up and recent advances in analysis of biogenic amines in foodstuffs. TrAC - Trends Anal Chem 78:84–94 . https://doi.org/10.1016/j.trac.2016.02.007
20. Erim FB (2013) Recent analytical approaches to the analysis of biogenic amines in food samples. TrAC - Trends Anal Chem 52:239–247 . https://doi.org/10.1016/j.trac.2013.05.018
21. He L, Xu Z, Hirokawa T, Shen L (2017) Simultaneous determination of aliphatic, aromatic and heterocyclic biogenic amines without derivatization by capillary electrophoresis and application in beer analysis. J Chromatogr A 1482:109–114 . https://doi.org/10.1016/j.chroma.2016.12.067
22. Li DW, Liang JJ, Shi RQ, Wang J, Ma YL, Li XT (2019) Occurrence of biogenic amines in sufu obtained from Chinese market. Food Sci Biotechnol 28:319–327 . https://doi.org/10.1007/s10068-018-0500-4
23. Huisman H, Wynveen P, Nichkova M, Kellermann G (2010) Novel ELISAs for screening of the biogenic amines GABA, glycine, β-phenylethylamine, agmatine, and taurine using one derivatization procedure of whole urine samples. Anal Chem 82:6526–6533 . https://doi.org/10.1021/ac100858u
24. Kaur N, Chopra S, Singh G, Raj P, Bhasin A, Sahoo SK, Kuwar A, Singh N (2018) Chemosensors for biogenic amines and biothiols. J Mater Chem B 6:4872–4902 . https://doi.org/10.1039/c8tb00732b
25. Gruendler P (2007) Introduction in Chemical Sensors. In: Chemical sensors. Springer, pp 1–13
26. McGrath MJ, Scanaill CN, McGrath MJ, Scanaill CN (2013) Sensing and Sensor Fundamentals. In: Sensor Technologies. pp 15–50
27. Sugiyasu K, Swager TM (2007) Conducting-polymer-based chemical

sensors: Transduction mechanisms. Bull Chem Soc Jpn 80:2074–2083 . https://doi.org/10.1246/bcsj.80.2074

28. Schultz JS, Taylor RF (1996) Introduction to chemical and biological sensors. In: Handbook of Chemical and Biological Sensors. pp 1–9
29. Fraden J (2004) Chemical Sensors. In: Handbook of Modern Sensors. Springer, pp 499–532
30. Narayanaswamy R (1993) Optical Chemical Sensors: Transduction and Signal Processing. Analyst 118:317-322. https://doi.org/10.1039/AN9931800317
31. Sabri N, Aljunid SA, Salim MS, Fouad S (2015) Recent Trends in Physics of Material Science and Technology. 204:299–311 . https://doi.org/10.1007/978-981-287-128-2
32. Jer PCA, Ara AN, Conceic M (2007) Optical sensors and biosensors based on sol – gel films. 72:13–27 . https://doi.org/10.1016/j.talanta.2006.09.029
33. Pan J, Cha T, Chen H, Choi JH (2013) Carbon nanotube-based optical platforms for biomolecular detection. Woodhead Publishing Limited 270-297.
34. Lobnik A, Turel M, Urek ŠK (2012) Optical Chemical Sensors : Design and Applications. In: Advances in Chemical Sensors. pp 1–28
35. Nagl S, Wolfbeis OS (2008) Classification of Chemical Sensors and Biosensors Based on Fluorescence and Phosphorescence. 5: 325-346
36. Wolfbeis OS (2005) Materials for fluorescence-based optical chemical sensors. J. Mater Chem 15:2657–2669 . https://doi.org/10.1039/b501536g
37. Lakowicz J.R. (2006) Fluorescence Sensing. In: Principles of Fluorescence Spectroscopy. pp 623–673
38. Gruendler P (2007) Optical Sensors. In: Chemical sensors. pp 199–225
39. Lakowicz J.R. (2006) Introduction to fluorescence. In: Principles of Fluorescence Spectroscopy. pp 1–26

40. Hapke B (2017) Reflectance Methods and Applications, 3rd ed. Elsevier Ltd. , pp 931-935
41. Ebralidze II, Laschuk NO, Poisson J, Zenkina O V. (2019) Colorimetric Sensors and Sensor Arrays. In: Nanomaterials Design for Sensing Applications. Elsevier Inc., pp 1–39
42. Water LC, Countsb RW, Palausky A, Jenkins RA (2008) Colorimetric strip tests : a comparison of visual and reflectometric measurements for quantitative applications. Hazard Mater 43:1–12 . https://doi.org/10.1016/0304-3894(95)00022-M
43. Ding B, Wang M, Wang X, Yu J, Sun G (2010) Electrospun nanomaterials for ultrasensitive sensors Increasing demands for ever more sensitive sensors for global. Mater Today 13:16–27 . https://doi.org/10.1016/S1369-7021(10)70200-5
44. Steiner MS, Meier RJ, Duerkop A, Wolfbeis OS (2010) Chromogenic sensing of biogenic amines using a chameleon probe and the red-green-blue readout of digital camera images. Anal Chem 82:8402–8405 . https://doi.org/10.1021/ac102029j
45. Lee B, Scopelliti R, Severin K (2011) A molecular probe for the optical detection of biogenic amines. Chem Commun 47:9639–9641 . https://doi.org/10.1039/c1cc13604f
46. Calvino C, Piechowicz M, Rowan SJ, Schrettl S, Weder C (2018) A Versatile Colorimetric Probe based on Thiosemicarbazide–Amine Proton Transfer. Chem - A Eur J 24:7369 – 7373 . https://doi.org/10.1002/chem.201801551
47. Roales J, Pedrosa JM, Guillén MG, Lopes-Costa T, Pinto SMA, Calvete MJF, Pereira MM (2015) Optical detection of amine vapors using ZnTriad porphyrin thin films. Sensors Actuators, B Chem 210:28–35 . https://doi.org/10.1016/j.snb.2014.12.080
48. Xiao-Wei H, Zhi-Hua L, Xiao-Bo Z, Ji-Yong S, Han-Ping M, Jie-Wen Z,

Li-Min H, Holmes M (2016) Detection of meat-borne trimethylamine based on nanoporous colorimetric sensor arrays. Food Chem 197:930–936 . https://doi.org/10.1016/j.foodchem.2015.11.041

49. Diaz YJ, Page ZA, Knight AS, Treat NJ, Hemmer JR, Hawker CJ, Read de Alaniz J (2017) A Versatile and Highly Selective Colorimetric Sensor for the Detection of Amines. Chem - A Eur J 23:3562–3566 . https://doi.org/10.1002/chem.201700368
50. Yu H, Zhuang D, Hu X, Zhang S, He Z, Zeng M, Fang X, Chen J, Chen X (2018) Rapid determination of histamine in fish by thin-layer chromatography-image analysis method using diazotized visualization reagent prepared with: P -nitroaniline. Anal Methods 10:3386–3392 . https://doi.org/10.1039/c8ay00336j
51. Omanovic-Miklicanin E, Valzacchi S (2017) Development of new chemiluminescence biosensors for determination of biogenic amines in meat. Food Chem 235:98–103 . https://doi.org/10.1016/j.foodchem.2017.05.031
52. Dole T, Koltun S, Baker SM, Goodrich-Schneider RM, Marshall MR, Sarnoski PJ (2017) Colorimetric Evaluation of Mahi-Mahi and Tuna for Biogenic Amines. J Aquat Food Prod Technol 26:781–789 . https://doi.org/10.1080/10498850.2017.1297879
53. Bueno L, Meloni GN, Reddy SM, Paixão TRLC (2015) Use of plastic-based analytical device, smartphone and chemometric tools to discriminate amines. RSC Adv 5:20148–20154 . https://doi.org/10.1039/c5ra01822f
54. Banimuslem H, Hassan A, Basova T, Esenpinar AA, Tuncel S, Durmuş M, Gürek AG, Ahsen V (2015) Dye-modified carbon nanotubes for the optical detection of amines vapours. Sensors Actuators, B Chem 207:224–234 . https://doi.org/10.1016/j.snb.2014.10.046
55. del Pozo M, Casero E, Quintana C (2017) Visual and spectrophotometric

determination of cadaverine based on the use of gold nanoparticles capped with cucurbiturils or cyclodextrins. Microchim Acta 184:2107–2114 . https://doi.org/10.1007/s00604-017-2226-z

56. Tseng SY, Li SY, Yi SY, Sun AY, Gao DY, Wan D (2017) Food Quality Monitor: Paper-Based Plasmonic Sensors Prepared Through Reversal Nanoimprinting for Rapid Detection of Biogenic Amine Odorants. ACS Appl Mater Interfaces 9:17306–17316 . https://doi.org/10.1021/acsami.7b00115
57. Lin T, Wu Y, Li Z, Song Z, Guo L, Fu F (2016) Visual monitoring of food spoilage based on hydrolysis-induced silver metallization of au nanorods. Anal Chem 88:11022–11027 . https://doi.org/10.1021/acs.analchem.6b02870
58. Yurova NS, Danchuk A, Mobarez SN, Wongkaew N, Rusanova T, Baeumner AJ, Duerkop A (2018) Functional electrospun nanofibers for multimodal sensitive detection of biogenic amines in food via a simple dipstick assay. Anal Bioanal Chem 410:1111–1121 . https://doi.org/10.1007/s00216-017-0696-9
59. Płotka-Wasylka JM, Morrison C, Biziuk M, Namieśnik J (2015) Chemical Derivatization Processes Applied to Amine Determination in Samples of Different Matrix Composition. Chem Rev 115:4693–4718 . https://doi.org/10.1021/cr4006999
60. Schaude C, Meindl C, Fröhlich E, Attard J, Mohr GJ (2017) Developing a sensor layer for the optical detection of amines during food spoilage. Talanta 170:481–487 . https://doi.org/10.1016/j.talanta.2017.04.029
61. Khairy GM, Azab HA, El-Korashy SA, Steiner MS, Duerkop A (2016) Validation of a Fluorescence Sensor Microtiterplate for Biogenic Amines in Meat and Cheese. J Fluoresc 26:1905–1916 . https://doi.org/10.1007/s10895-016-1885-1
62. Mohr GJ (2004) A tricyanovinyl azobenzene dye used for the optical

detection of amines via a chemical reaction in polymer layers. Dye Pigment 62:77–81 . https://doi.org/10.1016/j.dyepig.2003.11.011

63. Morsy MK, Zór K, Kostesha N, Alstrøm TS, Heiskanen A, El-Tanahi H, Sharoba A, Papkovsky D, Larsen J, Khalaf H, Jakobsen MH, Emnéus J (2016) Development and validation of a colorimetric sensor array for fish spoilage monitoring. Food Control 60:346–352 . https://doi.org/10.1016/j.foodcont.2015.07.038
64. Bustamante Fonseca SE, Rivas BL, García Pérez JM, Vallejos Calzada S, García F (2018) Synthesis of a polymeric sensor containing an occluded pyrylium salt and its application in the colorimetric detection of trimethylamine vapors. J Appl Polym Sci 135:4–9 . https://doi.org/10.1002/app.46185
65. Chen LY, Wang CW, Yuan Z, Chang HT (2015) Fluorescent gold nanoclusters: Recent advances in sensing and imaging. Anal Chem 87:216–229 . https://doi.org/10.1021/ac503636j
66. Huang C, Wang S, Zhao W, Zong C, Liang A, Zhang Q, Liu X (2017) Visual and photometric determination of histamine using unmodified gold nanoparticles. Microchim Acta 184:2249–2254 . https://doi.org/10.1007/s00604-017-2253-9
67. El-Nour KMA, Salam ETA, Soliman HM, Orabi AS (2017) Gold Nanoparticles as a Direct and Rapid Sensor for Sensitive Analytical Detection of Biogenic Amines. Nanoscale Res Lett 12:2008–2009 . https://doi.org/10.1186/s11671-017-2014-z
68. Jin YJ, Kwak G (2018) Detection of biogenic amines using a nitrated conjugated polymer. Sensors Actuators, B Chem 271:183–188 . https://doi.org/10.1016/j.snb.2018.05.091
69. Nedeljko P, Turel M, Lobnik A (2017) Hybrid sol-gel based sensor layers for optical determination of biogenic amines. Sensors Actuators, B Chem 246:1066–1073 . https://doi.org/10.1016/j.snb.2017.02.011

70. Qi X, Wang WF, Wang J, Yang JL, Shi YP (2018) Highly selective colorimetric detection of putrescine in fish products using o-phthalaldehyde derivatization reaction. Food Chem 259:245–250 . https://doi.org/10.1016/j.foodchem.2018.03.131
71. Seto D, Soh N, Nakano K, Imato T (2010) An amphiphilic fluorescent probe for the visualization of histamine in living cells. Bioorganic Med Chem Lett 20:6708–6711 . https://doi.org/10.1016/j.bmcl.2010.09.003
72. Seto D, Maki T, Soh N, Nakano K, Ishimatsu R, Imato T (2012) A simple and selective fluorometric assay for dopamine using a calcein blue-Fe2+ complex fluorophore. Talanta 94:36–43 . https://doi.org/10.1016/j.talanta.2012.02.025
73. Sahudin MA, Su'ait MS, Tan LL, Lee YH, Abd Karim NH (2019) Zinc(II) salphen complex-based fluorescence optical sensor for biogenic amine detection. Anal Bioanal Chem 411:6449–6461 . https://doi.org/10.1007/s00216-019-02025-4
74. Ramon-Marquez T, Medina-Castillo AL, Fernandez-Gutierrez A, Fernandez-Sanchez JF (2016) Novel optical sensing film based on a functional nonwoven nanofibre mat for an easy, fast and highly selective and sensitive detection of tryptamine in beer. Biosens Bioelectron 79:600–607 . https://doi.org/10.1016/j.bios.2015.12.091
75. Pandith A, Dasagrandhi C, Kim H-R, Kim H-S (2018) Selective discrimination of putrescine and cadaverine based on a Fe^{3+} - morpholinoanthracene ensemble in solution and solid state and logic gate aided biological applications in mixed aqueous medium. Sensors Actuators, B Chem 254:842–854 . https://doi.org/10.1016/j.snb.2017.07.115
76. Pospiskova K, Safarik I, Sebela M, Kuncova G (2013) Magnetic particles-based biosensor for biogenic amines using an optical oxygen sensor as a transducer. Microchim Acta 180:311–318 .

https://doi.org/10.1007/s00604-012-0932-0

77. Xu XY, Lian X, Hao JN, Zhang C, Yan B (2017) A Double-Stimuli-Responsive Fluorescent Center for Monitoring of Food Spoilage based on Dye Covalently Modified EuMOFs: From Sensory Hydrogels to Logic Devices. Adv Mater 29:1–7 . https://doi.org/10.1002/adma.201702298
78. Ren W, Qin M, Hu X, Li F, Wang Y, Huang Y, Su M, Li W, Qian X, Tang KL, Song Y (2018) Bioinspired Synergy Sensor Chip of Photonic Crystals-Graphene Oxide for Multiamines Recognition. Anal Chem 90:6371–6375 . https://doi.org/10.1021/acs.analchem.8b01549
79. Wang QH, Fang GZ, Liu YY, Zhang DD, Liu JM, Wang S (2017) Fluorescent Sensing Probe for the Sensitive Detection of Histamine Based on Molecular Imprinting Ionic Liquid-Modified Quantum Dots. Food Anal Methods 10:2585–2592 . https://doi.org/10.1007/s12161-017-0795-4
80. Wang Z, Liu F, Lu C (2014) Evolution of biogenic amine concentrations in foods through their induced chemiluminescence inactivation of layered double hydroxide nanosheet colloids. Biosens Bioelectron 60:237–243 . https://doi.org/10.1016/j.bios.2014.04.013
81. Liao W, Lu X (2016) Determination of chemical hazards in foods using surface-enhanced Raman spectroscopy coupled with advanced separation techniques. Trends Food Sci Technol 54:103–113 . https://doi.org/10.1016/j.tifs.2016.05.020
82. Gao F, Grant E, Lu X (2015) Determination of histamine in canned tuna by molecularly imprinted polymers-surface enhanced Raman spectroscopy. Anal Chim Acta 901:68–75 . https://doi.org/10.1016/j.aca.2015.10.025
83. Janči T, Valinger D, Gajdoš Kljusurić J, Mikac L, Vidaček S, Ivanda M (2017) Determination of histamine in fish by Surface Enhanced Raman Spectroscopy using silver colloid SERS substrates. Food Chem 224:48–54 . https://doi.org/10.1016/j.foodchem.2016.12.032

84. Xie Z, Wang Y, Chen Y, Xu X, Jin Z, Ding Y, Yang N, Wu F (2017) Tuneable surface enhanced Raman spectroscopy hyphenated to chemically derivatized thin-layer chromatography plates for screening histamine in fish. Food Chem 230:547–552 . https://doi.org/10.1016/j.foodchem.2017.03.081

85. Tan A, Zhao Y, Sivashanmugan K, Squire K, Wang AX (2019) Quantitative TLC-SERS detection of histamine in seafood with support vector machine analysis. Food Control 103:111–118 . https://doi.org/10.1016/j.foodcont.2019.03.032

86. Wu Z, Xu E, Jiao A, Jin Z, Irudayaraj J (2017) Bimodal counterpropagating-responsive sensing material for the detection of histamine. RSC Adv 7:44933–44944 . https://doi.org/10.1039/c7ra07362c

87. Wang L, Xu XM, Chen YS, Ren J, Liu YT (2018) HPTLC-FLD-SERS as a facile and reliable screening tool: Exemplarily shown with tyramine in cheese. J Food Drug Anal 26:688–695 . https://doi.org/10.1016/j.jfda.2017.07.007

2 Motivation and Structure of the Thesis

The focus of this thesis lies on the development of dipsticks for the detection and determination of biogenic amines in food samples. BA concentrations that are considered to be determined are not noticeable by the human nose but still may represent a health risk. According to the WHO, higher than 200 diseases can be transferred by food. As an example, in the U.S. 48 million people (one in six) go through foodborne disease every year. Of these, 128,000 are hospitalized and 3000 die from these diseases [1]. Biogenic amines are biologically active substances and food involving high concentrations of biogenic amines may cause various food poisoning diseases. Histamine, tyramine, β-phenylethylamine and tryptamine may have bad effects on the nervous and the vascular system. Tyramine, β-phenylethylamine and tryptamine may lead to intoxication known as ‘‘cheese reaction’’ causing hypertensive crises and severe headaches [2]. High levels of the aliphatic polyamines spermidine and spermine may increase the development of food allergies [3]. Tyramine, spermidine, spermine, putrescine and cadaverine may be precursors of carcinogenic nitrosamines, mainly in meat products because nitrate and nitrite salts are usually added to those as preserving agents. Histamine intoxication called as ‘‘histamine poisoning’’ includes different symptoms: skin irritation, rashes, dilatation of peripheral blood vessels resulting in hypotension and headache, contraction of intestinal smooth muscle causing diarrhea and vomiting [2]. Histamine is considered as the most toxic biogenic amine causing great concerns in clinical and food chemistry and is contained in seafood samples intrinsically at notable concentration levels. Recently, the number of food poisoning cases which are connected to histamine levels in fish increase. That’s why the focus of this study was on seafood samples. The BA concentration which may be risky is between 0.3 and 1.0 mM. BAs in amounts lower than 1.0 mM can mostly not be detected by the human nose but still are dangerous [4].

Detection of biogenic primary amines should be carried out by new probes in aqueous solution using reflectance and fluorescence spectroscopy as simple detection concepts suitable for the readout of dipsticks [5]. Colorimetric sensor arrays based on detecting a color change by acquiring photos of the sensor and RGB analysis were shown for monitoring meat and fish freshness [6]. Unlike arrays, dipsticks only need a one-point readout and are therefore much quicker and easier to be read out and thus deliver their response much faster. So we decided to go into the same direction and quantify the biogenic amine content based on optical detection either by semi-quantitative analysis (i.e. by naked eye based on the color change) on dipsticks or by photographic determination of the BA concentration based on fluorescence emission or reflectance measurements.

The development of dipsticks is beneficial since they are practical, simple, portable, easy to use and thus do not require trained staff. Moreover, they have a much lower cost compared to instrumental methods of analysis [7]. In addition to that, colorimetric sensing of BAs using dipsticks provides a simple response based on the color change and this leads to a yes/no answer besides the quantitative analysis [4]. Quantitative analysis using nanofibers enhances the sensitivity because of the high porosity and the high volume-to-surface area ratio of these materials. Nanofibers containing chromogenic and fluorescent dyes can be used for the selective detection of primary amines. Hence, the detection of BAs seemed feasible by using nanofiber mat dipsticks to benefit from their characteristics mentioned above and provide an optical readout upon reaction with BAs. Two types of dipsticks (Py-1-CA and S0378-CA) were planned to be prepared and used for the detection of BAs based on fluorescence and reflectometry, respectively.

Chapter 1 introduces on the formation of BAs in different kinds of food and their harmful effects when they exceed the permitted limits. It also explains the general concept of sensors and focuses on the optical sensors for BAs and

their advantages. Hence, it covers the optical sensors for determination of biogenic amines (BAs) in food over the last ten years. Moreover, it includes optical sensors for BAs with the classical sensor design where a probe for recognition such as organic dyes, metal-ligand complexes, nanomaterials, enzymes, etc. is immobilized in a membrane and/or placed on a suitable support which can be paper [4, 8, 9], glass [8, 10], TLC plates [7, 11, 12], microtiter plates [13] and test-tubes [14]. This chapter describes in detail the various optical readout methods which can be used for BA determination such as reflectometric readout [15, 16], photometric readout [17], luminescence readout [18], chemiluminescence readout [19], total internal reflection ellipsometry [20] and surface-enhanced Raman spectroscopy(SERS) [21].

Chapter 3 discusses in detail a quantitative determination method for BAs using functional electrospun nanofibers via fluorescence detection. Since electrospun nanofibers have high immobilization efficiency, they can improve the sensitivity of the optical detection [22] with sensor membranes or of dipsticks. This chapter includes how the Py-1-CA nanofibers were prepared by electrospinning, how all of the spinning conditions were optimized, and how fiber morphology was characterized. Electrospun nanofibers were prepared from a negatively charged polymer CA to extract the cationic Py1 conjugate formed upon the reaction of the Py-1 dye with biogenic amines. By doping the nanofibers with the fluorescent dye Py-1 the quantitative determination of BAs was carried out by evaluating the enhancement of the fluorescence emission upon the reaction of the amine moiety of the BA with the pyrylium group of Py-1 [4]. The optical response of the dye to various amines in solution was studied in detail in earlier work [23]. We show also the optimization of the reaction conditions (time of incubation in the ethanol chamber) with tyramine with the dipsticks to obtain the highest response. Using the mentioned procedure, a calibration plot for determination of tyramine was obtained. Other BAs show a very similar response. The selectivity of the dipsticks was tested for tyramine,

histamine, cadaverine, spermidine, putrescine, 2-aminoethylmethacrylate, dimethylamine, triethylamine. The fibers are selectively reactive to primary amines. Due to the comparable response to all BAs, the dipsticks were successfully applied to determine the total content of BAs in shrimp samples. Ageing of shrimp at 4° C was studied and the total amine content was determined to be 14.1, 16.4, 38.8 µmol/g for days 0, 3 and 6, respectively.

Chapter 4 describes in detail the detection of biogenic amines using S0378-CA dipsticks based on reflectometry. This chapter includes all the steps for the preparation of the reflectometric dipstick sensors and their application for the determination of BAs. First, the fabrication of the NIR dye-embedded nanofibers (S0378-CA) by electrospinning and optimizing the electrospinning conditions for obtaining the homogenous sensing fiber mat is described. The mat has a bright green color which allows sensitive reflectance measurements. Then, the nanofiber morphology as obtained by SEM and light microscopy is characterized. Next, the reaction between the dipsticks and BAs is optimized with respect to reaction conditions such as temperature and time. After that, various BAs (spermidine, tyramine, putrescine, and histamine) are calibrated after optimizing the conditions of the whole method (spinning, reaction, and reflectometry measurement). The selectivity of the dipsticks towards nucleophiles, secondary and tertiary amines and proteins (dimethylamine, triethylamine, human serum albumin and cysteine) is determined. Finally, the dipsticks are applied to shrimp samples. Ageing of shrimp at room temperature was studied and the total amine content was determined to be 7.5, 12.8, 21.7 µmol/g for days 0,1,6.

Chapter 5 introduces the final steps that were made to transfer the principles of signal generation from the dipsticks into a lab-on-a-chip microfluidic total analysis system. Its advantages are discussed and details about lamination and its fabrication and the possible bonding techniques to create a multi layered microfluidic chip are shown. Then, it is described, how a

microfluidic chip was fabricated, in which S0378-CA nanofibers were embedded for the detection of BAs. It includes how the design of the chip, wax melting conditions for bonding the support to the nanofiber-ITO layer, and reaction conditions with BAs were optimized in order to calibrate tyramine. Unfortunately, the lab-on-a-chip microfluidic total analysis system could not be developed to reach a final state due to time constraints at the end of the PhD thesis.

2.1 References

1. Ruiz-Capillas C, Herrero AM (2019) Impact of biogenic amines on food quality and safety. Foods 8:62 . https://doi.org/10.3390/foods8020062

2. Önal A (2007) A review: Current analytical methods for the determination of biogenic amines in foods. Food Chem 103:1475–1486 . https://doi.org/10.1016/j.foodchem.2006.08.028

3. Sugita Y, Takao K, Toyama Y, Shirahata A (2007) Enhancement of intestinal absorption of macromolecules by spermine in rats. Amino Acids 33:253–260 . https://doi.org/10.1007/s00726-007-0532-1

4. Steiner MS, Meier RJ, Duerkop A, Wolfbeis OS (2010) Chromogenic sensing of biogenic amines using a chameleon probe and the red-green-blue readout of digital camera images. Anal Chem 82:8402–8405 . https://doi.org/10.1021/ac102029j

5. Saravanakumar M, Umamahesh B, Selvakumar R, Dhanapal J, Ashok kumar SK, Sathiyanarayanan KI (2020) A colorimetric and ratiometric fluorescent sensor for biogenic primary amines based on dicyanovinyl substituted phenanthridine conjugated probe. Dye Pigment 178:108346 . https://doi.org/10.1016/j.dyepig.2020.108346

6. Magnaghi LR, Capone F, Zanoni C, Alberti G, Quadrelli P, Biesuz R (2020) Colorimetric sensor array for monitoring, modelling and comparing spoilage processes of different meat and fish foods. Foods 9: 684. https://doi.org/10.3390/foods9050684

7. Xiao-Wei H, Zhi-Hua L, Xiao-Bo Z, Ji-Yong S, Han-Ping M, Jie-Wen Z, Li-Min H, Holmes M (2016) Detection of meat-borne trimethylamine based on nanoporous colorimetric sensor arrays. Food Chem 197:930–936 . https://doi.org/10.1016/j.foodchem.2015.11.041

8. Lee B, Scopelliti R, Severin K (2011) A molecular probe for the optical detection of biogenic amines. Chem Commun 47:9639–9641 . https://doi.org/10.1039/c1cc13604f

9. Calvino C, Piechowicz M, Rowan SJ, Schrettl S, Weder C (2018) A Versatile Colorimetric Probe based on Thiosemicarbazide–Amine Proton Transfer. Chem - A Eur J 24:7369–7373 . https://doi.org/10.1002/chem.201801551

10. Roales J, Pedrosa JM, Guillén MG, Lopes-Costa T, Pinto SMA, Calvete MJF, Pereira MM (2015) Optical detection of amine vapors using ZnTriad porphyrin thin films. Sensors Actuators, B Chem 210:28–35 . https://doi.org/10.1016/j.snb.2014.12.080

11. Diaz YJ, Page ZA, Knight AS, Treat NJ, Hemmer JR, Hawker CJ, Read de Alaniz J (2017) A Versatile and Highly Selective Colorimetric Sensor for the Detection of Amines. Chem - A Eur J 23:3562–3566 . https://doi.org/10.1002/chem.201700368

12. Yu H, Zhuang D, Hu X, Zhang S, He Z, Zeng M, Fang X, Chen J, Chen X (2018) Rapid determination of histamine in fish by thin-layer chromatography-image analysis method using diazotized visualization

reagent prepared with: P -nitroaniline. Anal Methods 10:3386–3392 . https://doi.org/10.1039/c8ay00336j

13. Omanovic-Miklicanin E, Valzacchi S (2017) Development of new chemiluminescence biosensors for determination of biogenic amines in meat. Food Chem 235:98–103 . https://doi.org/10.1016/j.foodchem.2017.05.031

14. Dole T, Koltun S, Baker SM, Goodrich-Schneider RM, Marshall MR, Sarnoski PJ (2017) Colorimetric Evaluation of Mahi-Mahi and Tuna for Biogenic Amines. J Aquat Food Prod Technol 26:781–789 . https://doi.org/10.1080/10498850.2017.1297879

15. Kielwein G, Treptow H, Askar A, Dross A, Wittkowski R (1988) Biogene Amine in Lebensmitteln. In: Molecular Nutrition food research. pp 420–423

16. Khairy GM, Azab HA, El-Korashy SA, Steiner MS, Duerkop A (2016) Validation of a Fluorescence Sensor Microtiterplate for Biogenic Amines in Meat and Cheese. J Fluoresc 26:1905–1916 . https://doi.org/10.1007/s10895-016-1885-1

17. El-Nour KMA, Salam ETA, Soliman HM, Orabi AS (2017) Gold Nanoparticles as a Direct and Rapid Sensor for Sensitive Analytical Detection of Biogenic Amines. Nanoscale Res Lett 12:2008–2009 . https://doi.org/10.1186/s11671-017-2014-z

18. Ren W, Qin M, Hu X, Li F, Wang Y, Huang Y, Su M, Li W, Qian X, Tang KL, Song Y (2018) Bioinspired Synergy Sensor Chip of Photonic Crystals-Graphene Oxide for Multiamines Recognition. Anal Chem 90:6371–6375 . https://doi.org/10.1021/acs.analchem.8b01549

19. Wang Z, Liu F, Lu C (2014) Evolution of biogenic amine concentrations

in foods through their induced chemiluminescence inactivation of layered double hydroxide nanosheet colloids. Biosens Bioelectron 60:237–243 . https://doi.org/10.1016/j.bios.2014.04.013

20. Banimuslem H, Hassan A, Basova T, Esenpinar AA, Tuncel S, Durmuş M, Gürek AG, Ahsen V (2015) Dye-modified carbon nanotubes for the optical detection of amines vapours. Sensors Actuators, B Chem 207:224–234 . https://doi.org/10.1016/j.snb.2014.10.046

21. Xie Z, Wang Y, Chen Y, Xu X, Jin Z, Ding Y, Yang N, Wu F (2017) Tuneable surface enhanced Raman spectroscopy hyphenated to chemically derivatized thin-layer chromatography plates for screening histamine in fish. Food Chem 230:547–552 . https://doi.org/10.1016/j.foodchem.2017.03.081

22. Matlock-Colangelo L, Baeumner AJ (2014) Biologically Inspired Nanofibers for Use in Translational Bioanalytical Systems. Annu Rev Anal Chem 7:23–42 . https://doi.org/10.1146/annurev-anchem-071213-020035

23. Azab HA, El-Korashy SA, Anwar ZM, Khairy GM, Duerkop A (2012) Reactivity of a luminescent “off-on” pyrylium dye toward various classes of amines and its use in a fluorescence sensor microtiter plate for environmental samples. J Photochem Photobiol A Chem 243:41–46 . https://doi.org/10.1016/j.jphotochem.2012.05.029

3 Functional Electrospun Nanofibers for Multimodal Sensitive Quantitation of Biogenic Amines in Food via a Simple Dipstick Assay

3.1 Abstract

Electrospun nanofibers (ENFs) are promising materials for rapid diagnostic tests like lateral flow assays and dipsticks because they offer an immense surface area while excluding minimal volume, a variety of functional surface groups and can entrap functional additives within their interior. Here, we show that ENFs on sample pads are superior in comparison to standard polymer membranes for the optical detection of biogenic amines (BAs) in food using a dipstick format. Specifically, cellulose acetate (CA) fibers doped with 2 mg/mL of the chromogenic and fluorogenic amine-reactive chameleon dye Py-1 were electrospun into uniform anionic mats. Those extract cationic BAs from real samples and Py-1 transduces BA concentrations into a change of color, reflectance and fluorescence. Dropping a BA sample onto the nanofiber mat converts the weakly fluorescent pyrylium dye Py-1 into a strongly red emitting pyridinium dye. For the first time, a simple UV-lamp excites fluorescence and a digital camera acts as detector. The intensity ratio of the red to the blue channel of the digital image is dependent on the concentration of most relevant BAs indicating food spoilage from 10-250 µM. This matches the permitted limits for BAs in foods and no false positive signals arise from secondary and tertiary amines. BA-detection in seafood samples was also demonstrated successfully. The nanofiber mat-dipsticks were up to 6-fold more sensitive than those using a polymer membrane with the same dye embedded. Hence, nanofiber-based tests are not only superior to polymer-based dipstick assays, but will also improve the performance of established tests related to food safety, medical diagnostics and environmental testing.

This chapter has been published:

Nadezhda S. Yurova, Alexandra Danchuk, Sarah N. Mobarez, Nongnoot Wongkaew, Tatiana Yu. Rusanova, Antje. J. Baeumner, Axel Duerkop, Anal. Bioanal. Chem. 2018, 410:1111-1121; DOI: 10.1007/s00216-017-0696-9

Author contributions:

Sarah Mobarez shared in the experimental work and revision of the manuscript. The experimental work was mainly done by Nadezhda S. Yurova and Alexandra Danchuk. Antje J. Baeumner and Nongnoot Wongkaew contributed with strategic discussions. Axel Duerkop is the corresponding author. Axel Duerkop was the leader of this project.

3.2 Introduction

Rapid testing of biogenic amines (BAs) is of increasing interest because they are potential indicators of the different stages of freshness of protein-rich food, cheese and fermented food. BAs can have adverse effects on human health even in concentrations that cannot be recognized by the human nose [1-3]. It is therefore not surprising that many instrumental methods for the analysis of BAs have been proposed. Among them are chromatography [4], capillary electrophoresis [5], sensors, flow-injection analysis [6] and ELISA [7-8]. All of them are suitable for a precise determination of individual concentrations of BAs in a laboratory environment with well-educated staff and with costs per sample being less important, which makes translation into "in-field" operations impossible.

In-field BA determination requires inexpensive and simple on-site methods for quantitation of BAs. Here, the aim is not to obtain a detailed concentration of each individual BA in the sample but rather an overall concentration level of all BAs potentially contained within to judge on the freshness or potential danger of a food sample [9-10]. Therefore, rapid tests such as dipsticks are advantageous because they can be easily operated by an inexperienced worker in the field and because they are also cheap enough to be widely available. There are many visual tests for determination BAs in food. It has been reported that a nonporous colorimetric sensor array for trimethylamine (TMA) detection was developed [11]. In this work, a sol–gel method was used to obtain a TiO_2 nanoporous film as substrate material to improve the sensitivity and stability of the colorimetric sensor. Several other optical-based sensors have been described for the detection of BAs using various chromogenic reagents, including Meldrum's activated furan (MAF) for the determination of amines in solution, on solid supports, and in the vapor phase [12], simultaneous using of

GJM-492 and Remazol Brilliant Blue (RBBR) for detection of ammonia and biogenic amines [13] or immobilizing of the indicator dye ETH4001 for the development of a spermidine and spermine sensing system [14]. Moreover, there are further colorimetric chemical sensors based on various classes of indicator dyes, such as phthalocyanines [15], porphyrins [16], calixarenes [17] and others. Recently, the application of gold nanoparticles (AuNPs) has acquired much attention for the development of different sensors. Tyramine-protected AuNPs were used as a probe for colorimetric and fluorescence turn-on detection of spermine and spermidine based on AuNP aggregation in the presence of diamines [18]. An optical method relying on the application of a Cu^{2+} complex of organic nanoparticles for the simultaneous quantification of spermidine and spermine in vapors and aqueous phase [19] and a sensor based on AuNPs for rapid detection of histidine and histamine in meat samples [20] were proposed. The aforementioned sensors commonly suffer from the fact that some require a large number of different reagents and only one of them permits both colorimetric and luminescence readout [18]. As luminescence is in general more sensitive than a colorimetric readout, the creation of dipsticks offering luminescent readout with additional colorimetric detection of BAs can provide a dual response by providing both, a yes/no answer and quantitative information [21].

Electrospun nanofibers are an emerging field in biosensing and chemosensing because they have a high porosity and immense surface area, are easy to handle, can be mass-produced and can be reusable. Furthermore, electrospun nanofibers provide excellent loading capacities for immobilization of recognition molecules that can introduce an optical response into a fiber net [22]. Commonly, polymeric materials are used for the production of fibers like polymethyl methacrylate (PMMA), polyacrylamide (PAM), polystyrene (PS), polyvinylpyrrolidone (PVP), polyvinyl alcohol (PVA), polycarbonate (PC) or

cellulose acetate [23]. By spinning a charged polymer, additional functionality can be introduced into the resulting fiber mat because the charged surface of the resulting nanofibers can serve to enrich a counter-charged analyte. That means that charged electrospun nanofibers could adopt functionality similar to a solid-phase extraction material. Hence, for the quantitation of BAs (which are commonly cationic in aqueous solution of neutral pH), a negatively charged polymer should be chosen. By additional doping the fibers with an appropriate chromogenic fluorescent probe for BAs, a new material for analyte extraction and optical readout of dipsticks with three different methods could be obtained.

We therefore embedded a blue dye (Py-1) [24] that is responsive to BAs into electrospun nanofibers made of cellulose acetate (CA) to obtain uniform, flexible, blue colored anionic nanofibers that respond to the presence of various BAs in three different ways. First, a color change from blue to red can be seen by naked eye. Secondly, the reflectance of the fibers at 611 nm changes upon dipping into a liquid sample containing BAs. Finally, there is a pronounced increase in fluorescence at 588 nm in proportion to the concentration of BAs. Fluorescence emission was acquired from dipsticks as a digital image upon illumination with a simple handheld UV-lamp. From the images acquired in RAW-format the intensities of the red, green and blue channels are extracted with public-domain software and the red-to-blue intensity ratio was used for the calibration of BA concentrations. The fibers on the dipsticks selectively respond to primary amines but not to secondary or tertiary amines and were successfully tested with real samples.

3.3 Materials and Methods

3.3.1 Materials

Py-1 was from ActiveMotif Chromeon (www.chromeon.com). The buffer N-cyclohexyl- 2-amino ethanesulfonic acid (CHES) was from Roth (www.carlroth.de). Spermidine, putrescine, cadaverine, 2-aminoethylmetacrylate, dimethylamine were purchased from Sigma-Aldrich (www.sigmaaldrich.com) and histamine from Fluka, all as hydrochloride salts. Tyramine and trimethylamine, each as free base, were from Sigma. All amines were of analytical grade. Poly-styrene-co-acrylonitrile (SAN) (M_w 185,000 Da), poly-methyl methacrylate (PMMA) (M_w 996,000 Da), cellulose acetate (CA) (M_w 30,000 Da, 39.8 wt% acetyl content), and poly-vinylpyrrolidone (PVP) (M_w 1,300,000 Da) were obtained from Sigma-Aldrich. The polyurethane polymer (HydroMed D4) was obtained from AdvanSource Biomaterials (www.advbiomaterials.com). Indium tin oxide (ITO) coated on PET (polyethylene terephthalate) with a surface resistivity 60 Ω/sq was purchased from Sigma-Aldrich.

Stock solutions of BA (10.0 mM) were prepared in CHES buffer (pH 9.5). Working standard solutions of compounds were freshly prepared by diluting stock solutions with CHES. CHES buffer (5.00 mM) was prepared by dissolving of solid CHES (0.1036 g) in 100 mL of deionized water. The pH of CHES was adjusted with sodium hydroxide (1.00 M).

3.3.2 Apparatus

The electrospinning was performed using a commercial electrospinning machine (Spraybase® power supply unit PLS000048 and Spraybase® syringe pump module PLS000004). Fiber mat thickness, fiber diameter, and images for

pore size determination were obtained by an Olympus LEXT OLS4000 3D Measuring Laser Microscope with 10 nm minimum z-resolution. pH was checked with a pH meter CG 842 from Schott (www. si-analytics.com). Fluorescence spectra of dipsticks were acquired in a solid sample holder (with 30° incident angle) with a Jasco FP-6300 luminescence spectrometer with 520 nm excitation and 5 nm slits for excitation and emission monochromator, respectively, 500 nm scan speed, 0.5 nm data pitch and a PMT voltage adjusted to "medium" in the software. All spectra are corrected. Reflectance spectra were acquired with an Ocean Optics Reflectance measurement kit, containing of a white light source, a y-shaped bifurcated optical fiber, a fiber holder and a Flame-S VIS-NIR spectrometer.

3.3.3 Electrospinning of Fibers Containing Py-1

The polymer CA (0.720 g) and Py-1 (8.00 mg) were dissolved in a mixture of 3.00 mL of acetic acid and of 1.00 mL of acetone. Then, this spinning dope should be stirred for about 48 hours until Py-1 is completely dissolved and the mixture is homogeneous. The spinning dope should be protected from light while stirring. The CA-Py-1 electrospun nanofibers were fabricated using the electrospinning machine with the following parameters: plastic syringe 5 mL (covered with aluminum foil); voltage: 17 kV; flow rate: 0.002 mL/min, tip-to-collector distance: 11 cm. An ITO film (size: 7×5 cm) was used as a supporting material. The resulting materials were prepared with different electrospinning times (15, 30, 60 min). Electrospun fiber mats on ITO should be stored dry and dark.

3.3.4 Preparation of Dipsticks and BA determination

The dipsticks with CA-Py-1-nanofibers (Ø = 8 mm) were cut from the ITO sheets with a hole puncher and mounted into a multi stick holder which can house several sticks in a row, circumvented by black, solvent resistant plastic. After that 5.00 µL of BA (in CHES buffer, pH 9.5) was added on the circles with a micropipette. The multi stick holder was immersed into an ethanol chamber (4 mL of ethanol) for spreading of the drop of analyte to the full size of the stick. After spreading, the spots were dried at ambient air (20 min). Then again, the holder was placed into the ethanol chamber for color development (20 min) of the sticks.

3.3.5 Acquisition of Images and Evaluation

For the fluorimetric determination of BA, pictures were taken in a dark room using a UV lamp (254 nm) for excitation. The lamp was positioned under a 50°-illumination angle and fixed with respect to an adjusted position of the multi stick holder. The digital camera was mounted on top over the multi stick holder on a Novoflex MagicStudio Repro-Stand which permits reproducible distances between the objective of the camera and the stick holder. Images were acquired by means of a Canon EOS 550D camera equipped with a 67 mm UV filter using the following preset parameters f = 5,5; 1/13 sec exposure time, ISO 6400, 57 mm distance and custom white balance. The resulting photos were processed with the use of Photoshop CS6. In this regard, the spot was highlighted with the Lasso tool, the color was averaged over the area of the whole stick and the colorimetric parameters such as R, G, and B were determined by the software.

ImageJ software was used to determine pore size of the fiber mats. Here, the microscopic image was changed to 8-bit and the threshold was set at 35%. A

pore of the fiber mat was treated as a particle in which Feret sizes larger than 0.5 μm^2 were taken into account.

3.3.6 Preparation of Real Samples

Shrimp samples were purchased from a local discounter supermarket and stored at -22°C. A 10.0 g portion was mixed with 100 mL of methanol in a beaker and homogenized in a blender at high speed for 2 min. The homogenisate was transferred into a conical flask and placed in a 60 °C water bath for 30 min. The extract was filtered through a porcelain Buchner funnel with blue ribbon filter paper (Schleicher und Schüll: 589^3, www.whatman.com) for three times to yield particle-free samples. Then, 80 µL of triethylamine were added and the extract was mixed. From this mixture, 25.0 µL aliquots were taken and histamine solution was added to reach concentrations of 0-140 µM of added histamine after dilution to 500 µL overall volume with CHES buffer (5.00 mM; pH 9.5). After that, 5.00 µL of aliquot solutions were then added on dipsticks mounted into a multi stick holder and developed and imaged as described in the sections above.

3.4 Results and Discussion

3.4.1 Choice of Materials, Conditions of Spinning and Fiber Morphology

The main idea (Fig. 1) of this research was to spin functional anionic nanofibers that could act as a solid-phase extraction material for BAs (that are cationic in aqueous samples) on the sample pads of dipstick assays. By designing a spinning dope with an appropriate chromogenic fluorescent probe (Py-1) for

BAs new nanofibers for both analyte extraction and optical readout of dipsticks should be obtained. Those nanofibers were tested with respect to their response to biogenic amines with various optical detection methods and to their applicability for BA monitoring during ageing in real samples. The amine reactive probe Py-1 was chosen because of its chromogenic and fluorogenic properties. It is blue (λ_{abs}^{max}=605 nm) and virtually non-fluorescent (φ=0.01) in its non-conjugated form in solution but shows a dramatic color change to red (λ_{abs}^{max}=503 nm) accompanied by a strong increase in fluorescence intensity (φ=0.5) when covalently reacted with primary amino groups [21]. This enables a fluorescence readout of the reacted dye even in presence of unreacted Py-1. The optical response of the dye to various amines in solution was studied in detail in earlier work [24].

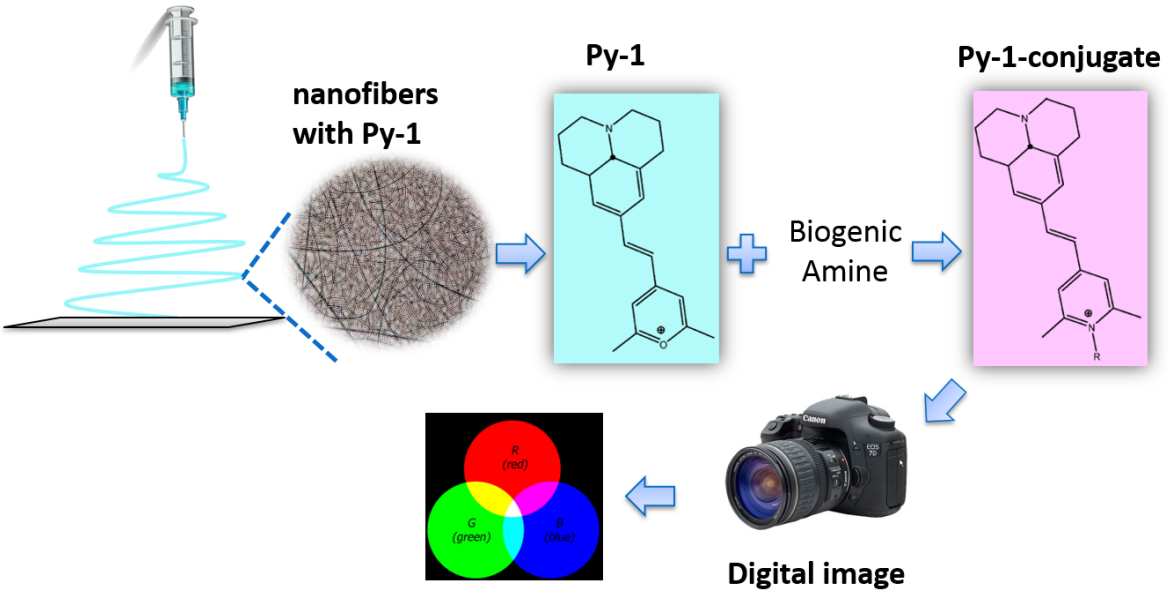

Fig.1. Schematic rendering the nanofiber-based BA detection dipstick assay.

Prior electrospinning both dye and polymer are dissolved in a solvent mixture to yield the so-called spinning dope. Solutions of poly-styrene-acrylonitrile (SAN), poly-vinylpyrrolidone (PVP), poly-methyl methacrylate (PMMA), Hydromed D4 and cellulose acetate (CA) were tested for their ability to dissolve the Py-1

dye, the stability of the dye embedded in the polymer and for their optical response towards BAs. The polymer solutions (SAN - 35%, PVP - 14%, PMMA - 5%, D4 - 20% and CA - 18%) and the dye solution (Py-1 - 1 g/L) were mixed on a microscope glass slide and after drying on air, a drop of BA solution (tyramine, 10 mM) was applied to evaluate the response of the respective spinning dope to the analyte. The tested polymers should have a threshold polarity as to enable a quick access of the polar BAs into the polymer and show a distinct change of color upon reaction with a BA.

Table 1. Stability of polymers with embedded Py-1 and visual response to tyramine.

№	**Polymer**	**Characterization**	**Response to tyramine solution**
1	poly-styrene-acrylonitrile	high hydrophobicity, stability of color for 1 month	no
2	poly-vinyl-pyrrolidone	green to brown after 2 days at room temperature / after 1 hour at 165 °C	changing color from green to red
3	poly-methyl-methacrylate	disappearance of color after 2 hours at room temperature	no
4	Hydromed D4	disappearance of color after 1 hour at room temperature	changing color from green to pink
5	Cellulose Acetate	stability of color for 3 weeks	changing color from blue-green to pink

As can be seen from table 1, only three polymers (2, 4 and 5) enable a response of Py-1 to the amine. In the case of poly-styrene-acrylonitrile, the polymer is

highly hydrophobic, which makes the analyte penetration into the polymer very difficult. This is also obvious from the fact that no color change is observed upon addition of the amine solution. Also PMMA does not respond to tyramine and the dye is unstable in the polymer. PVP and D4 are not suitable for long-term use due to decomposition of the dye when mixed within. In the case of PVP, the crosslinking reaction at 165 ° C (to render the polymer water-insoluble) leads to the decomposition of the dye. Only CA retains the color of the unreacted dye for a long time and displays a distinct color change upon reaction with a BA. Accordingly, CA was chosen for the spinning of nanofibers.

For the optimization of the electrospinning process, Py-1 was dissolved in the CA spinning dope solution in 1 or 2 mg/mL, respectively. The latter concentration showed a brighter color of the BA-Py-1 conjugate, and this concentration was selected for further study. Spinning for 30 min onto ITO slides yields homogeneous, well-formed nanofibers (Figure 2). A number of different collector substrates were studied, including aluminum foil, glass slides and filter paper which all lead to non-uniform distributions of nanofibers on the surface, upon spinning times >15 min. In contrast, spinning onto indium tin oxide (ITO) resulted in homogeneously distributed nanofibers (and color). This is presumably due to the high planarity of the ITO sheets which yields a more homogenous electric field on the collector plate during the electrospinning process.

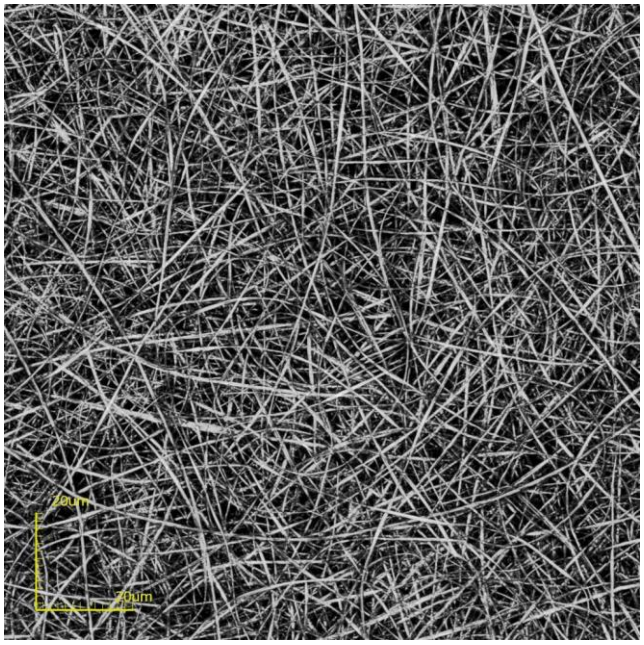

Fig. 2. Microscopic image of CA-Py-1 nanofibers on ITO with 30 min electrospinning time (c(Py-1) = 2 mg/mL). The microscopic pictures were taken by a 3D laser scanning microscope with 2,160x magnification (100x objective lens).

Characterizations of fiber morphology with respect to fiber mat thickness, pore size, and diameter were performed by a 3D Measuring Laser Microscope. CA-Py-1 nanofibers were then prepared on ITO with different electrospinning times (15, 30, 60 min). The thickness of the resulting fiber mats were determined to be 0.65±0.01 µm, 6.9±1.6 µm and 11.2±0.4 µm and the respective fiber mats are displayed in Fig. 3a-c. For the mats that are spun for 30 min this is about the same thickness as of common polymeric sensor membranes. The related pore sizes derived from the 2D-microscopic image are 2.6 ± 1.3 µm as determined by the Feret diameter (example shown in Fig. 3d) from 1896 pores (n=3). In addition, within a specified area the density of pores is very high (~1.48×10^5 pores/mm^2), enabling a huge accessible sensing area for BAs. The fibers have an average diameter of 168 ± 18 nm, as to determination with the 3D Measuring Laser Microscope with 2160x magnification.

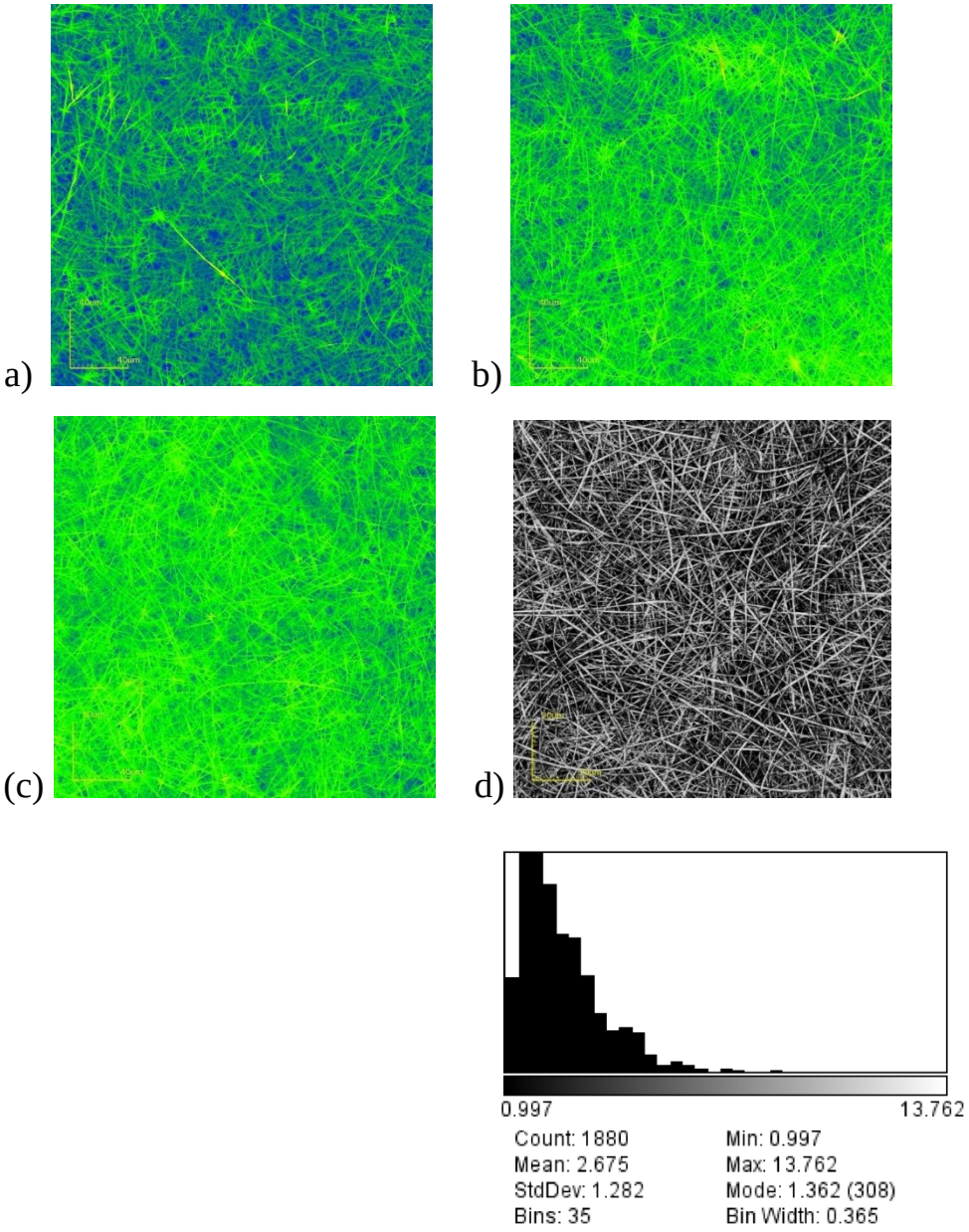

Fig. 3. Morphology of Py1-nanofibers electrospun for (a) 15, (b) 30, and (c) 60 min as taken by a 3D laser scanning microscope (Olympus LEXT 3D Measuring Laser Microscope OLS4000) with 1080x magnification (50x objective lens). d) Representative sample for calculation of the pore size as indicated by the Feret diameter (magnification: 2,160x; determination area: 132.13 µm x 96.77 µm; threshold for ImageJ set at 35%; count = number of pores in total area).

3.4.2 Optical Properties of Nanofibers and Acquisition of Images

The CA fiber mat containing Py-1 as amine reactive probe is blue and virtually non-fluorescent (see Fig. 4, A2), and reacts with primary amine groups in aqueous solution of pH 8-9.5 at room temperature to give a covalent red conjugate (see Figure 3, B2) [21]. This color change is visible at 210 µM which is close to the BA concentrations (0,3-1 mM) in foods that can induce serious health problems [21]. A visible red color of the dipsticks upon testing a sample therefore should be understood as a warning that the sample might be suspicious. The visual color change can also be derived from the reflectance spectra of the dipsticks monitored in absence and presence of TYR, respectively (see Fig. 5). The reflectivity at 611 nm significantly increases in presence of TYR because the blue form of Py-1 is no longer present and converted to the red one. This means that more light is reflected in the yellow/orange range of the spectrum thus leading to the faint red color of the dipstick shown in Fig. 4, B2. Hence, reflectance spectroscopy could be used for evaluation of the dipsticks, as well, albeit its sensitivity will not be very high.

While the change of reflectance and visual color is not too pronounced due to the small amount of dye doped into the CA nanofibers, the dye concentration is sufficient for fluorescence analysis. The dye amount is smaller than in a plain polymer sensor membrane because the porosity of a fiber mat is much higher than that of a layer of knife coated polymer. Doping of electrospun nanofibers with a fluorophore therefore helps reducing assay costs in comparison to polymer membranes. The fluorescence change from unreacted Py-1 (A_1) in the fiber mat to orange red (B_1) upon formation of the conjugate between Py-1 and tyramine when the fiber mat is excited at 254 nm with a UV lamp, is highly pronounced. The blue color of the spot in A_1 is the common background luminescence from the PET support of the ITO sheet and stronger than the weak red emission from Py-1. This is confirmed by the fluorescence

spectra of Py-1 in the nanofiber mat where the initially barely detectable emission of unreacted Py-1 (λ_{em}^{max}= 663 nm) in the fiber mat increases by a factor of about 10 upon formation of the conjugate between Py-1 and tyramine (λ_{em}^{max}= 588 nm). Compared to the emission spectra in solution [25] the emission maximum of unreacted Py-1 remains almost unchanged whereas the emission maximum of reacted Py-1 shifts 15 nm shortwave in the mat. The excitation maximum of the reacted form of Py-1 embedded in the nanofibers is found at 517 nm.

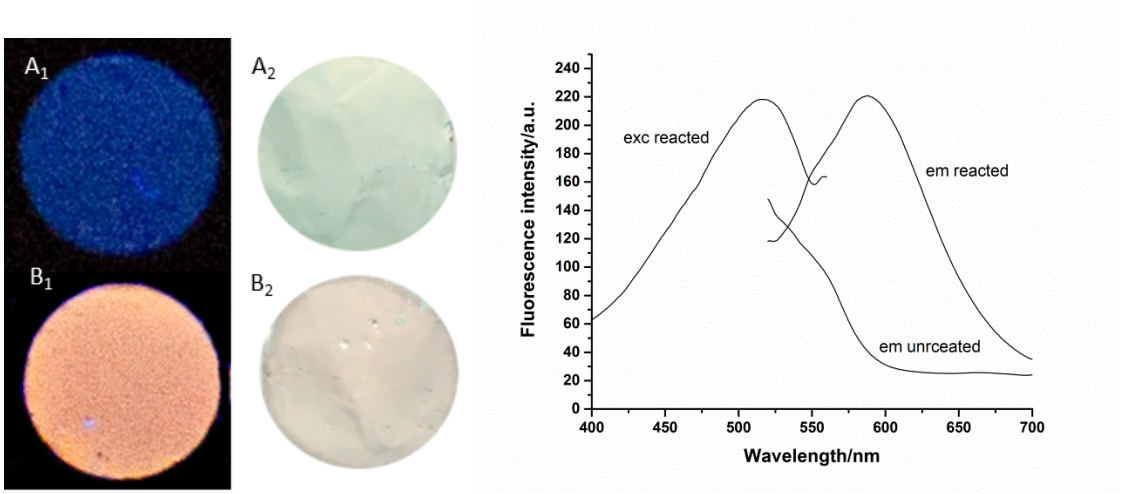

Fig. 4. left: Images of CA-Py-1 nanofiber mats before (A_1 and A_2) and after (B_1 and B_2) reaction with tyramine under excitation with UV light 254 nm (A_1 and B_1) and under visible light (A_2 and B_2); right: fluorescence spectra of unreacted and reacted (with 210 µM tyramine) CA-Py-1 nanofiber mats, respectively (λ_{em}= 588 nm for excitation and λ_{exc}= 517 nm for emission spectra; the excitation spectrum of the unreacted dipstick is omitted for clarity).

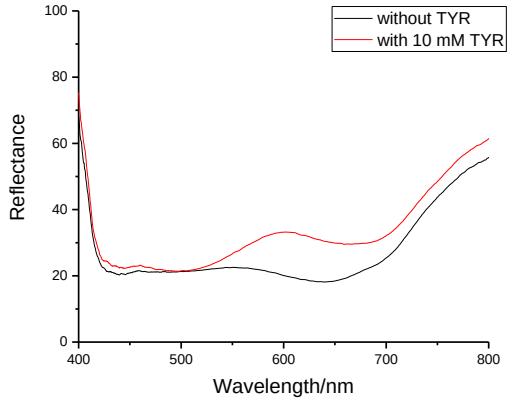

Fig. 5. Change of reflectance spectra of dipsticks upon reaction with 10 mM TYR.

3.4.3 Assay Procedure for Quantitation of BAs

A simple assay protocol was developed (Fig. 6) using the optimized nanofiber mats in a dipstick format for the fluorimetric detection of BA. Nanofiber mat circles (Ø = 8 mm) were cut and fit into a multi stick holder to enable the readout of multiple dipsticks in a row under the same conditions for fluorescence excitation and detection. The mats are surrounded by black solvent resistant plastic to suppress stray light and ensure an even dark background when acquiring the digital images. As the extracts of BAs from real samples are typically delivered in an aqueous/alcoholic mixture and this environment assists in the even distribution of the small BA volume over the fiber mat, the stick holder was located in an ethanol chamber after addition of BA (in CHES buffer, pH 9.5). After spreading, the spots were dried at ambient air (20 min). Then again, the holder was placed into the ethanol chamber for color development (20 min). It should also be noted that it is known from earlier work that the BA conjugation with Py-1 works more rapid and reproducible in an alcoholic environment and the emission of the conjugate is brighter when derivatized in an alcohol [26].

The incubation time of the BA determination was studied in more detail using fiber mats with three different electrospinning times (15, 30, 60 min).

Digital images in RAW-format were taken each 5 min under fluorescence excitation by a UV-lamp at 254 nm under a 50° illumination angle. The intensity of the red, green, and blue channel was extracted via Adobe Photoshop CS6 software. Data from the red channel contained the emission intensity information of the amine-Py-1 conjugate. The blue channel contained the low emission intensity information from the PET support of the ITO sheet. Finally, the intensity of the red channel was divided by the one of the blue channel and the red-to-blue intensity ratio was used as a parameter for BA detection. Using excitation by a UV-lamp for dipstick assays containing Py-1 is new and was never described in earlier publications, so far. This omission of a noncommercial excitation source further simplifies the assay procedure and makes it amenable to less qualified users which is beneficial for rapid diagnostic test procedures.

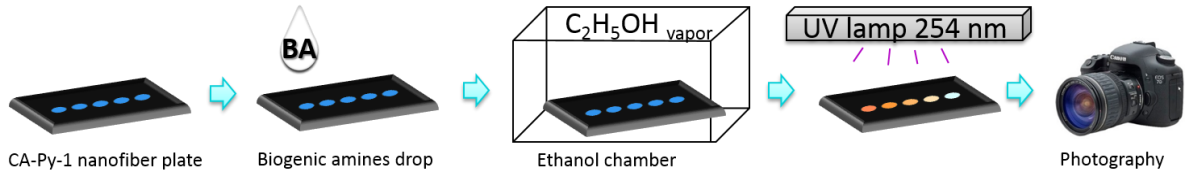

Fig. 6. Schematic of the fluorimetric BA assay using a multi- stick holder.

The ratio of the luminescence found in the red to the blue channel of the digital image of replicate tests was followed over time. As can be seen from Fig. 7 the development of the change of the fluorescence takes 35-40 minutes after addition of the BA. Over the first 20 min after BA addition, the drop is spreading (1 min) and the fluorescence intensity ratio is almost constant over the remaining time. After 20 min, there is a pronounced increase of the R/B signal for about additional 20 min. At incubation times longer than 40 min (after addition of the BA drop) no further significant increase in signal is observed. Further analyses were therefore done using a 40 min overall incubation time.

Furthermore, a significant increase in the fluorescence intensity ratio with development in the ethanol vs. ambient air chamber is noted, as expected, based on earlier results using polymer films [26]. Electrospinning time only modestly affects the increase of the luminescence intensity ratio of the dipstick tests over the whole incubation time and the highest increase is found for the fiber mats with 30 min spinning time. Small variations in spinning time will therefore not negatively affect the reproducibility of the assay.

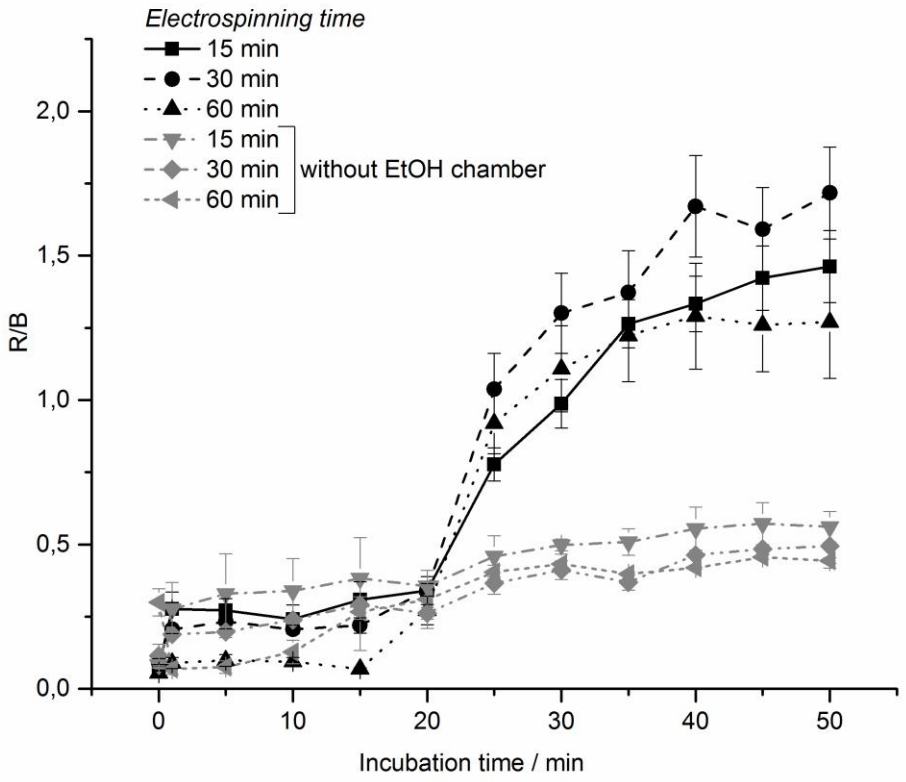

Fig.7. Effect of incubation time on luminescence response (expressed as R/B-ratio) of dipstick assays upon addition of tyramine (c(TYR) = 1 mM); 0-20 min: drying of sensing spot after BA addition; 20-50 min: color development (n=3).

3.4.4 Calibration and Sensitivity

The effect of different BA concentrations on the luminescence intensity ratio of the dipstick assay was studied with tyramine as a model. The calibration curves for fiber mats with three different electrospinning times (15, 30, 60 min) are shown in Fig. 8. We used 8 concentrations of tyramine (0.01; 0.025; 0.05; 0.1; 0.25; 0.5; 0.75; 1.0 mM) and three replicates for each concentration. The R/B fluorescence intensity ratio is well linear proportional to the concentration of tyramine in the range from 10.0 to 100 µM of tyramine, as shown in the inset of Fig. 8. This is lower by about one order of magnitude compared to sticks consisting of a kinfe-coated polymer membrane with Py-1 [21]. The signal increase reaches saturation at 250 µM of tyramine. The LOD is defined as the analyte concentration yielding a red/blue (R/B) signal equal or higher than the average value produced by the blank sample plus three standard deviations. The LOD of Tyramine is 0.009 mM using a mat with 15 min of electrospinning, 0.003 mM for 30 min and 0.006 mM for 60 min of electrospinning, respectively. These LODs are lower by up to a factor of 6 compared to earlier work [21]. Parameters of the calibration curves for tyramine detection are shown in table 2. The correlation coefficients are on a comparatively high level considering that rapid diagnostics tests such as dipstick assays always show less reproducibility than sophisticated instrumental detection methods. Compared to earlier data [21] with R^2 from 0.92-0.95 the dipstick assays based on electrospun nanofibers show considerable better perfomance. The slope of the calibration plots slightly increase with electrospinning time. This behaviour could be expected because the thickness and density of the nanofiber mat increase with spinning time. This means that more reactive Py-1 is available per surface area and therefore can lead to a higher change of the luminescence intensity ratio. As to their luminescence response, the mats are stable for more than 3 months (longer times could not be tested, yet).

Table 2. Parameters of calibration curves of tyramine detection

Electrospinning time, min	**Equation of calibration curve**	**R^2**
15	y = 11.26x + 0.416	0.98
30	y = 11.803x + 0.522	0.96
60	y = 12.027x + 0.503	0.98

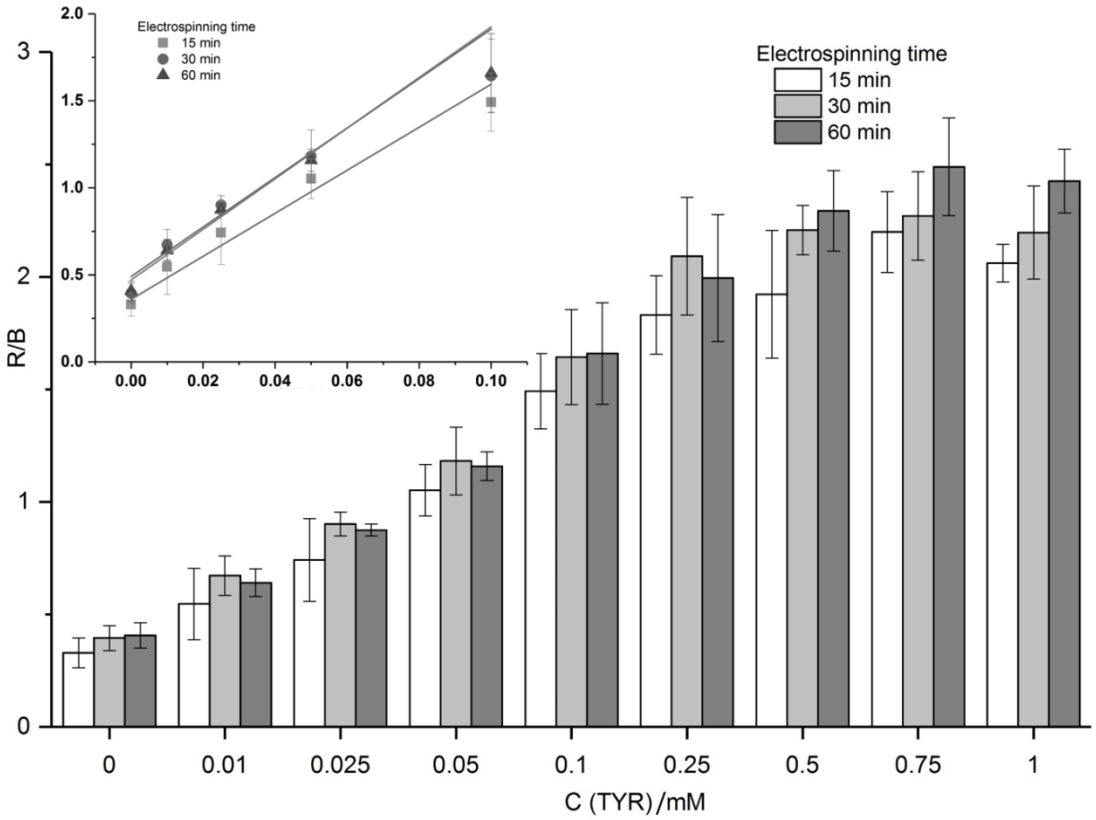

Fig. 8. Response of CA-Py-1 nanofiber based tests to different tyramine concentrations, the insert shows the calculated calibration curves (n=3).

The concentration range of BAs relevant to induce health risks is between 0.3 and 1.0 mM. BAs in concentrations below 1.0 mM are not detectable by the

human nose in most cases but may be indicative of food spoilage and, hence, represent a health risk [21]. The linear range of the determination of tyramine with the dipsticks using luminescent electrospun nanofibers therefore is just below this critical range of interest. This is advantageous because low but uncritical concentrations as e.g. naturally occurring in shrimp [21] can be detected as well as increasing concentrations over prolonged storage. The latter case might require appropriate dilution during sample preparation, as described in the experimental section.

3.4.5 Selectivity Studies

The selectivity of the new CA-Py-1-nanofiber-based dipstick assays were tested with the following amines: tyramine, histamine, cadaverine, spermidine, putrescine, 2-aminoethylmethacrylate, dimethylamine, triethylamine. These particular amines were chosen to cover monoamines and polyamines as well as aliphatic, aromatic, and heteroaromatic amines. We added BAs in an excess concentration (10 mM) and acquired the fluorescence intensity ratio readout of digital images for the mats obtained with different spinning times (i.e. thickness). As can be seen from Fig. 9, the nanofiber mats selectively respond to primary amines but not to secondary or tertiary amines. This is comparable to earlier findings with Py-1 embedded in other polymers [25, 27]. On comparing the average R/B signals of tyramine, histamine, cadaverine, spermidine, putrescine, 2-aminoethylmethacrylate, respectively, at the same spinning times, it is noted that the fiber mats with a 30 min spinning time respond most comparably to the presence of different BAs. This is further confirmed from the average relative standard deviations (RSDs) of the R/B values calculated for those BAs for the same spinning time which are 21.5%, 16.5%, 17.3% for 15, 30 and 60 min, accordingly. This suggests the applicability of the mats to detect

the overall concentration of various BAs in real samples and that they can be used as a pre-screening tool to determine the total amine content (TAC) in real samples before more advanced analytical methods are applied to determine individual concentration of each BA in a sample.

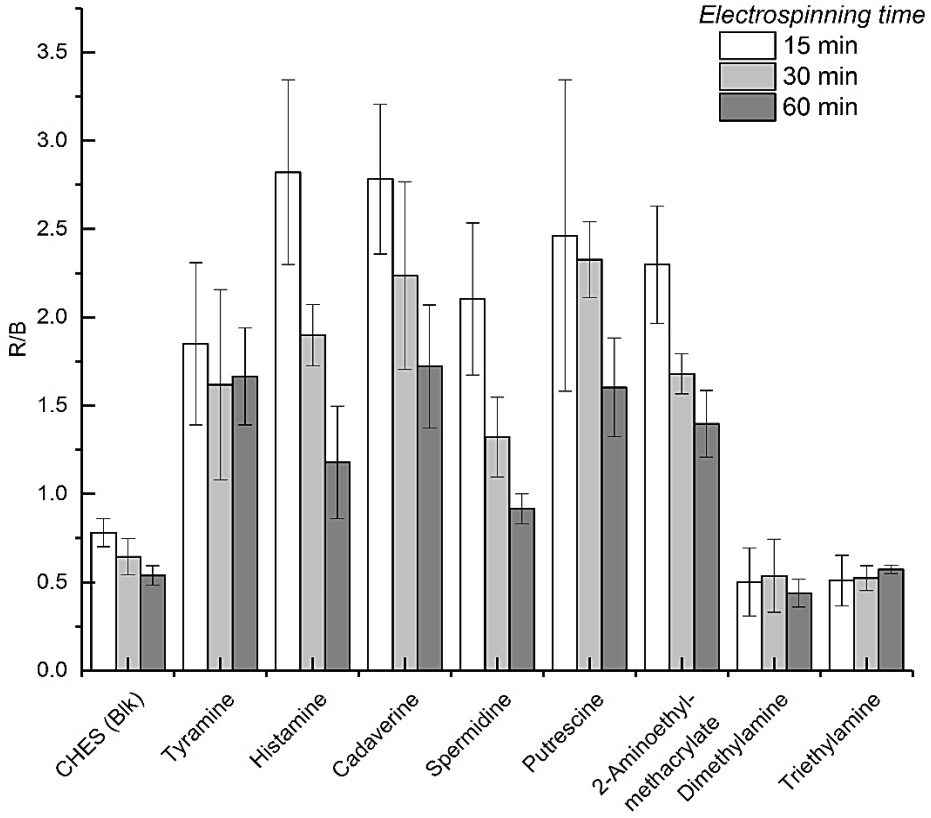

Fig. 9. Selectivity of the dipstick assays (obtained with various spinning time) towards various types of amines in 10 mM concentration (n=3).

3.4.6 Quantitation of BAs in Real Samples

We finally tested the response of the dipsticks to BAs in shrimp samples over a 6 day storage period at 4°C. The extraction of the shrimp samples follows the AOAC method 35.1.32 [28] and a standard addition method was applied. We choose histamine as BA to be added because it commonly accounts for the

major fraction of all BAs contained in real meat or seafood samples [29]. As the mats spun for 30 min respond quite similar to various BAs (Fig. 9), the overall variation of the R/B response of the dipsticks induced by the presence of various BAs in a real sample was regarded acceptable. Hence, all BAs in the sample will contribute to the fluorescence response of the dipstick and are expressed in equivalents of histamine, similarly as done in earlier work [10, 30]. We found concentrations of 14.1±0.3 µmol/g, 16.4±1.5 µmol/g and 38.8±2.6 µmol/g (n=4, each) of histamine, on days 0, 3 and 6, respectively. The slow increase of the BA concentration over 3 days and a distinctly higher content after 6 days of storage correspond well with ageing profiles of real samples found in earlier work [31] and show the suitability of the dipsticks for BA quantitation in real samples.

3.5 Conclusion

New dipsticks using multimodal electrospun nanofibers for the determination of BAs with inexpensive instrumentation for chromogenic, fluorescence or reflectance detection are presented. The nanofibers are based on cellulose acetate doped with the amine-reactive Py-1 dye. The readout can be done fluorimetrically upon excitation with a simple UV-lamp with a digital camera using the intensity ratio of the red versus the blue channel. The dipstick assay selectively responds to primary amines and is more sensitive by about one order of magnitude towards tyramine with respect to linear range and LOD than those based on a polymer film. On the one hand, the dipstick assay can be used for simple yes/no analysis by the naked eye or it allows semi-quantitative evaluation via comparison to a calibration color scale or using reflectance spectrometry. These sensitive tests can therefore be used for rapid determination of the total content of biogenic amines detection in food. This work

demonstrates that the main advantage of using electrospun nanofibers as an immobilization matrix in rapid tests is a higher sensitivity and a lower consumption of the reagent for BAs due to the high porosity and surface area of the fiber mat that can improve the optical response of dipsticks.

3.6 References

1. Bedia Erim F. Recent analytical approaches to the analysis of biogenic amines in food samples. Trends Anal Chem. 2013; doi: 10.1016/j.trac.2013.05.018
2. Kalac P, Gloria MBA. Biogenic amines in cheeses, wines, beers and sauerkraut. In: Dandrifosse G, editor. Biological Aspects of Biogenic Amines, Polyamines and Conjugates. Scarborough: Research Signpost; 2009, pp. 267-310.
3. Fogel WA, Lewinski A, Jochem J. Histamine in food: Is there anything to worry about?. Biochem Soc Trans. 2007; doi: 10.1042/BST0350349
4. Özdestan Ö, Üren A. A method for benzoyl chloride derivatization of biogenic amines for high performance liquid chromatography. 2009; doi: 10.1016/j.talanta.2009.02.001
5. He L, Xu Z, Hirokawa T, Shena L. Simultaneous determination of aliphatic, aromatic and heterocyclic biogenic amines without derivatization by capillary electrophoresis and application in beer analysis. J Chromatogr A. 2017; doi: 10.1016/j.chroma.2016.12.067
6. Önal A. A review: current analytical methods for the determination of biogenic amines in foods. Food Chem. 2007; doi: 10.1016/j.foodchem.2006.08.028
7. Marcobal A, Polo MC, Martín-Alvarez PJ, Moreno-Arribas MV. Biogenic amine content of red Spanish wines: comparison of a direct ELISA and an

HPLC method for the determination of histamine in wines. Food Res Int. 2005; doi: 10.1016/j.foodres.2004.10.008

8. Luo L, Xu ZL, Yang JY, Xiao ZL, Li YJ, Beier RC, Sun YM, Lei HT, Wang H, Sheng YD. Synthesis of novel haptens and development of an enzyme-linked immunosorbent Assay for quantification of histamine in foods. J Agric Food Chem. 2014; doi: 10.1021/jf504689x
9. Bidmanova S, Steiner MS, Stepan M, Vymazalova K, Michael A. Gruber M, Duerkop A, Damborsky J, Prokop Z, Wolfbeis OS. Enzyme-Based Test Strips for Visual or Photographic Detection and Quantitation of Gaseous Sulfur Mustard. Anal Chem. 2016; doi: 10.1021/acs.analchem.6b01272
10. Khairy GM, Azab HA, El-Korashy SA, Steiner MS, Duerkop A. Validation of a Fluorescence Sensor Microtiterplate for Biogenic Amines in Meat and Cheese. J Fluoresc. 2016; doi: 10.1007/s10895-016-1885-1
11. Huang X, Li Z, Zou X, Shi J, Mao H, Zhao J, Hao L, Holmes M. Detection of meat-borne trimethylamine based on nanoporous colorimetric sensor arrays. Food Chem. 2016; doi: 10.1016/j.foodchem.2015.11.041
12. Diaz YJ, Page ZA, Knight AS, Treat NJ, Hemmer JR, Hawker CJ, Alaniz JR. A Versatile and Highly Selective Colorimetric Sensor for the Detection of Amines. Chem Eur J. 2017; doi: 10.1002/chem.201700368
13. Schaude C, Meindl C, Fröhlich E, Attard J, Mohr GJ. Developing a sensor layer for the optical detection of amines during food spoilage. Talanta. 2017; doi: 10.1016/j.talanta.2017.04.029
14. Nedeljko P, Turel M, Lobnik A. Hybrid sol-gel based sensor layers for optical determination of biogenic amines. Sens Actuat B. 2017; doi: 10.1016/j.snb.2017.02.011
15. Sutarlie L, Yang KL., Colorimetric responses of transparent polymers doped with metal phthalocyanine for detecting vaporous amines. Sens Actuat B. 2008; doi: 10.1016/j.snb.2008.07.011

16. Roales J, Pedrosa JM, Guillén MG, Lopes-Costa T, Pinto SMA, Calvete MJF, Pereira MM. Optical detection of amine vapors using ZnTriad porphyrin thin films. Sens Actuat B. 2015; doi: 10.1016/j.snb.2014.12.080
17. Wöllner K, Vollprecht M, Leopold N, Kasper M, Busche S, Gauglitz G. Interaction behaviour of a PDMS-calixarene system and polar analytes characterised by microcalorimetry and spectroscopic methods. Anal Bioanal Chem. 2007; doi: 10.1007/s00216-007-1600-9
18. Rawat KA, Bhamore JR, Singhal RK, Kailas SK. Microwave assisted synthesis of tyrosine protected gold nanoparticles for dual (colorimetric and fluorimetric) detection of spermine and spermidine in biological samples. Biosens Bioelectron. 2017; doi: 10.1016/j.bios.2016.07.069
19. Chopra S., Singh A., Venugopalan P., Singh N., Kaur N. Organic Nanoparticles for Visual Detection of Spermidine and Spermine in Vapors and Aqueous Phase. ACS Sustainable Chem. Eng. 2016; doi: 10.1021/acssuschemeng.6b01295
20. El-Nour KMA, Salam ETA, Soliman HM, Orabi AS. Gold Nanoparticles as a Direct and Rapid Sensor for Sensitive Analytical Detection of Biogenic Amines. Nanoscale Res Lett. 2017; doi: 10.1186/s11671-017-2014-z
21. Steiner MS, Meier RJ, Duerkop A, Wolfbeis OS. Chromogenic Sensing of Biogenic Amines Using a Chameleon Probe and the Red−Green−Blue Readout of Digital Camera Images. Anal Chem. 2010; doi: 10.1021/ac102029j
22. Matlock-Colangelo L, Baeumner AJ. Biologically Inspired Nanofibers for Use in Translational Bioanalytical Systems. Ann Rev Anal Chem. 2014; doi: 10.1146/annurev-anchem-071213-020035

23. Mercante LA, Scagion VP, Migliorini FL, Mattoso LHC, Correa DS. Electrospinning-based (bio)sensors for food and agricultural applications: A review. Trends Anal Chem. 2017; doi: 10.1016/j.trac.2017.04.004
24. Azab HA, El-Korashy SA, Anwar ZM, Khairy GM, Duerkop A. Reactivity of a Luminescent "off-on" Pyrylium Dye Towards Various Classes of Amines and its use in a Fluorescence Sensor Microtiter Plate for Environmental Samples. J. Photochem. Photobiol. A. 2012; doi: 10.1016/j.jphotochem.2012.05.029
25. Wetzl BK, Yarmoluk SM, Craig DB, Wolfbeis OS. Chameleon Labels for Staining and Quantifying Proteins. Angew. Chem. Int. Ed. 2004; doi: 10.1002/anie.200460508
26. Steiner MS, Meier RJ, Spangler C, Duerkop A, Wolfbeis OS. Determination of Biogenic Amines by Capillary Electrophoresis Using a Chameleon-Type of Fluorescent Stain. Microchim. Acta. 2009; doi: 10.1007/s00604-009-0247-y
27. Caro B, Guen-Robin FL, Salmain M, Jaouen G. 4-Benchrotrenyl Pyrylium Salts as Protein Organometallic Labelling Reagents. Tetrahedron. 2000; doi: 10.1016/S0040-4020(99)00947-3
28. AOAC. AOAC Official Methods of Analysis. th ed.16 Washington; AOAC, 1995. Method 35.1.32.
29. Stadnik J, Dolatowski ZJ Biogenic amines in meat and fermented meat products. Acta Sci Pol Technol Aliment. 2010;9:251–63.
30. Alonso-Lomillo MA, Dominguez-Renedo O, Matos P, Arcos-Martinez MJ. Disposable biosensors for determination of biogenic aminesAnal . Chim Acta. 2010; doi: 10.1016/j.aca.2010.03.012
31. Azab HA, El-Korashy SA, Anwar ZM, Khairy GM, Steiner MS, Duerkop A. High-Throughput Sensor Microtiter Plate for Determination of Biogenic

Amines in Sea Food using Fluorescence or Eye-Vision. Analyst. 2011; doi: 10.1039/C1AN15049A

4 Dipsticks with Reflectometric Readout of an NIR Dye for Determination of Biogenic Amines

4.1 Abstract

Electrospun nanofibers (ENFs) are great analytical tools for quantitative analysis since they are inexpensive, easily produced in uniform homogenous mats and provide a high surface-area to volume ratio. Additionally, a high immobilization efficiency of an optical indicator as recognition element inside ENFs leads to high sensitivity and promotes a relatively fast response of the sensor membrane formed. We therefore show for the first time the use of an NIR-dye as chemosensor inside ENFs on dipsticks for the detection of biogenic amines (BAs) in food. For this purpose, cellulose acetate (CA) fibers were doped with the chromogenic and fluorogenic amine-reactive chameleon dye S0378 and electrospun into uniform mats. The free form of the dye is green and the dye-BA conjugate is blue. The reaction of the S0378 dye with various primary amines was monitored by reflectance measurements at 635 nm where the intrinsic absorption of biological material is low. The difference of the reflectance before and after the reaction is proportional to BA levels that can induce food poisoning but are not accessible to the human nose. The dynamic range for histamine detection is 0.1–1 mM. The dipsticks are selective to primary amines (no matter if mono or diamines) and show low interference towards most nucleophiles. A minute interference of proteins in real samples can be overcome by appropriate sample pretreatment. Hence, the ageing of seafood samples could be followed via their TAC (total amine content) via standard addition. This demonstrates that optically doped ENFs represent viable sensor and transducer materials for food analysis with dipsticks.

This chapter is intended for submission in Chemosensors.

Author contributions:

The experimental work and writing the manuscript was carried out by Sarah Mobarez. The article was revised by the Sarah Mobarez and Axel Duerkop who is corresponding author and leader of this project. Antje J. Baeumner contributed with strategic discussions. Nongnoot Wongkaew and Marcel Simsek contributed with useful discussions and sharing skills and experience especially for data analysis.

4.2 Introduction

Biogenic amines (BAs) are important compounds that can determine the quality of food [1]. High levels of amines in food are produced by bacterial decarboxylation of amino acids and have been recognized as an important reason for seafood intoxication [2]. Hence, the determination of biogenic amines concentration in fresh food is in high need to determine its freshness status. Papageorgiou and co-workers gave a review on food and beverage products that should be regularly tested since they contain BAs or may develop certain contents over (storage) time [3]. This raises interest in research on rapid and inexpensive optical detection methods and tools like dipsticks to determine BAs in food, not only for individual concentration levels but also as a sum parameter. According to the European Food Safety Authority (EFSA), the U.S. Food and Drug Administration (FDA) as well as the World Health Organization (WHO) there are limits for BA concentrations in food to control the food quality. Histamine is one of the most bioactive and toxic BAs. Histamine exists in the majority of foods and plays an important role in food intolerances [4]. If the histamine concentration in food exceeds 500 ppm there is a high risk for food poisoning [3]. 5-10 mg of histamine might induce skin irritation, rashes, dilatation of peripheral blood vessels resulting in hypotension and headache, or contractions of intestinal smooth muscles causing diarrhoea and vomiting [5]. 10 mg is regarded a borderline for toxicity and 100 mg can result in medium toxic responses and 1000 mg is considered as very toxic [3].

Optical detection of BAs is challenging because those are weak absorbers of visible light as most of them lack conjugated aromatic π-electron systems. The solution to this problem can be labelling or derivatization of BAs with chromophores or fluorophores. Additionally, the analyte has to be extracted from out of a complex matrix in food analysis. Therefore, the combination of separation techniques such as GC, HPLC or capillary electrophoresis with

optical, electrochemical or mass spectrometric detection after BA derivatization was used, recently [6–10]. Eventually, ELISAs [11] are used for BA determination in food samples. Those are highly selective and sensitive on the one hand but expensive, time consuming, and require highly trained staff, on the other hand. Nevertheless, extraction and purification steps are still required for sample preparation. In order to overcome these limitations, reasonably fast, low-cost and portable chemo and biosensors are desired for rapid on-site analysis of BAs in food [12].

Frequently, chromogenic and fluorogenic dyes, such as acid-base indicators [13–15], porphyrins [16] , phthalocyanines [17], chameleon dyes [18, 19], coumarin derivatives [20], azo dyes [21] or nanomaterials are applied for optical BA determination. Cellulose-based microparticles bonded with a pH-indicator and a blue reference dye yielded in slow traffic light-responding (1.5 h) colorimetric sensors [15]. Another study described the highly specific and sensitive detection of histamine in mackerel using TLC with visualization by spraying the sheets with ninhydrin and diazonium reagents [22]. Further, an array of five pH-indicators was shown to respond quickly (10 min) and to differentiate between isobutylamine, triethylamine, isopentylamine in ppm concentrations range via RGB readout using a mobile phone [14]. Unlike arrays, dipsticks only need a one-point readout and are therefore much quicker and easier to be read and thus deliver their response much faster. The development of dipsticks is beneficial since they are practical, simple, portable, easy to use and thus do not require trained staff. Moreover, they have a much lower cost compared to instrumental methods of analysis [13]. In addition to that, colorimetric sensing of BAs using dipsticks provides a simple response based on the color change and this leads to a yes/no answer besides the quantitative analysis [18].

Direct sensing of BAs was recently carried out using a filter paper-based dipsticks containing an amine-reactive chromogenic probe and a reference dye. Quantitative determination of BAs could be successfully achieved either visually based on a color change or via luminescence. Digital images of the luminescence of sensor spots were taken and the BA concentrations were derived from the red-to-green intensity ratio via image J software. [18]. As an alternative sensor concept to paper as support for the hydrogel carrying the sensing matrix we employed electrospun nanofibers on ITO sheets. Dipsticks containing these nanofiber mats showed an up to six-fold higher sensitivity compared to those based on hydrogel sensor membranes containing the same dye [23]. This is due to the high surface area to volume ratio and the high porosity of electrospun nanofibers. Moreover, electrospun nanofibers were designed such that they were counter-charged with respect to BAs so to achieve an additional enrichment effect.

Reflectometric detection of optical sensors raises interest, since it is a fast and simple technique. Reflectometric sensors require a light source (which could be an inexpensive LED), a filter to select the detection wavelength and a detector (which can be a low-cost digital camera). Evaluation of data can be then carried out by free available software). Hence, a complete sensor (array) can be obtained for a few hundred US-$ or less including detection equipment. BA sensing was carried out reflectometrically by a digital camera and data were analyzed using the color space of the CIE system. These sensors were applied for quantitation of various amines and ammonia produced during food ageing in food packages. Fish freshness was monitored reflectometrically using a colorimetric sensor of creatine in the fish body which is an indicator for the fish ageing [24].

We now intended to simplify our dipsticks compared to earlier research by choosing sensor layers that only contain one dye instead of two. Moreover,

we wanted to simplify the detection of the optical signal by choosing reflectometry instead of having a two-step process of a) making a digital image and b) converting its data into concentration-dependent intensities by a software. Finally, we intended to shift the detection wavelength much further to the NIR-range, because most real samples show less self-absorption and scatter in this wavelength region. Thereby, we expected to gain further improvements regarding resolution and a reduced background in real samples.

In this work, we use for the first time an NIR chromogenic dye that is reactive to BAs and embedded into a mat of electrospun nanofibers to form reflectometric dipstick sensors. The electrospun nanofibers made from cellulose acetate (CA) are prepared by a simple standard electrospinning procedure and contain the S0378 cyanine dye which absorbs at 800 nm. Primary amines react with the dye by an S_N1 nucleophilic substitution mechanism which is accompanied by a color change from green to blue. Hence, the concentration of BAs can be determined based on reflectance detection which a simple and fast readout. The equal response towards monoamines and diamines makes the dipsticks an ideal tool for determination of the total amine content (TAC) in real samples which was demonstrated by monitoring the ageing of shrimp samples over time.

4.3 Materials and methods

4.3.1 Materials

S0378 was from FEW Chemicals (www.few.de). The buffer N-cyclohexyl-2-amino ethanesulfonic acid (CHES) was from Roth (www.carlroth.de). Spermidine (SPR), putrescine (PUT), and histamine (HIS) were purchased from Sigma-Aldrich (www. sigmaaldrich.com), all as hydrochloride salts. Tyramine (TYR), Cysteine (CYS), Triethylamine (TEA) and dimethylamine, each as free base, were from Sigma, Mann research laboratories, Merck and Fluka

respectively. Cellulose acetate (CA) (Mw 30,000 Da, 39.8 wt% acetyl content) and human serum albumin (HSA) and all organic solvents (methanol, acetic acid and acetone) were obtained from Sigma-Aldrich. All chemicals were of analytical grade. Indium tin oxide (ITO) coated on polyethylene terephthalate (PET) with a surface resistivity 60 Ω/sq and 127 µm thickness was purchased from Sigma-Aldrich. Stock solutions of BA (10.0 mM) were prepared in CHES buffer (pH 9.7). Standard solutions of the BAs were freshly prepared by diluting stock solutions with CHES buffer. CHES buffer (5.00 mM) was prepared by dissolving of solid CHES (0.1036 g) in 100.0 mL of deionized water. The pH of CHES was adjusted with sodium hydroxide solution (1.00 M, from Merck (www.merckgroup.com)).

4.3.2 Apparatus

The electrospinning was performed using a home-built electrospinning setup (see figure S1) with an iseg T1 CP300p high voltage power supply (www.iseg-hv.com) and a syringe pump. Fiber mat thickness, fiber diameter, and images for pore size determination were obtained by a scanning electron microscope (Zeiss/LEO 1530, Germany) at 5.0 kV. Samples for SEM were cut with a pair of scissors and sputtered with gold for 30 s (≈ 7 nm layer thickness).

Reflectance spectra were acquired with an AB2 luminescence spectrometer with a 150 W xenon light source. The light was guided to the dipstick by a y-shaped bifurcated optical fiber, a fiber holder and the samples were illuminated under an average illumination angle of 33°. The inner central fiber bundle at the tip of the bifurcated optical fiber collects the reflected light from the dipstick and guides it back into the spectrometer. Two wavelengths (650 and 635 nm) were used for illumination and the dipsticks were placed in home-made black plastic holders below the tip of the optical fiber to ensure a flat and reproducible positioning of the dipsticks with respect to the incident

light beam. The distance between the dipstick and the tip of the optical fiber is small (3 mm) to increase the collected reflected light and improve the sensitivity. The measurements were done in synchronous mode of the spectrometer i.e. the emission was measured at the same wavelength as the excitation. The band passes are 4 nm for both, excitation and emission.

The absorbance spectra were acquired on a Varian Cary 50Bio photometer in quartz cells. The emission spectra were obtained using the AB2 luminescence spectrometer equipped with a cell holder with 90° arrangement of excitation and emission beam and no fiber optic. The excitation wavelength was 600 nm and the bandpasses for excitation and emission were 4 nm and 8 nm, respectively.

4.3.3 Electrospinning of S0378-CA fibers

The polymer CA (0.720 g) and S0378 (30.00 mg) were dissolved in a mixture of 3.00 mL of acetic acid and of 1.00 mL of acetone. Then, this spinning dope is first sonicated at room temperature for 30 min, then at 40° C for another 30 min and finally stirred for about 1 h until the mixture is completely homogeneous. The spinning dope is protected from light by Al-foil while stirring, storage, and electrospinning. The CA-S0378 electrospun nanofibers were fabricated using the electrospinning setup with the following parameters: Spinning dope in plastic syringe 5 mL (covered with aluminum foil); voltage 17 kV; flow rate 0.002 mL/min; tip-to-collector distance, 11 cm, 15 min spinning time. An ITO sheet (size 7 × 5 cm) was used as a supporting material. Electrospun fiber mats deposited on ITO should be stored in a desiccator.

4.3.4 Preparation of dipsticks and BA determination

The dipsticks with S0378-CA nanofibers (Ø = 8 mm) were cut from the ITO sheets with a toggle press from BERG & SCHMID (www.bergundschmid.de)

and placed on black, solvent-resistant plastic positioners. After that, 10.00 µL of either BA (in CHES buffer, pH 9.7) or extract from the real sample were added onto the spots. The reflectance was measured two times for each dipstick before and after the reaction with BAs. The reaction takes place at 130°C for 30 min in an oven.

4.3.5 Preparation of real samples

Histamine concentration in real samples is determined using methanolic extraction and a standard addition method for concentration determination. The extraction follows the AOAC method 35.1.32 [25] with slight modifications. Shrimp samples were purchased from a local supermarket and stored at −80 °C. A 10.0 g portion was mixed with 100 mL of methanol in a beaker and homogenized in a blender at the highest speed for 2 min. The homogenate was transferred into a conical flask and heated at 60 °C on a water bath for 30 min. 0.19 M Carrez solution I (potassium hexaferrocyanide) and 1.05 M Carrez solution II (zinc acetate) were prepared in distilled water. 2 mL of each Carrez solution was added to the shrimp extract before filtration of the homogenate for protein precipitation. The extract was filtered through a porcelain Buchner funnel with blue ribbon filter paper (Schleicher und Schüll: 589^3, www. whatman.com) twice to yield a clear solution. Then, different volumes were taken from the sample extract to achieve a suitable dilution factor on each ageing day and histamine solution was added to reach concentrations of 0–600 µM of added histamine after dilution to 500 µL overall volume with CHES buffer (5.00 mM; pH 9.7). After that, 10.00 µL of aliquot solutions were added onto dipsticks and the reflectance of each dipstick was measured, as indicated above.

4.4 Results and discussion

4.4.1 Choice of dye

The main idea of this work was to produce the first NIR-dye embedded electrospun nanofiber mats which act as sensor layers in dipsticks for visual and reflectometric evaluation of BAs. Upon reaction with BAs (from real samples) the embedded dye shows a color change from green (λ_{abs}^{max}= 800 nm) to blue (see figures 1 and 2). The S0378 dye was chosen because of its chameleon property and the reaction with the BA (e.g. tyramine) occurs in CHES buffer at pH 9.7. This pH is required to warrant a free electron pair to be present at the amino group of the BA for a nucleophilic attack at the electrophilic carbon atom in the center of the π-electron system of the cyanine dye. Then, the electron-withdrawing chloro group is replaced by the electron-donating amino group of the BA in an S_N1 reaction. This inexpensive cyanine dye was formerly used as long wavelength-absorbing protein label [26].

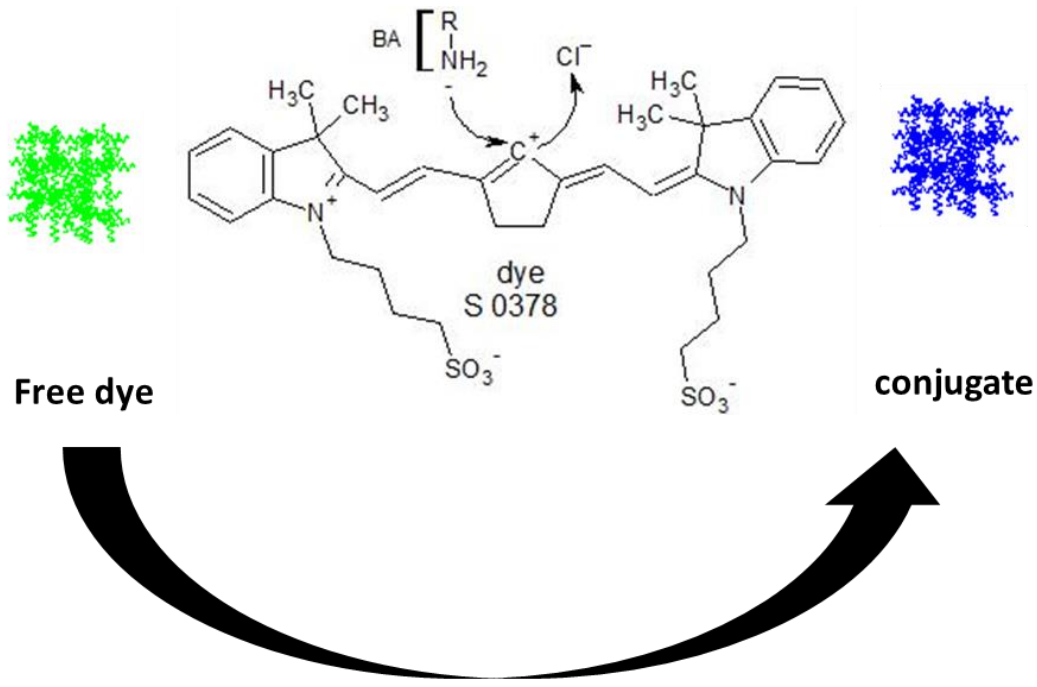

Fig. 1. Illustration of the reaction and of the color change of a mat of electrospun nanofibers containing the S0378 dye with biogenic amines.

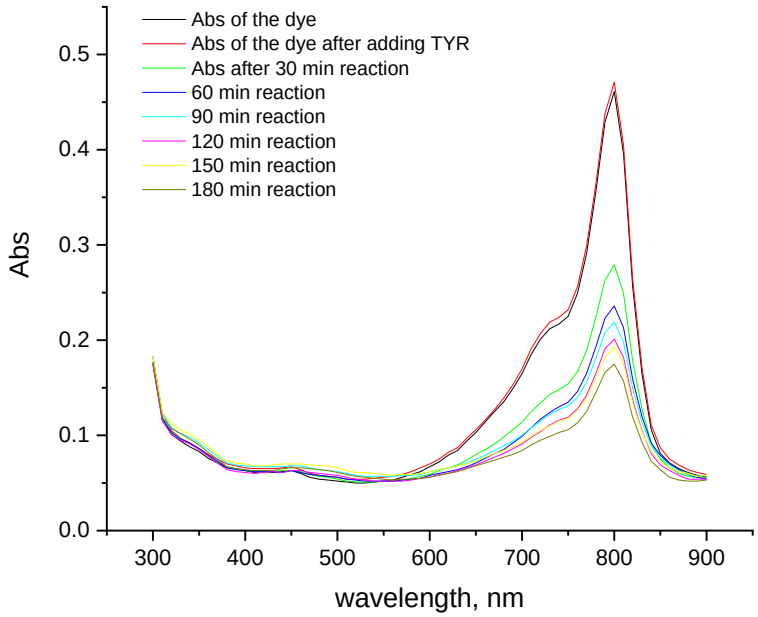

Fig. 2. Absorption spectra of 5 µM S0378 dye upon binding to 5 µM Tyramine at 80 °C over time in CHES buffer.

Furthermore, the emission maxima of S0378 at 663 nm and at 820 nm strongly decrease upon conjugation with BAs as shown in figure S2 Hence, the determination of BAs could be done by either fluorimetry or reflectometry. As we were aiming for a simple detection method suitable for the evaluation of dipsticks, reflectometry based on the color change was chosen in this work.

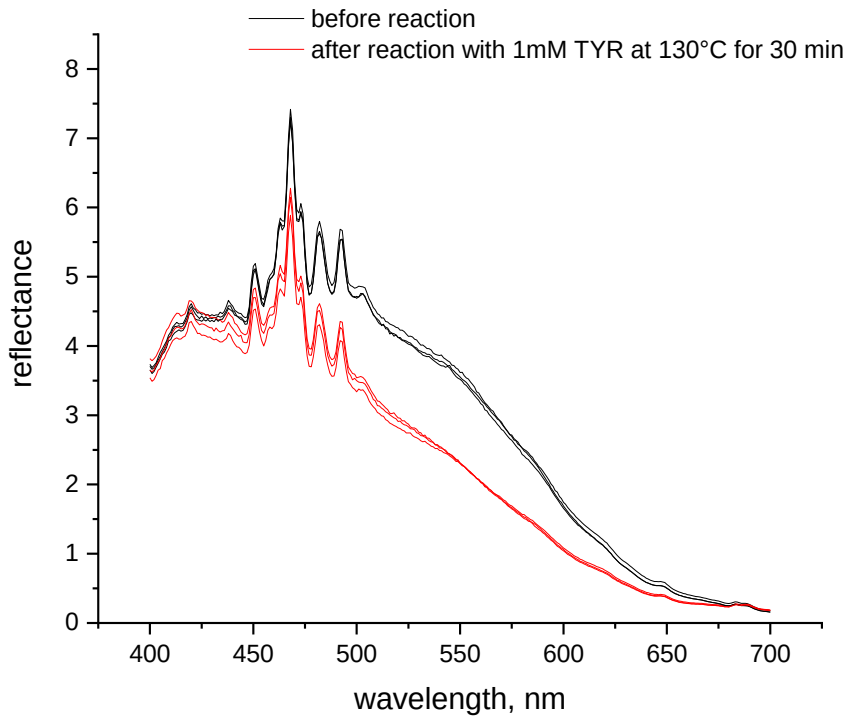

Fig. 3. Reflectance spectra of a mat of S0378-CA nanofibers on a dipstick in absence (red) and reacted with 1 mM of tyramine (n=3).

If the S0378 dye is spun into a fiber mat of CA polymer and reacted with tyramine, the reflectance spectra show an overall decrease (figure 3). The sharp peaks between 400 nm and 525 nm are the characteristic peaks of the xenon excitation lamp and hence instrumental artifacts. Therefore, a much longer detection wavelength closer to the absorption maximum of S0378 is advisable for the reflectance measurements. This is further supported by the fact that the self-absorption of biological matter strongly decreases at longer wavelengths, which in turn can lead to higher reflectance. Considering that it was intended to detect food extracts and the much higher reproducibility of the reflectance change at longer wavelengths we choose 650 nm for method optimization and 635 nm for quantitative reflectance detection in real samples.

4.4.2 Choice of nanofiber materials, conditions of spinning, reaction temperature and time, and fiber morphology

The spinning dope used for the electrospinning of the nanofibers was prepared by dissolving the S0378 dye and CA polymer in a solvent mixture of acetic acid and acetone. The electrospinning conditions, the polymer and the solvents used resemble those used in an earlier study [23] except for dye concentration and spinning time. The concentration of the dye molecules was increased in the same volume to enhance the sensitivity of the reflectance measurements. It was also tested if reducing of the spinning time to half the time (15 min) yields a more stable fiber mat and avoids detachment of the mat off the ITO sheet. Hence, the spinning time was varied between 15 min and 30 min and the dye concentration in the spinning dope between 7.5 mg/mL and 15 mg/mL. The effects on the change of the reflectance signal after a reaction of the fiber mat with histamine are shown in Fig. 4. Here, lower dye concentrations lead to lower changes of reflectance (Δ R). In all combinations of dye concentration and spinning time Δ R increases with increasing concentration of HIS. On comparing the change of Δ R at 0.8 mM of HIS with Δ R in absence of HIS there is not a too large difference among all the four combinations of dye concentration and reaction time. Therefore, a concentration of the dye in the spinning dope of 7.5 mg/mL and 15 min spinning time were chosen to save dye and time for preparation of the dipstick. Other spinning conditions did not provide a larger dynamic range in calibration plots for determination of BAs.

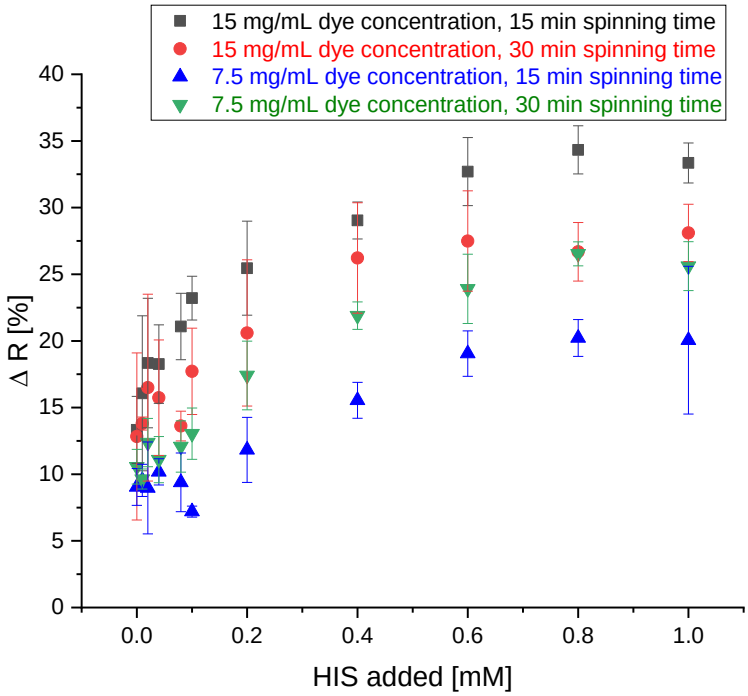

Fig. 4. Effect of dye concentration and spinning time on the change of reflectance of the dipstick at 650 nm upon reaction with HIS solutions of 0, 0.01, 0.02, 0.04, 0.08, 0.1, 0.2, 0.4, 0.6, 0.8, 1 mM, (n =4).

The reaction of S0378 dye and BAs on the dipsticks was allowed to develop at various temperatures after addition of histamine solution in CHES buffer (pH 9.7). Fig. 5 shows that the reaction between the dye embedded inside the electrospun nanofibers was carried out at 3 temperatures 70, 100, 130 °C for 30 min. The highest increase of the reflectance is observed at 130°C. As we were aiming to obtain a wide detection range and a more reproducible response of the dipsticks, the reaction with BAs was carried out at 130 °C in all subsequent measurements. Fig. S3 shows the response of the dipsticks after different development times (10, 20 and 30 min at 70°C). A development time of 30 min provided the highest change of reflectance and hence better sensitivity.

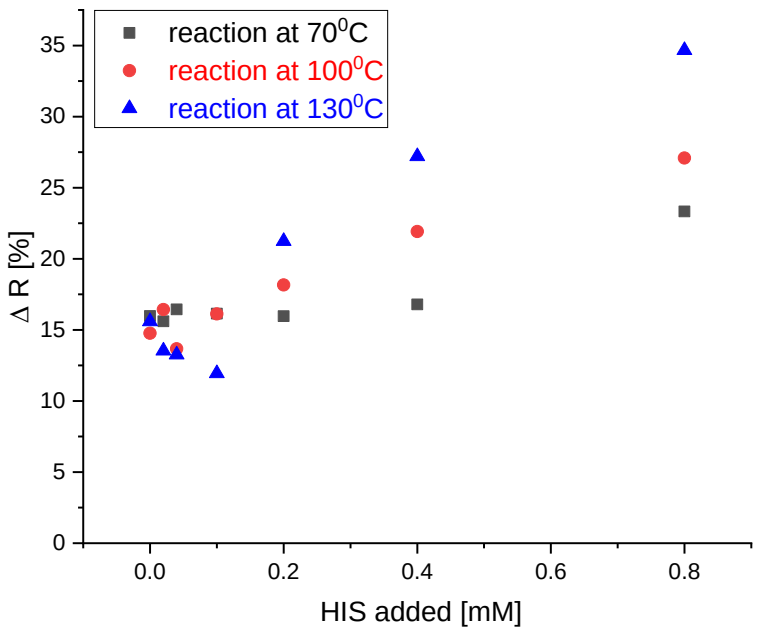

Fig. 5. Effect of reaction temperature on the reflectance of the dipstick at 650 nm to HIS solutions of 0, 0.02, 0.04, 0.1, 0.2, 0.4, 0.8 mM concentration (n=1).

Characterizations of fiber morphology with respect to fiber mat thickness, pore size, pore density, and diameter were performed by scanning electron microscope (SEM) images. An example of a nanofiber mat is displayed in Fig. 6. The thickness of the resulting fiber mat was determined to be 50.7 ± 8.4 µm. The pore sizes are 2.80 ± 0.15 µm as determined by the Feret diameter (example shown in Fig. S4) from 1330 pores. In addition, the density of pores is very high (~ 1.94×10^5 pores/mm^2), thus providing a great surface area for interaction with BAs. The average diameter of the fibers is 496 ± 318 nm (n=82). The fibers are round and have an overall shape of two fibers fused with one another (see figure S5). Hence, there is a short and a long axis to describe the fiber size, and the average ratio between the diameters along the short and long fiber axis is 0.62. This also explains the large standard deviation of the fiber diameter. The surface of the fibers is not smooth but rather undulated.

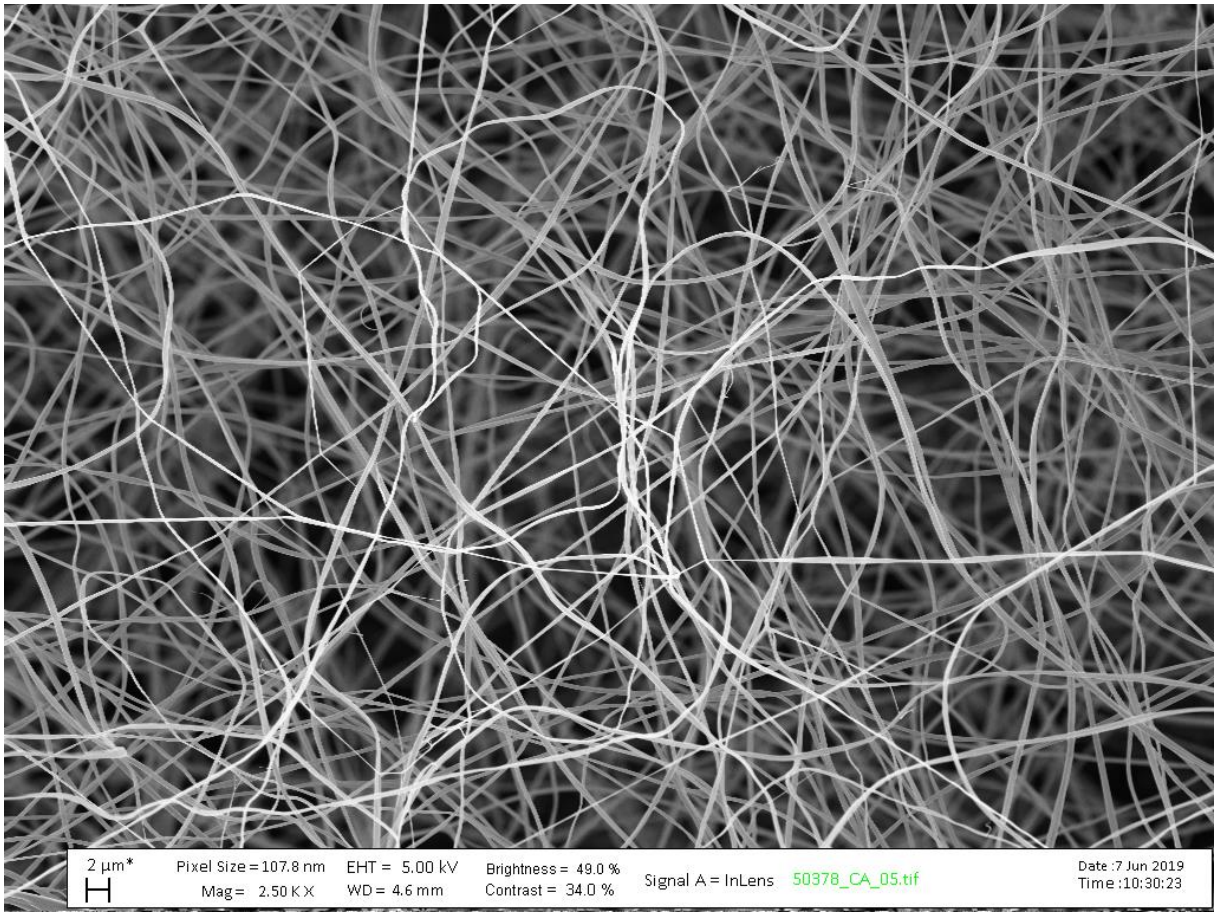

Fig. 6. Morphology of S0378-CA nanofibers electrospun for 15 min as taken by SEM with 2500-fold magnification.

4.4.3 Visible color change of dipsticks

The S0378-CA fiber mats on the dipsticks are greenish and turn blue upon the reaction with a primary biogenic amine (like histamine in aqueous solution of pH 9.5–10). This is due to the S_N1 nucleophilic substitution of the chlorine atom by the nitrogen atom of the BA. The blue color becomes more intense with increasing the BA concentration as shown in Fig. 7. This color change is most visible starting from a BA concentration 0.2 mM which nicely coincides with BA concentrations (0.3–1 mM) in foods that can induce serious health problems [18] but cannot be detected by the human nose. We chose reflectance detection based on the color change to determine BAs because it has a low instrumental demand and reasonable sensitivity. With an appropriate device at hand, in-field

use of the dipsticks seems feasible, eventually even with less qualified personnel, at a later stage of application. Further, reflectometry is the typical and well established method for evaluation of dipsticks and also the vision of the human eye is based on perception of reflected light.

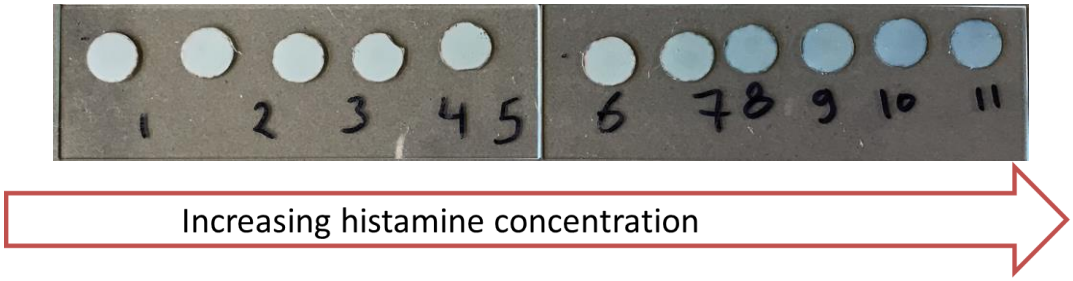

Fig. 7. Visible color change of dipsticks with S0378-CA nanofibers with histamine solutions of different concentrations at 130° C for 30 min. (1) blank solution (CHES buffer), (2) 0.02, (3) 0.04, (4) 0.06, (5) 0.08, (6) 0.1, (7) 0.2, (8) 0.4, (9) 0.6, (10) 0.8, (11) 1 mM, respectively, of histamine.

4.4.4 Assay procedure for quantitation of BAs

Nanofiber mat circles (Ø = 8 mm) were cut with a toggle press and placed on a positioning device made of black solvent resistant plastic to absorb stray light. The dipsticks were illuminated by a y-shaped bifurcated optical fiber (red light) at 33° illumination angle and the original reflectance of each dipstick was measured as shown in figures S6 und S7. A series of BA solutions of different concentrations was prepared and added onto the dipsticks for calibration. The real sample extracts were delivered to the dipsticks as a methanolic/aqueous mixture using the standard addition method. After adding of the BA solution onto the dipstick, the liquid was spreading all over the dipstick area. The dipsticks were then transferred to glass slides to allow the reaction with the S0378 dye embedded in the fibers to occur in an oven at 130°C for 30 min. Then, the reflectance of all dipsticks was measured again. The reflectance of each dipstick was measured before and after the reaction with BAs. This

considers potential differences of the reflectance of each dipstick originating from minute differences of the thickness of the fiber mats and of mispositioning. The percentage of the reflectance change was calculated by dividing the absolute difference of the dipstick reflectance before and after the reaction by the reflectance before the reaction multiplied by 100 %. The reflectance change (ΔR [%]) was then plotted against the concentration of the BA.

4.4.5 Calibration and sensitivity

The effect of different BA concentrations on the reflectance of the dipsticks was studied for four biogenic amines (spermidine, tyramine, putrescine, and histamine). Their calibration plots are shown in figures 8 and 9. We used eleven concentrations (blank, 0.01, 0.02, 0.04, 0.08, 0.1, 0.2, 0.4, 0.6, 0.8, 1 mM) to cover the whole dynamic range of the dipstick until the saturation of the change of reflectance was reached. Four replicates for each concentration were used. The calibration curves for all BAs are not linear but rather resemble saturation curves. The signal increase is steeper at lower concentrations (0-0.1 mM) than at higher concentrations (0.2-0.6 mM) and then the signal reaches saturation for all of the tested BAs at 0.6 mM, except histamine. The dynamic ranges are 0.04.-0.6, 0.08-0.60, 0.10-0.60, 0.10-1.0 mM for SPR, TYR, PUT, and HIS respectively. The LOD is the concentration which is corresponding to the blank signal plus three standard deviations. The LODs were found to be 30, 30, 80, 90 μM for SPR, TYR, PUT, and HIS respectively. The dynamic range and LOD of all BAs are shown in table 1. All BAs have a similar response and sensitivity, even though one could expect to see a higher sensitivity for the diamines like putrescine and spermidine. Obviously, the average distance to the proximate S0378 dye (embedded into either the same or neighbor fiber) is larger than the average length of the two BAs, so that no additional reaction occurs. Moreover,

the steric hindrance of the secondary amino group on a S0378-spermidine conjugate is obviously too high to get access to the rigid conjugated π-system of a neighboring NIR dye. Also, a further S_N1 reaction of the secondary amino group with another S0378 molecule seems to be prevented. The very similar response of the NIR dye to all BAs is very beneficial for its use in dipsticks. Those are intended as screening tools for the determination of the overall content of BAs in a sample. In this case, a very similar response (i.e. color change) of the dipsticks towards all BAs is beneficial to determine the sum content of all BAs, irrespective of their chemical structure. This will reduce potential errors that might occur from overestimation of the S0378 dye towards diamine BAs.

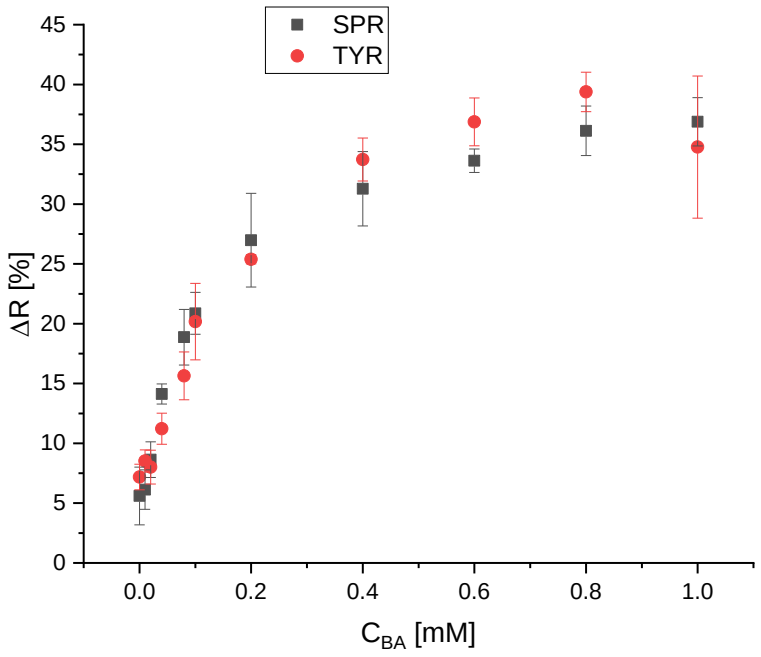

Fig. 8. Calibration plot of the reflectometric response of the dipsticks for spermidine and tyramine (illumination wavelength=635 nm), (n=4).

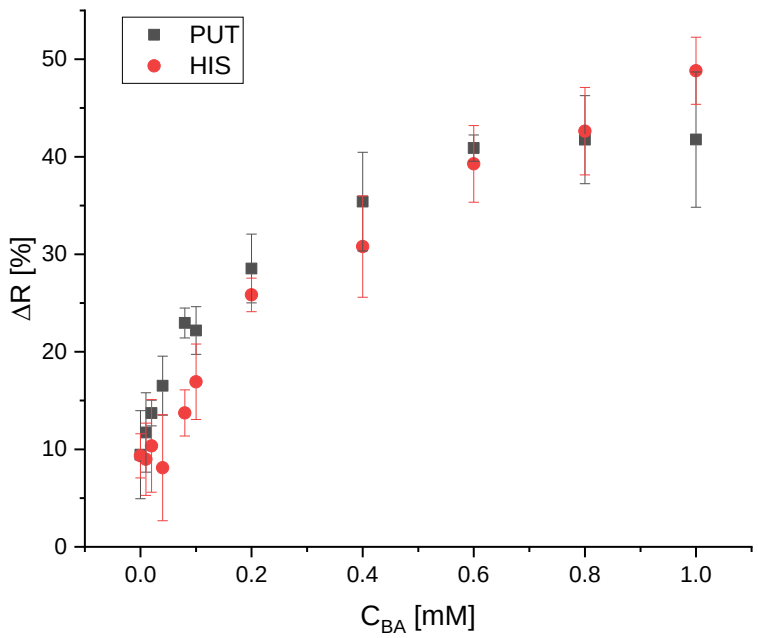

Fig. 9. Calibration plot of the reflectometric response of the dipsticks for putrescine and histamine (illumination wavelength=635 nm), (n =4 (PUT), n=6 (HIS).

Table 1. Dynamic range and LOD derived from the reflectometric response of the dipsticks towards various BAs.

BA	**LOD / mM**	**Dynamic range / mM**
SPR	0.03	0.04-0.60
TYR	0.03	0.08-0.60
PUT	0.08	0.10-0.60
HIS	0.09	0.10-1.0

The concentration range of BAs in foods that might be potentially dangerous for health is between 0.3 and 1.0 mM. The LODs and working ranges of the dipsticks are even sufficient to detect concentrations lower than 0.3 mM (Table 1). This is an advantage because uncritical concentrations of BAs as, e.g., naturally occurring in seafood are accessible. Moreover, one can follow the increase of the concentration of BAs during the ageing of seafood using a suitable dilution (see later section on quantitation of BAs in real samples). This makes the dipsticks ideal tools to control food freshness or spoilage.

4.4.6 Selectivity studies

The selectivity of the S0378 - CA nanofibers was tested with the following substances: dimethylamine (DMA), triethylamine (TEA), human serum albumin (HSA), cysteine (CYS), (figure S8). These particular substances were chosen to test the selectivity of the response of the dipsticks towards secondary amines, tertiary amines, proteins, and thiols. Being nucleophiles, those could interfere in the reaction of S0378 with a BA. We studied the effect of different interferents depending on their concentrations on the reflectance of the dipstick (Fig. 10).

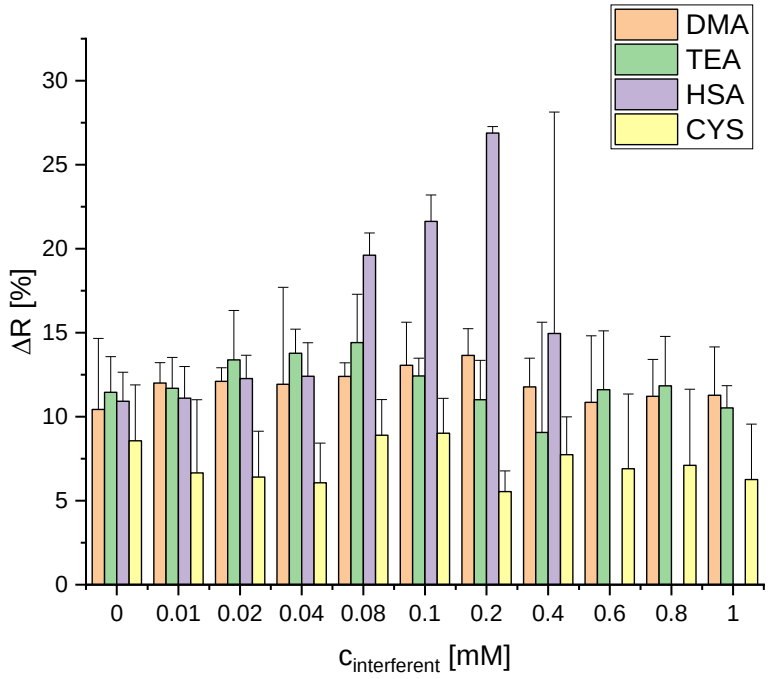

Fig. 10. Selectivity of the dipstick towards DMA, TEA, HSA and CYS (n = 4; illumination wavelength=635 nm)

No significant interference to the reflectance is observed for DMA and TEA. The dye does not react with secondary or tertiary amines but only primary amino groups. This is probably due to their higher steric hindrance and the low accessibility of the carbenium ion located between the four methyl groups at the two indole moieties of S0378. The embedding of the dye inside the fibers of the CA hydrogel should also contribute, here. CYS only slightly decreases the reflectance response of the dipsticks in general but has no concentration dependent effect. Although CYS has a primary amino group this group is still lowly protonated at the pH of the reaction (9.7) because its pK_a is 10.77 [27]. This means that deprotonated (and hence nucleophilic CYS) is present only to a minute degree. CYS therefore mostly exists as zwitter ion in which the amino group is not available to react. Although the thiol group could act as an interfering nucleophile and react with the NIR dye, it obviously is less reactive

under the conditions of the dipstick reaction. HSA shows an interference only at relatively high concentrations (0.04-0.2 mM). This could be expected because it has various primary amino groups that could react with the dye. On the other hand, the CA polymer in the dipsticks particularly hinders the access of larger macromolecules like proteins. Therefore, the reaction of free amino groups of HSA is only possible at relatively high concentrations of the protein. At c_{HSA}>0.2 mM, the fibers are destroyed. The reason for this is still unknown. The interference of proteins, however, is not relevant for the use of the dipsticks in real samples because the common sample pretreatments for determination of BAs which use carrez solutions (this work), methanol [19, 25, 27] or trichloroacetic acid [18] warrant quantitative removal of proteins prior use of the dipstick.

Additionally, the selectivity of the dipsticks towards tyramine in the presence of HSA interferent was tested. HSA (0.04 mM) was added to solutions with increasing concentrations of TYR and ΔR[%] was measured and compared to the ΔR of solutions of TYR of the same concentrations without HSA. The addition of HSA up to 0.04 mM does not affect the calibration plot of tyramine, as shown in fig. 11. Obviously, the reaction rate of S0378 inside the fibers with primary amines is considerably higher than the reaction rate with amines of proteins due to steric hindrance. Hence, the dipsticks react selectively to primary (biogenic) amines as found in food samples, provided that an appropriate sample preparation is done.

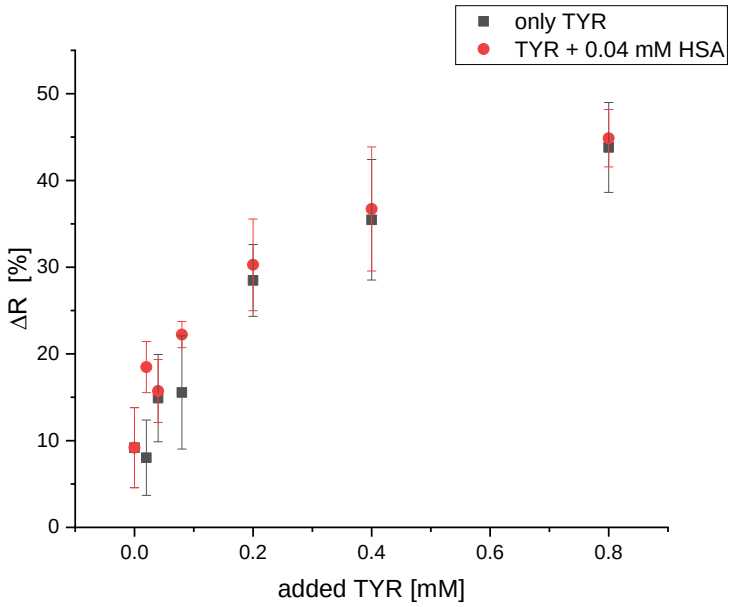

Fig. 11. Effect of HSA interferent (0.04 mM) on the calibration plot of dipsticks with TYR (illumination wavelength=635 nm), (n=4).

4.4.7 Quantitation of BAs in real samples

We finally tested the response of the dipsticks to BAs in shrimp samples over a 6-day storage period at room temperature. The extraction of the shrimp samples follows the AOAC method 35.1.32 [25] and standard additions were done. The methanolic extraction procedure works best in that it is fast, simple, and eliminates the interference of proteins to a major degree. Proteins denature and precipitate in methanol and can be removed with filtration. Carrez solution I (potassium hexaferrocyanide) and Carrez solution II (zinc acetate) were added to the shrimp extract before filtration to completely precipitate the proteins and avoid any interference. We chose histamine as BA as the standard to be added because it is the major BA present in seafood samples. For each ageing day, a suitable dilution factor was used to remain in the dynamic range of the dipsticks for determination of HIS. The ageing of shrimp at room temperature as derived from the standard addition plots are shown in Fig. S9. The R^2 values for all of

the linear fitting plots of the real samples exceed 0.96. These correlation coefficients are good considering that dipsticks are always less reproducible than instrumental detection methods [18, 23].

With respect to the shrimp ageing at room temperature, the increase of the HIS concentrations found can also be translated into a total content of biogenic amines (TAC). The TAC is then expressed in equivalents of histamine (µmol HIS / g sample). Since histamine is the major biogenic amine occurring in seafood, its concentration is representative for the TAC [28]. Furthermore, the mean molar mass of the BAs found in food equals the molar mass of histamine. Histamine concentrations found in shrimp during ageing at room temperature were 7.54 ± 0.96, 12.76 ± 0.77, and 21.73 ± 3.19 µmol/g (n = 4, each) on days 0, 1, and 6, respectively, as shown in table 2. (Fig. 12). These results agree well with ageing profiles of real shrimp samples found in earlier work [29].

Table 2. The determined histamine concentration in shrimp over various days of ageing at room temperature.

635 nm	Dilution factor	Intercept	Slope	TAC [µmol/g]	%uncertainity	R2
day 0	1:10	11.97	79.38	7.54±0.96	12.7	0.969
day 1	1:10	18.21	71.37	12.8±0.77	6.02	0.986
day 6	1:20	12.52	57.61	21.7±3.19	14.7	0.962

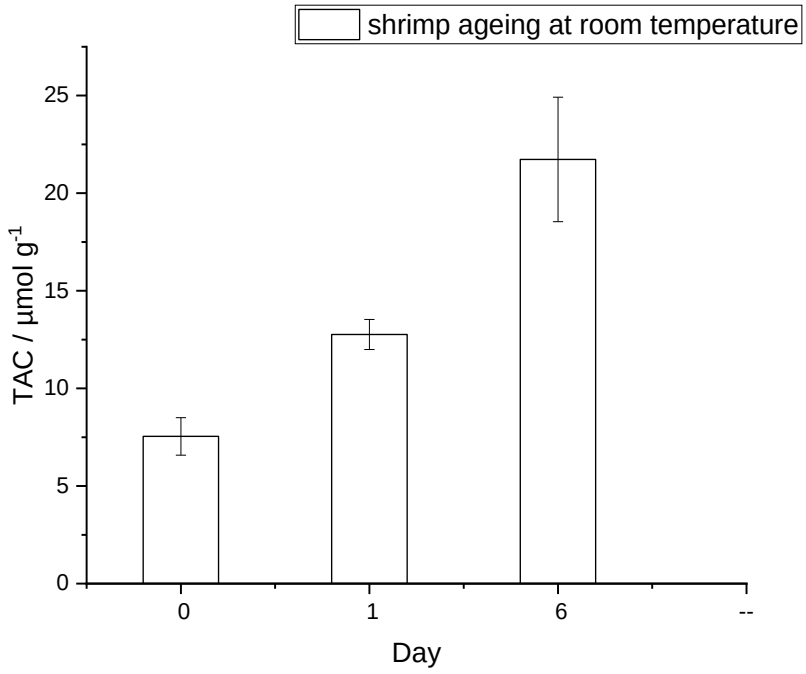

Fig.12. Bar plot of the TAC of shrimp ageing at room temperature over 6 days (illumination wavelength=635 nm), (n=4).

4.5 Conclusion

Chromogenic dipsticks based on electrospun CA nanofiber mats doped with S0378 dye are introduced for reflectometric determination of the content of biogenic amines (BAs) in food samples. S0378 is a chameleon amine-reactive dye which changes its color from green to blue when conjugated to primary amino groups. Hence, the reaction of dipsticks with BAs was monitored via reflectance measurement. The dipsticks can also be used for a yes/no qualitative analysis by the naked eye for determination of potentially dangerous concentrations of biogenic amines. Various biogenic amines such as histamine, tyramine, putrescine and spermidine, respectively, all show an equal reflectance response. The selectivity of the dipsticks towards primary amines over secondary and tertiary amines is very good and only high protein concentrations may interfere. For real samples, this fact is unimportant, since the sample

preparation usually involves steps for protein precipitation. Quantitative analysis of BAs in shrimp samples at room temperature successfully delivered a typical profile of the BA concentration upon ageing of the sample, in agreement with previous studies. Hence, these dipsticks show that electrospun nanofibers are very useful sensor materials for monitoring food freshness using innovative and a simple devices.

4.6 References

1. Oliveira J, Mantoanelli F, Moreira L, Elisabete G, Pereira A (2020) Dansyl Chloride as a Derivatizing Agent for the Analysis of Biogenic Amines by CZE - UV. Chromatographia 83:767–778 . https://doi.org/10.1007/s10337-020-03896-x

2. Chong CY, Bakar FA, Russly AR, Jamilah B, Mahyudin NA (2011) The effects of food processing on biogenic amines formation. Int. Food Res. J. 18:867–876 .

3. Papageorgiou M, Lambropoulou D, Morrison C, Kłodzińska E, Namieśnik J, Płotka-Wasylka J (2018) Literature update of analytical methods for biogenic amines determination in food and beverages. TrAC - Trends Anal Chem 98:128–142 . https://doi.org/10.1016/j.trac.2017.11.001

4. Kettner L, Seitl I, Fischer L (2020) Evaluation of porcine diamine oxidase for the conversion of histamine in food-relevant amounts. J Food Sci 85:843–852 . https://doi.org/10.1111/1750-3841.15069

5. Dong H, Xiao K (2017) Modified QuEChERS combined with ultra high performance liquid chromatography tandem mass spectrometry to determine seven biogenic amines in Chinese traditional condiment soy

sauce. Food Chem 229:502–508 . https://doi.org/10.1016/j.foodchem.2017.02.120

6. Önal A (2007) A review: Current analytical methods for the determination of biogenic amines in foods. Food Chem 103:1475–1486 . https://doi.org/10.1016/j.foodchem.2006.08.028

7. Mohammed GI, Bashammakh AS, Alsibaai AA, Alwael H, El-Shahawi MS (2016) A critical overview on the chemistry, clean-up and recent advances in analysis of biogenic amines in foodstuffs. TrAC - Trends Anal Chem 78:84–94 . https://doi.org/10.1016/j.trac.2016.02.007

8. Erim FB (2013) Recent analytical approaches to the analysis of biogenic amines in food samples. TrAC - Trends Anal Chem 52:239–247 . https://doi.org/10.1016/j.trac.2013.05.018

9. He L, Xu Z, Hirokawa T, Shen L (2017) Simultaneous determination of aliphatic, aromatic and heterocyclic biogenic amines without derivatization by capillary electrophoresis and application in beer analysis. J Chromatogr A 1482:109–114 . https://doi.org/10.1016/j.chroma.2016.12.067

10. Li DW, Liang JJ, Shi RQ, Wang J, Ma YL, Li XT (2019) Occurrence of biogenic amines in sufu obtained from Chinese market. Food Sci Biotechnol 28:319–327 . https://doi.org/10.1007/s10068-018-0500-4

11. Huisman H, Wynveen P, Nichkova M, Kellermann G (2010) Novel ELISAs for screening of the biogenic amines GABA, glycine, β-phenylethylamine, agmatine, and taurine using one derivatization procedure of whole urine samples. Anal Chem 82:6526–6533 . https://doi.org/10.1021/ac100858u

12. Danchuk AI, Komova NS, Mobarez SN, Doronin SY, Burmistrova NA,

Markin A V., Duerkop A (2020) Optical sensors for determination of biogenic amines in food. Anal. Bioanal. Chem. https://doi.org/10.1007/s00216-020-02675-9

13. Xiao-Wei H, Zhi-Hua L, Xiao-Bo Z, Ji-Yong S, Han-Ping M, Jie-Wen Z, Li-Min H, Holmes M (2016) Detection of meat-borne trimethylamine based on nanoporous colorimetric sensor arrays. Food Chem 197:930–936 . https://doi.org/10.1016/j.foodchem.2015.11.041

14. Bueno L, Meloni GN, Reddy SM, Paixão TRLC (2015) Use of plastic-based analytical device, smartphone and chemometric tools to discriminate amines. RSC Adv 5:20148–20154 . https://doi.org/10.1039/c5ra01822f

15. Schaude C, Meindl C, Fröhlich E, Attard J, Mohr GJ (2017) Developing a sensor layer for the optical detection of amines during food spoilage. Talanta 170:481–487 . https://doi.org/10.1016/j.talanta.2017.04.029

16. Roales J, Pedrosa JM, Guillén MG, Lopes-Costa T, Pinto SMA, Calvete MJF, Pereira MM (2015) Optical detection of amine vapors using ZnTriad porphyrin thin films. Sensors Actuators, B Chem 210:28–35 . https://doi.org/10.1016/j.snb.2014.12.080

17. Banimuslem H, Hassan A, Basova T, Esenpinar AA, Tuncel S, Durmuş M, Gürek AG, Ahsen V (2015) Dye-modified carbon nanotubes for the optical detection of amines vapours. Sensors Actuators, B Chem 207:224–234 . https://doi.org/10.1016/j.snb.2014.10.046

18. Steiner MS, Meier RJ, Duerkop A, Wolfbeis OS (2010) Chromogenic sensing of biogenic amines using a chameleon probe and the red-green-blue readout of digital camera images. Anal Chem 82:8402–8405 . https://doi.org/10.1021/ac102029j

19. Khairy GM, Azab HA, El-Korashy SA, Steiner MS, Duerkop A (2016) Validation of a Fluorescence Sensor Microtiterplate for Biogenic Amines in Meat and Cheese. J Fluoresc 26:1905–1916 . https://doi.org/10.1007/s10895-016-1885-1

20. Lee B, Scopelliti R, Severin K (2011) A molecular probe for the optical detection of biogenic amines. Chem Commun 47:9639–9641 . https://doi.org/10.1039/c1cc13604f

21. Mohr GJ (2004) A tricyanovinyl azobenzene dye used for the optical detection of amines via a chemical reaction in polymer layers. Dye Pigment 62:77–81 . https://doi.org/10.1016/j.dyepig.2003.11.011

22. Yu H, Zhuang D, Hu X, Zhang S, He Z, Zeng M, Fang X, Chen J, Chen X (2018) Rapid determination of histamine in fish by thin-layer chromatography-image analysis method using diazotized visualization reagent prepared with: P -nitroaniline. Anal Methods 10:3386–3392 . https://doi.org/10.1039/c8ay00336j

23. Yurova NS, Danchuk A, Mobarez SN, Wongkaew N, Rusanova T, Baeumner AJ, Duerkop A (2018) Functional electrospun nanofibers for multimodal sensitive detection of biogenic amines in food via a simple dipstick assay. Anal Bioanal Chem 410:1111–1121 . https://doi.org/10.1007/s00216-017-0696-9

24. Fazial FF, Tan LL, Zubairi SI (2018) Bienzymatic creatine biosensor based on reflectance measurement for real-time monitoring of fish freshness. Sensors Actuators, B Chem 269:36–45 . https://doi.org/10.1016/j.snb.2018.04.141

25. AOAC (1995) AOAC Official Methods of Analysis, 16th ed., AOAC, Washington. 35.1.32

26. Gorris HH, Saleh SM, Groegel DBM, Ernst S, Reiner K, Mustroph H, Wolfbeis OS (2011) Long-wavelength absorbing and fluorescent chameleon labels for proteins, peptides, and amines. Bioconjug Chem 22:1433–1437 . https://doi.org/10.1021/bc200192k

27. Harris DC (1971) Quantitative Chemical Analysis

28. Hwang DF, Chang SH, Shiau CY, Cheng C. (1996) Biogenic amines in the flesh of sailfish (Istiophorus platypterus) responsible for scombroid poisoning. food sci 60:926–928

29. Azab H., El-Korashy SA, Anwar Z., Khairy GM, Steiner MS, Duerkop A (2011) High-throughput sensing microtiter plate for determination of biogenic amines in seafood using fluorescence or eye-vision. R Soc Chem 136:4492–4499 . https://doi.org/10.1039/c1an15049a

4.7 Supporting information

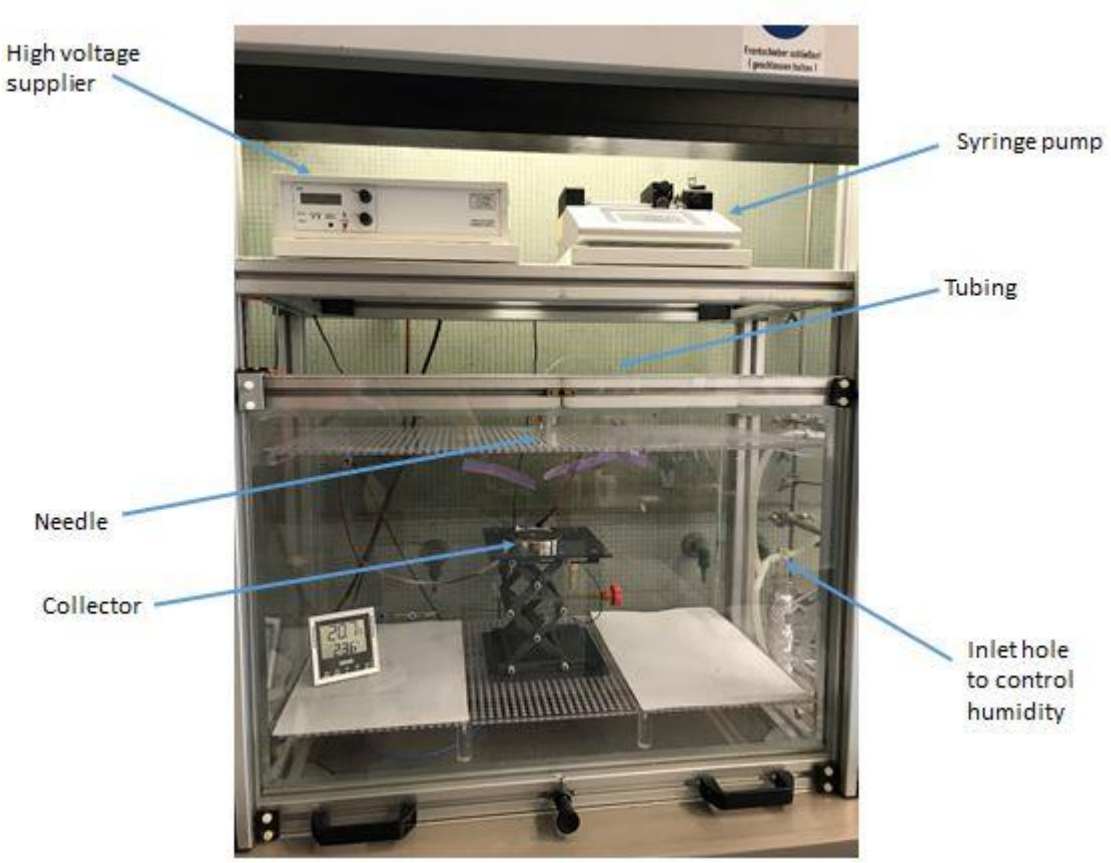

Fig. S1. Image of the electrospinning setup with voltage supply and syringe pump.

The spinning chamber is made of acrylic glass. The voltage (from an iseg T1 CP300p high voltage power supply, www.iseg-hv.com) is applied to the needle and the collector is grounded. The distance between the needle and the collector is adjusted using a height-adjustable platform below the collector. The spinning dope was filled into a plastic syringe. After covering it with Al-foil, it was clamped in a syringe pump (Legato 180 from KD Scientific, www.kdscientific.com) and the flow rate was adjusted. The syringe was connected to the needle with a 75 cm polytetrafluoroethylene (PTFE) tubing

(inner diameter 500 µm). The ITO coated PET sheets were put on the collector and fixed with tape.

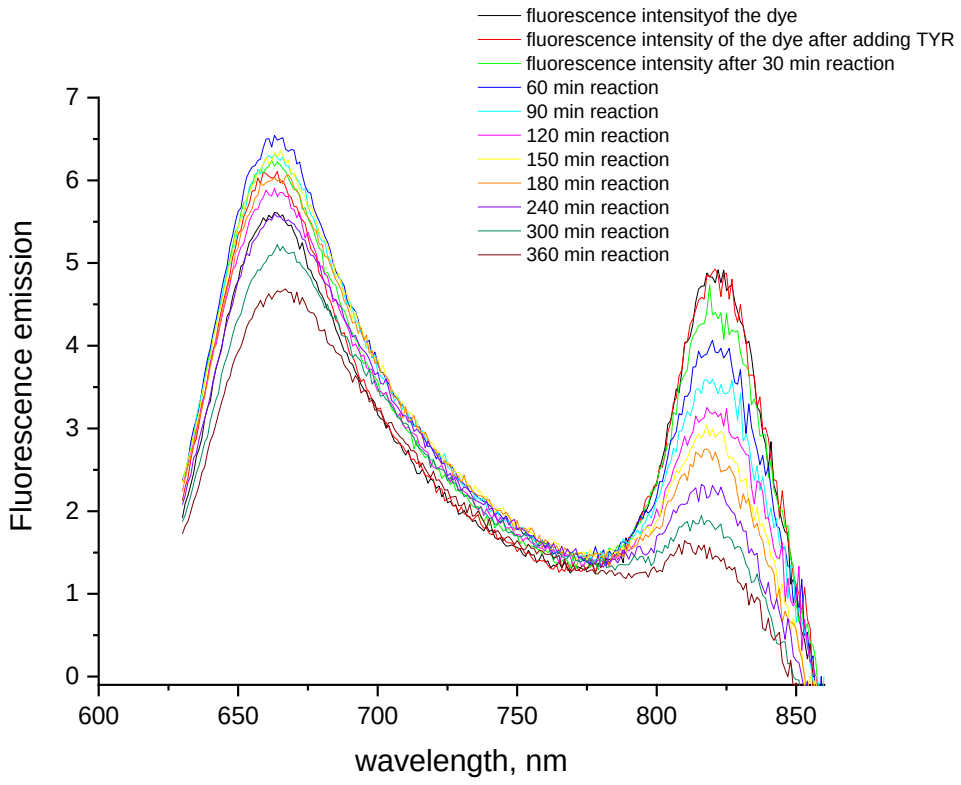

Fig. S2. Change of the fluorescence emission of 5 µM S0378 dye upon binding to 5µM Tyramine at 80 °C over time in CHES buffer (λ_{exc}= 600 nm).

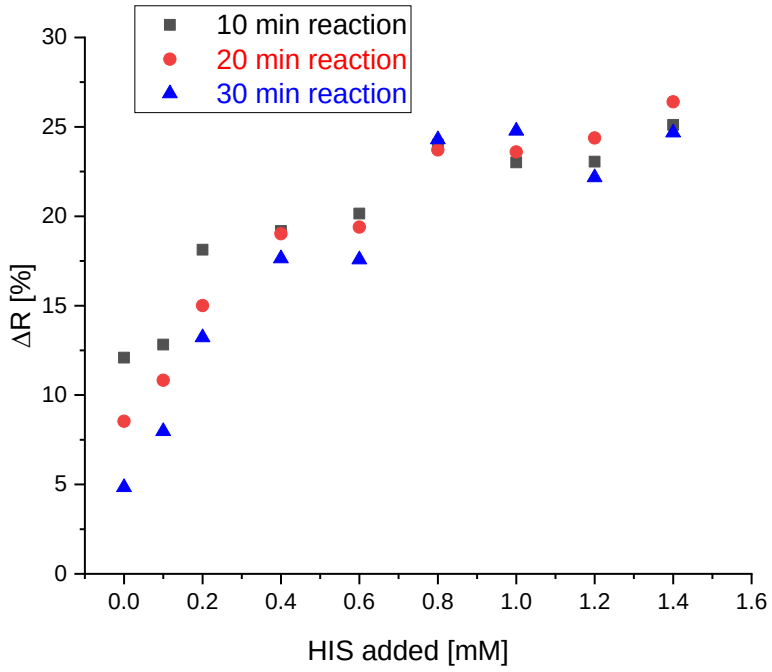

Fig. S3. Effect of reaction time on the reflectance of the dipstick at 650 nm to HIS solutions of 0, 0.02, 0.04, 0.1, 0.2, 0.4, 0.8 mM.

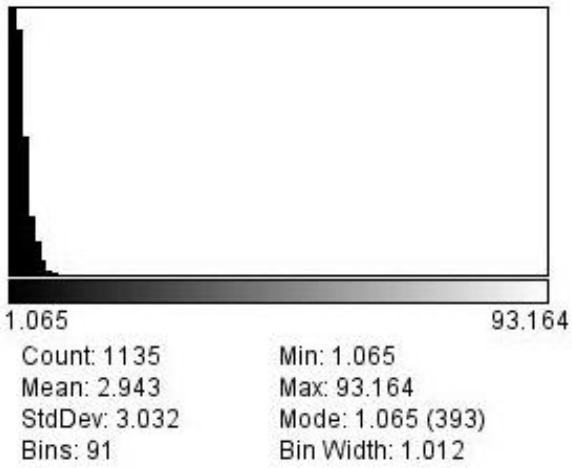

Fig. S4. Representative sample for calculation of the pore size as indicated by the Feret diameter (magnification: 2,500x; determination area: 97.6 µm x 68.21 µm; threshold for ImageJ set at 35%; count = number of pores in total area)

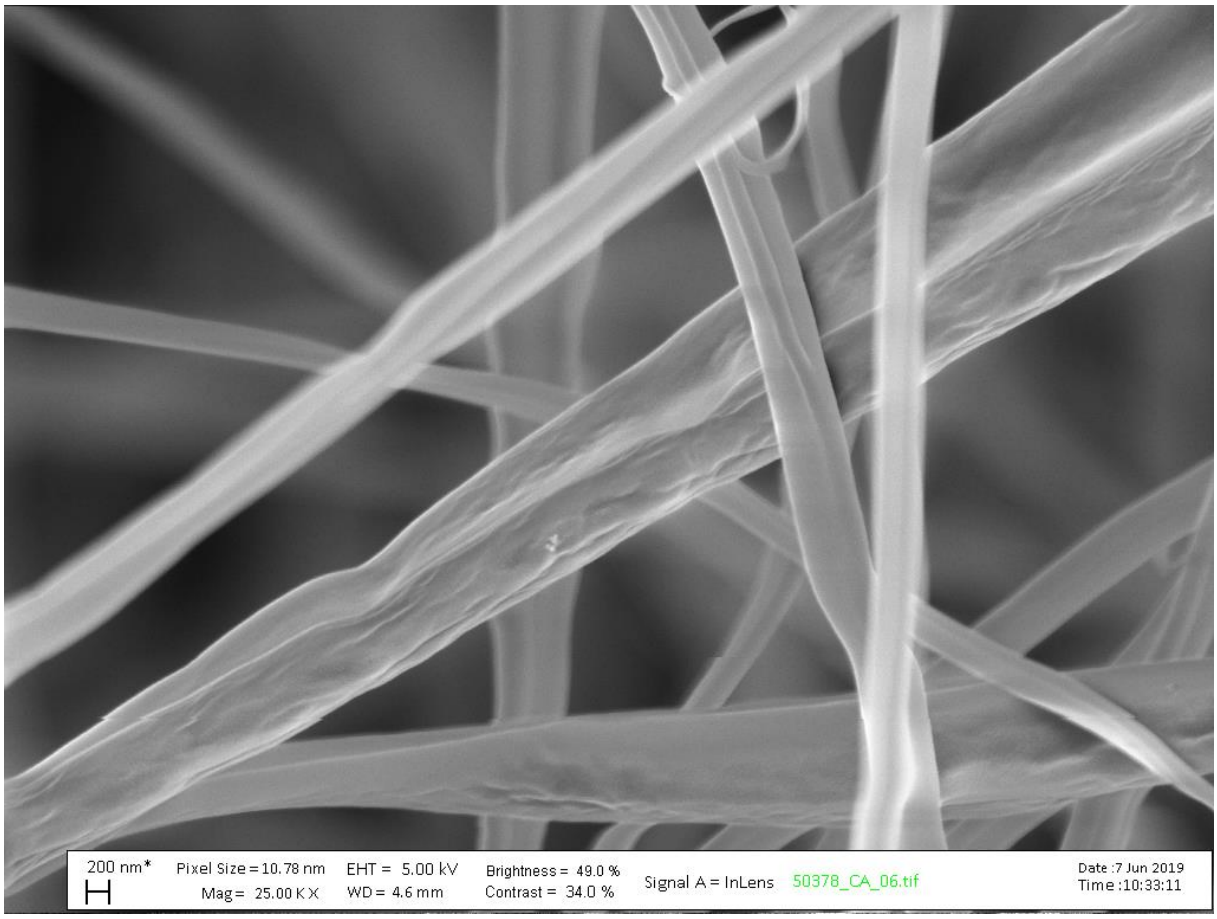

Fig. S5. Morphology of S0378- CA nanofibers electrospun for 15 min as taken by SEM with 2500-fold magnification.

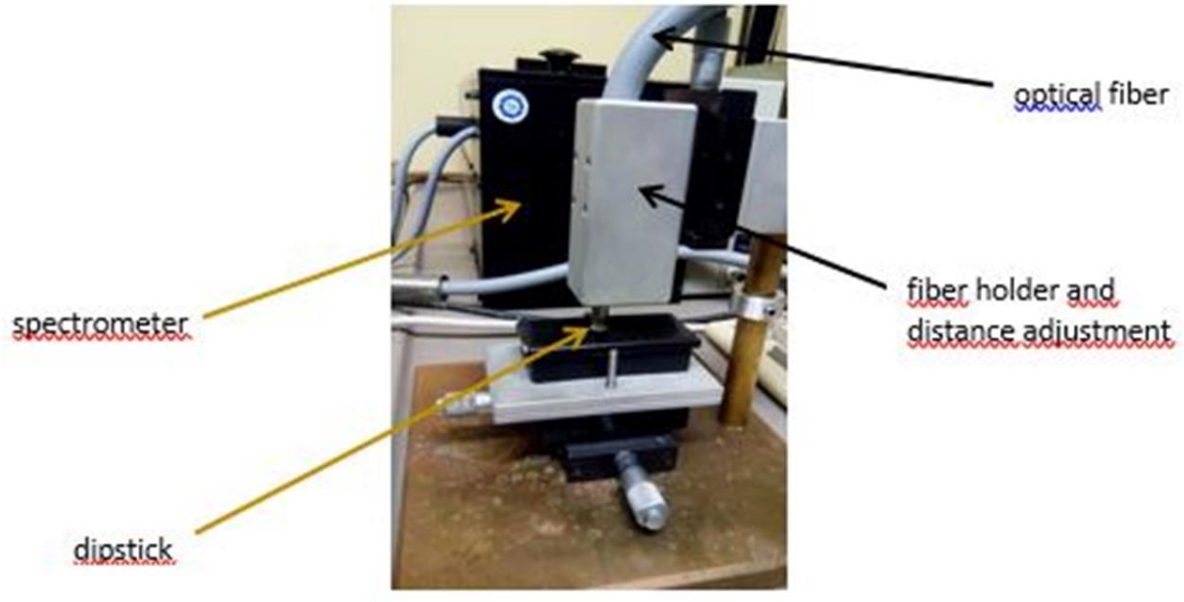

Fig. S6. Instrumental setup used for reflectometric measurements.

Fig. S7. Close-up view on the dipsticks on the sample holder during detection.

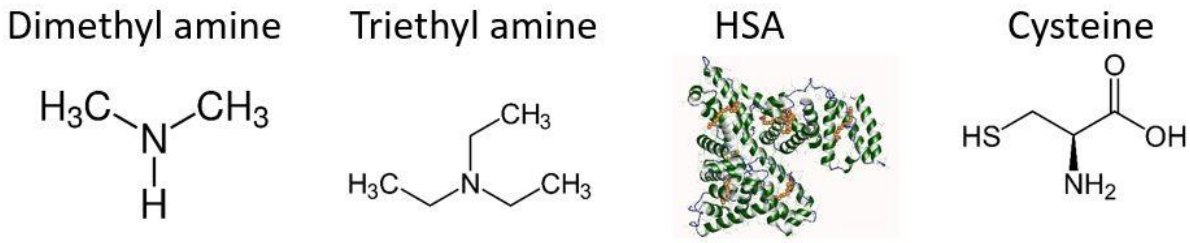

Fig. S8. Structure of the potential interferents tested with the dipsticks.

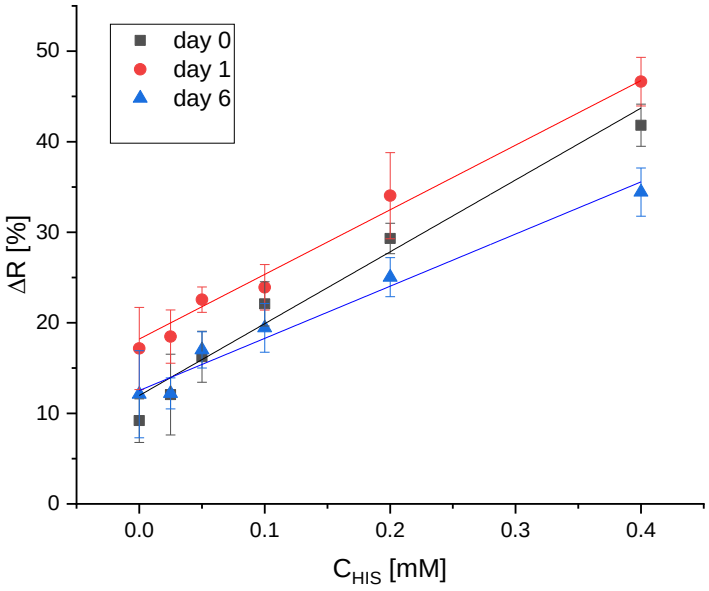

Fig. S9. Calibration plots obtained from the change of the reflectance upon ageing of shrimp at room temperature using standard additions and the dilution factors given in table 2 on days 0,1,6 (illumination wavelength=635 nm), (n=4).

5 Approaching a µ-TAS for the quantitation of Biogenic Amines in Food

5.1 Introduction

5.1.1 µ-TAS as an application of microfluidics and its advantages

One of the most frequent applications of microfluidics are lab-on-a-chip systems. Lab-on-a-chip is a revolutionary tool in chemical and biological analyses because it joins all steps of analysis (sample preparation, isolation, detection) on one platform having very small area. This brings about great advantages with respect to response times and cost of analysis over traditional chemical or biological methods of analysis and makes micro-total analysis systems (µ-TAS) ideal tools for point-of-care systems [1]. The introduction of lab-on-a-chip (LOC) techniques or µ-TAS with the aim of doing familiar laboratory scale techniques for separations and detections on chip is a result of transferring chemical processes onto a chip in the mid-1990s. Generally, the aim is to use miniaturized systems that can manipulate fluids to execute different operations on one platform, hence making this platform a multi-function unit cell [2]. Lab-on-a-chip (LOC) or µ-TAS is where one or more laboratory functions can be done on a single chip of centimeter to millimeter scale. The great advantages of microfluidics is the miniaturization which leads to lower fluid consumption and with it, less use of chemicals, but provides inexpensive mass production of the microfluidic device. Miniaturization can bring molecules closer to one another which results in more effective mixing and faster interactions. The small size of microfluidic channels leads to faster analysis and shorter response time, because of the high surface to volume ratio, shorter diffusion distances and smaller heating capacities [3].

A microfluidic system needs a list of components including reagents, samples, pumps, a channel design, substrate, and devices for mixing [4]. Various materials such as silicon, glass, elastomers, plastics, hydrogels, paper, etc. are being used for fabrication of the microfluidic devices [5]. Thus, depending on the required application, microsystems with different

characteristics of chemical compatibility, surface properties, thermal, and electrical conductivity are manufactured by choosing an appropriate material for their fabrication [6].

5.1.2 Laminates

5.1.2.1 Laminate Fabrication

Laminated microfluidic devices are chips which are fabricated as a pack of independently cut layers. These layers are bonded together to form channels and to establish microfluidic properties. Each layer can be thought of in a two-dimensional flow geometry, which is locked by the layers over and beneath it. The channel height is then determined by the thickness of the material that the layer is made of. The simplest device consists of three layers: an interface layer, a flow layer, and a bottom layer [7]. A three-layered microfluidic device, used for polymerase chain reaction PCR, is shown as an example in Fig. 1.

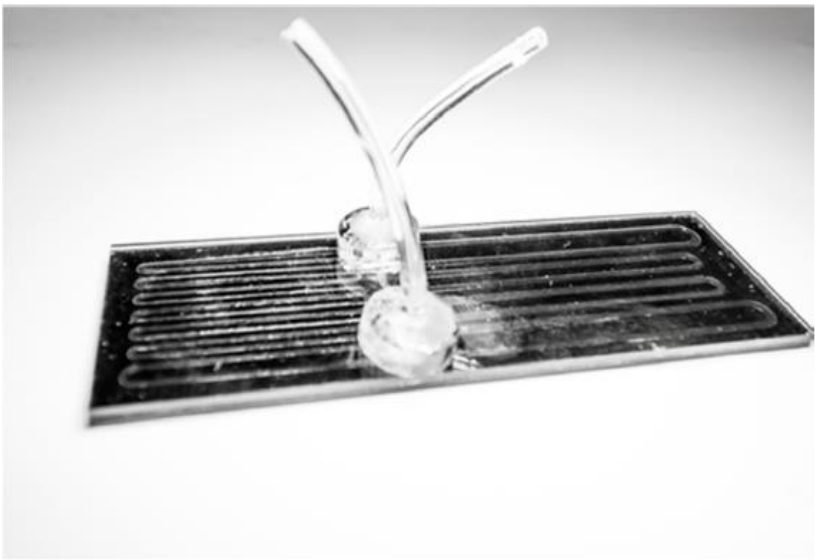

Fig. 1: Device for xPCR fabricated with double-sided adhesive tape sandwiched between two glass slides [8].

The device is constructed by packing a microscope slide, a flow layer cut from double-sided adhesive tape, and a microscope slide with ports cut into it, to set

up a closed channel [8] with acrylic ports glued on as interfaces. The positive properties of layered microfluidic devices are that they are inexpensive, simple, easy to be fabricated, and that the microchannel depth can be controlled by the material thickness. To produce a laminate device the main steps are (1) material selection, (2) cutting the required microfluidic properties into each layer, and (3) bonding the individual layers together [9, 10] . Laminate fabrication is compatible with a wide range of materials such as optically transparent plastics and thermoplastics, in addition to opaque layers, as desired. Adhesive transfer tapes [11], polymer layers (usually polycarbonate, PMMA, and COC) [12], and glass slides are the three materials commonly used in laminate microfluidic devices. Polymers (including acrylic and polycarbonate) and glass layers are commonly used because they are transparent, inexpensive and compatible with many samples. Each layer in the laminate microfluidic devices is cut separately. The way of cutting has a big influence on the functionality and dimensions of the chip. For prototyping and laboratory settings, cutting is usually carried out by a knife plotter (i.e., xurography) or laser since they are simple and fast [13]. Laser cutters provide better resolution and dimensional accuracy down to 25 µm and they are applicable to many substances and thicknesses [10, 14]. Depending on the materials used in the fabrication of the microfluidic devices, the suitable bonding method will be chosen. The mostly used binding methods are adhesives and thermal bonding. An example for the adhesive bonding is the double-sided tape which can be used as the flow layer or an adhesive layer between two different layers. Although adhesive bonding is simple, it has some drawbacks such as that the devices are not stable with high pressures (beyond 5 bar). Moreover, non-uniform bonding and channel heights [15] might occur. In the second type of bonding, the thermal bonding, the temperature of the independent layers is increased to the glass transition temperature of one or both of the materials, with applying force to the layers. When thermal bonding is applied properly the layers will become one solid phase. The negative points of

thermal bonding are being not applicable to all materials, change the properties of some materials upon heating, and creating bubbles between layers which can lead to leaking problems. The bonding method highly affects the stability of the device against pressure and the extent of the air bubbles present between the layers and hence the performance of the device. In the fabrication procedure of the microfluidic device there must be an aligning step or tool for the separated layers to be ready for the bonding process [16].

5.1.2.2 Paper based microfluidic devices

Paper-based assays have been formerly used for different diagnostic tests [17]. Recently, paper as a base for microfluidic devices was introduced by Whitesides and co-workers [18] who point out to the ability to do complex analysis on a paper with getting benefits from the low cost and reducing sample volumes. Paper has been used as analytical platform for a long time starting from litmus paper till the pregnancy test. Over the past few years there is a high interest in using paper for fabricating microfluidic devices. This increasing interest in paper-based microfluidics is because of many advantages. First, paper as a substrate makes a microfluidic device more simple because the need of including pumps in the system is decreasing since paper is a porous medium and able to pump aqueous solutions by capillary action. Second, paper has been applied prior chemical analysis such as for pH detection. Third, paper is of low cost, reproducibly manufactured and comes from renewable resources. Most of these devices were fabricated by patterning hydrophobic barriers in hydrophilic paper via photoresist or wax [18]. Others were formed by cutting paper using a laser [19]. Wax printing is a simple technique used for manufacturing of paper-based microfluidic devices. Physically, wax is hydrophobic, plastic (malleable) at room temperature, insoluble in water and upon melting has a relatively low viscosity. Wax printing is done by patterning hydrophobic wax barriers in hydrophilic paper via a wax- printer and a hot plate. This process includes two

main steps: (i) printing wax patterns on the paper surface and (ii) wax melting in the paper to obtain hydrophobic barriers. Wax printing is fast, of low cost, and useful for mass production of the desired design [11]. This procedure forms hydrophobic barriers in the paper which specify defined hydrophilic channels, solution reservoirs, and reaction chambers [20]. Other technique for creating paper-based microfluidic systems form physical boundaries (instead of hydrophobic boundaries). Yager and coworkers formed channels physically by cutting a nitrocellulose membrane using a CO_2 laser [21]. Others create the physical channels in paper by knife cutters or knife plotters [22]. In these devices, the physical barriers produced by laser or knife cutting prevent the flow of a fluid in a desired direction. Paper-based microfluidics have a common problem which is the relatively low mechanical strength of the paper, especially when it becomes wet. To solve this problem, glass or plastic layers are used underneath the paper and attached to it using double-sided tape [21].

5.1.3 Microfluidic systems including nanofibers

The coupling of nanofibers with microfluidic devices can overcome the disadvantages of the nanofibers including the low throughput and the relatively low mechanical strength [23]. Incorporating the nanofibers in microchips leads to increasing the surface area for immobilization and hence enhancing the sensitivity. For example, microfluidic immunoassays, like ELISA, involve immobilized antigens/antibodies on the transduction substrate. Lately, a electrospun polyether-sulfone nanofibrous membrane was used as the solid substrate for microfluidic immunoassays to increase the efficiency of capturing proteins and therefore, improve the whole diagnostic system [24]. Microfibers and nanofibers can be integrated within a microfluidic chip or incorporated into low refractive index polymers [25]. Then, the microfluidic chip protects the microfibers or nanofibers naturally and significantly decreases the volume of the solutions required in the analysis. Because of the networks of the

microchannel, the microfibers and nanofiber surface can be cleaned after each analysis resulting in a long lifetime of the sensor [26]. Nanofibers incorporated in functional polymers may display a charged surface. These fibers can be embedded into microfluidic channels to obtain great surface area and functional surfaces in a microfluidic device [27].

5.2 Materials and Methods

5.2.1 Materials

S0378 was from FEW Chemicals (www.few.de). The buffer N-cyclohexyl-2-amino ethanesulfonic acid (CHES) was from Roth (www.carlroth.de). Histamine (HIS) was purchased from Sigma-Aldrich (www. sigmaaldrich.com) as hydrochloride salts. Tyramine (TYR), as free base, was from Sigma. Cellulose acetate (CA) (Mw 30,000 Da, 39.8 wt% acetyl content) was obtained from Sigma-Aldrich. All organic solvents, acetic acid, and acetone were obtained from Sigma-Aldrich. Indium tin oxide (ITO) coated on polyethylene terephthalate (PET) with a surface resistivity 60 Ω/sq and 127 µm thickness purchased from Sigma-Aldrich. Stock solutions of BA (10.0 mM) were prepared in CHES buffer (pH 9.7). Standard solutions of the compounds were freshly prepared by diluting stock solutions with CHES buffer. CHES buffer (5.00 mM) was prepared by dissolving of solid CHES (0.1036 g) in 100.0 mL of deionized water. The pH of CHES was adjusted with sodium hydroxide solution (1.00 M, from Merck (www.merckgroup.com)). All chemicals were of analytical grade. Poly ester plastic sheets in A4-size were purchased from Exponent as Laser Films.

5.2.2 Apparatus

The electrospinning was performed using a home-built electrospinning machine with an iseg T1 CP300p high voltage power supply (www.iseg-hv.com) and a Spraybase® syringe pump module PLS000004. Fiber mat thickness, fiber

diameter, and images for pore size determination were obtained by a scanning electron microscopy (Zeiss/LEO 1530, Germany) at 5.0 kV. Therefore, the samples have been cut with a pair of scissors and sputtered with gold for 30 s (≈ 7 nm layer thickness).

Reflectance spectra were acquired with an AB2 luminescence spectrometer with a 150 W xenon light source. The light was guided to the dipstick by a y-shaped bifurcated optical fiber, a fiber holder and the samples were illuminated under an average illumination angle of 33°. The inner central fiber bundle at the tip of the bifurcated optical fiber collects the reflected light from the dipstick and guides it back into the spectrometer. Two wavelengths (650 and 635 nm) were used for illumination and the microfluidic chips were placed in home-made black plastic holders below the tip of the optical fiber to ensure a flat and reproducible positioning of the chips with respect to the incident light beam. The distance between the chips and the tip of the optical fiber is small (3 mm) to increase the signal and improve the sensitivity. The measurements were done in synchronous mode of the spectrometer i.e. the emission was measured at the same wavelength as the excitation. The band passes are 4 nm for both, excitation and emission.

5.2.3 Electrospinning of S0378-CA fibers

The polymer CA (0.720 g) and S0378 (30.00 mg) were dissolved in a mixture of 3.00 mL of acetic acid and of 1.00 mL of acetone. Then, this spinning dope is first sonicated at room temperature for 30 min, then at 40°C for another 30 min and finally stirred for about 1 h until the mixture is completely homogeneous. The spinning dope is protected from light by Al-foil while stirring, storage, and electrospinning. The CA-S0378 electrospun nanofibers were fabricated using the electrospinning machine with the following parameters: Spinning dope in plastic syringe 5 mL (covered with aluminum foil); voltage 17 kV; flow rate 0.002 mL/min; tip-to-collector distance, 11 cm, 15 min spinning time. An ITO

film (size 7 × 5 cm) was used as a supporting material. Electrospun fiber mats on ITO should be stored in desiccators.

5.2.4 Fabrication of the microfluidic chip

The fabrication of the microfluidic chip was carried out in several steps as shown in fig. 2. First, the design of the microfluidic chip was drawn using Microsoft PowerPoint software. Then, the design was printed on a transparent plastic sheet using a wax printer ColorQube 8580 from Xerox as shown in fig. 3. Next, the holes for applying solution onto the chip are punched (2 mm diameter) on the plastic sheet. After that, the plastic sheet layer is put onto the nanofibers deposited on an ITO layer and sandwiched in between two glass slides followed by heating the sandwich in the oven at 175°C for 25 s to allow the wax to melt. Finally, the melted wax will fill the pores between the nanofibers thus creating a hydrophobic barrier. Additionally, this provides a good contact between the two layers.

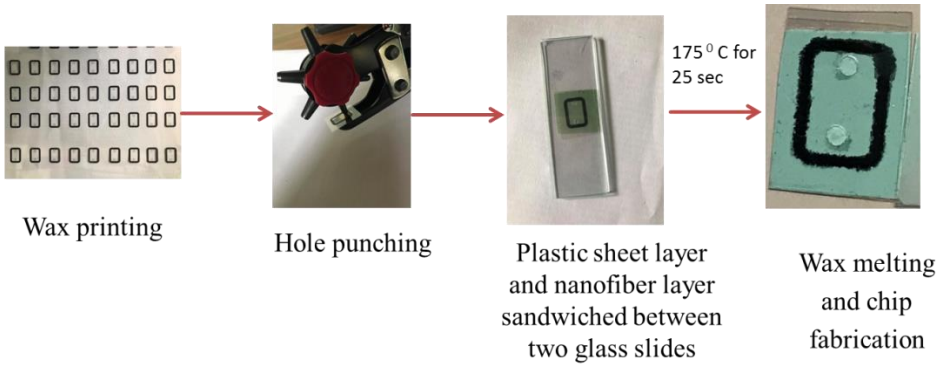

Fig. 2. The steps of microfluidic chip fabrication.

Fig. 3. ColorQube 8580 Xerox printer.

5.3 Results and discussion

5.3.1 Setting up the design of the microfluidic chip

Seven different designs of microfluidic chips as shown in fig. 4 were used for some preliminary experiments to define different sizes and wax barrier widths. The size of the designs vary to find the suitable size with respect to the sensitivity of the reflectance measurement and the nanofiber consumption. The width of the wax barrier was varied to prevent possible leakage of solution and to allow good contact between the two layers, and minimize wax spreading upon wax melting. Designs in each of those two design sets (2, 4, 6, and 7) and (3 and 5) have the same size but a different wax barrier width (either 1.02, 1.53, or 2.04 mm) and hole size (either 2, or 2.5 mm) in the plastic sheet. To find out the most suitable design, 5 µL of 1 mM HIS was added to each chip and allowed to react with the S0378-CA nanofibers at 130 °C for 10 min. Design 1 produces the highest reflectance signal and the best sensitivity, on the other hand, it has a relatively big size. Designs 3 and 5 have the smallest size and therefore a low fiber demand but they show the lowest response. That's why design 7 was chosen as the optimized design since it has medium size and a relatively high and sensitive response. Moreover, it provides a suitable hole size for applying the solution and a wax barrier width that prevents leaking. For design 7, the inner width is 0.78 cm, the inner length is 1.19 cm and the width of the wax barrier is 1.53 mm.

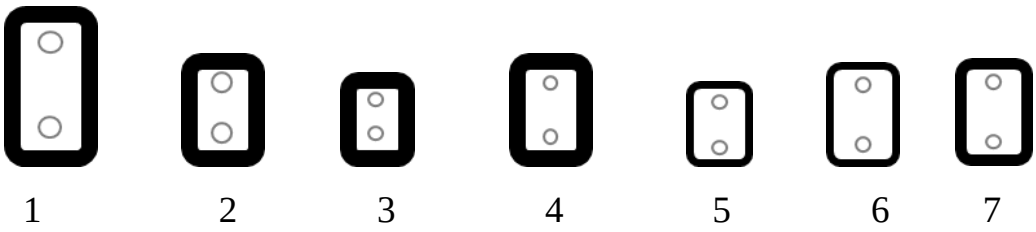

Fig. 4. Scheme of all of the deigns tested for the microfluidic chip.

5.3.2 Optimization of the wax melting conditions, and applied BAs volume

Different wax melting conditions were applied to the microfluidic chip to find out the suitable heating temperature and the time of heating so to provide a strong contact between the two layers. At the same time, the wax spreading has to be minimized to have a good surface area enabling the application and reaction with BAs and detection by the optical fiber via reflectance measurement. Different temperatures ranging from 165-185°C and melting times of 10-30 s were tested. The optimized temperature for wax melting is 175°C and 25 s for the heating period. The volume of BA solution applied to the chip was reduced compared to the dipsticks in chapter 4 to 5 µL. The volume was suitable for covering the whole area surrounded by the wax barrier as shown in fig. 5.

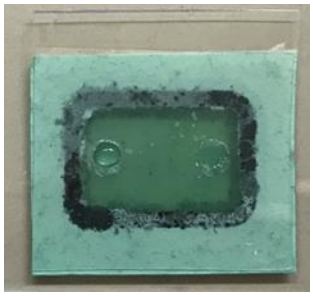

Fig. 5. Applying the BAs solution to the microfluidic chip.

5.3.3 Optimization of reaction temperature and time for TYR calibration

Three reaction temperatures 70, 100, 130°C were tried to find the best one for tyramine calibration on microfluidic chip. Previous optimized reaction conditions of the S0378-CA nanofibers with BAs mentioned in chapter 4 were tried first. The reaction of tyramine in the microfluidic chip at 130°C occurred for only 10 min since the fibers were unstable and decomposed after longer heating times in the microfluidic system. 5 µL of TYR solution of different concentrations were applied to the microfluidic chip of design 6 and allowed to react as shown in fig. 6. The reflectance of the nanofibers before and after the

reaction was measured to calculate ΔR[%]. The results show no response as shown in fig. 7 and therefore, the logical step was to lower down the reaction temperature. Leaking of solution was observed in some chips and that lead to increasing the wax barrier width and to choose design 7 as the final optimized one. The reaction of the chips with S0378-CA nanofiber sensor mats was carried out with TYR at 70 °C for 10, 20, and 30 min. The response was not sensitive, again, as shown in fig. 8.

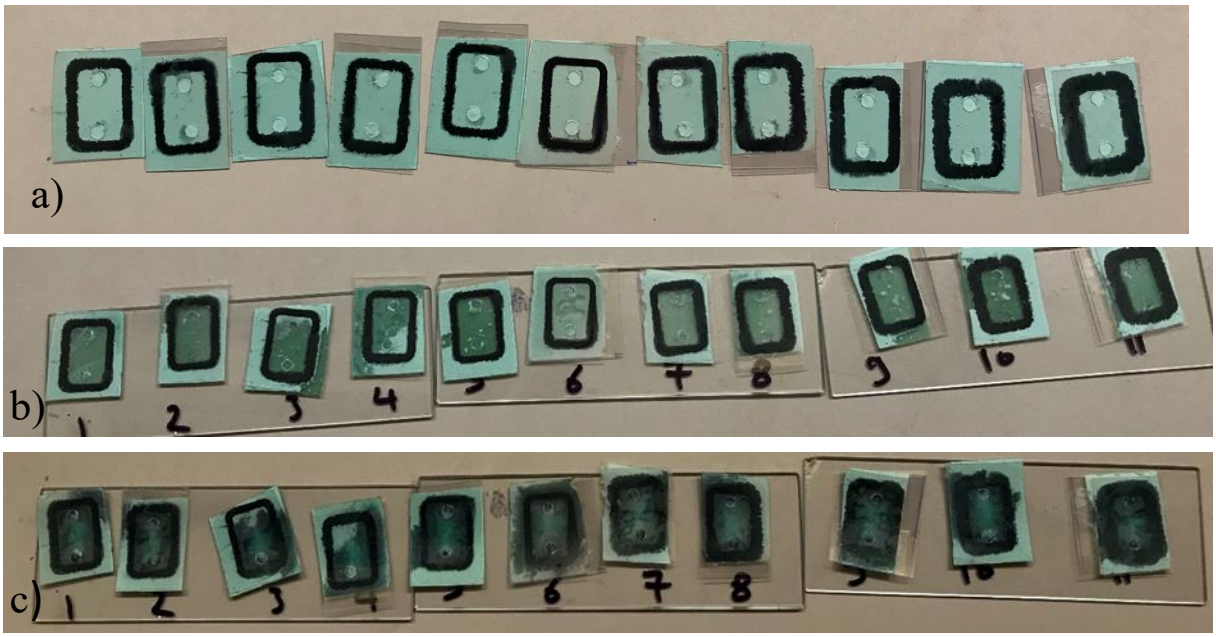

Fig. 6. a) The microfluidic chips before adding the TYR solution, b) after adding TYR solutions of different concentrations 1) blank solution (CHES buffer), 2) 0.02 mM, 3) 0.04 mM, 4) 0.06 mM, 5) 0.08 mM, 6) 0.1 mM, 7) 0.2 mM, 8) 0.4 mM, 9) 0.6 mM, 10) 0.8 mM, 11) 1 mM , c) after reaction at 130° C for 10 min.

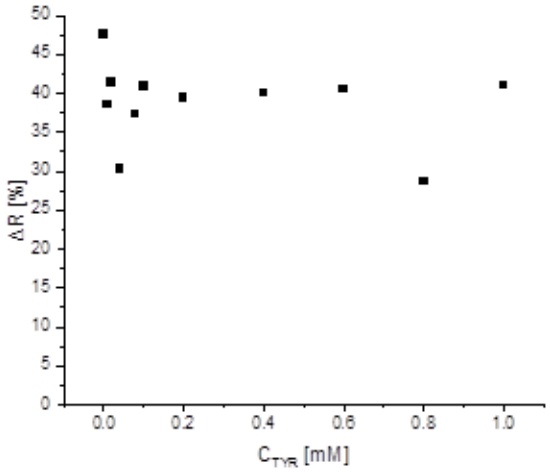

Fig. 7. Calibration plot of reflectance response of microfluidic chips towards TYR developed at 130° C.

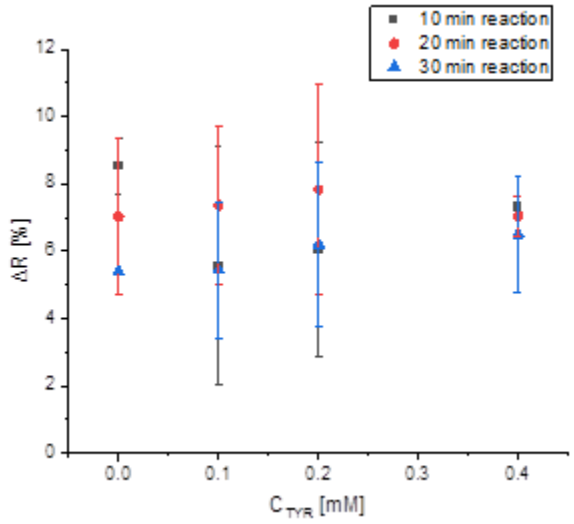

Fig. 8. Calibration plot of reflectance response of microfluidic chips towards TYR developed at 70 ° C for 10, 20, and 30 min (n= 2).

The reaction of the S0378-CA nanofibers was carried out with TYR at 100 °C for 10, 20, and 30 min. The reflectance response is shown in fig. 9. It shows a more concentration-dependent response than at melting temperatures of 70 °C and 130 °C. Regarding the reaction time, there is no big difference between 10, 20, and 30 min but the 10 min reaction has the most sensitive response since the

slope of the fitting graph is the steepest. Hence, the optimized reaction conditions for TYR calibration using S0378-CA nanofibers in microfluidics is 100 °C for reaction temperature and for 10 min for reaction time.

The same conditions were applied for histamine calibration. The reaction was allowed to take place at 100 °C and for 10, 20, and 30 min. The more sensitive response is found for the 30 min reaction time as shown in fig. 10.

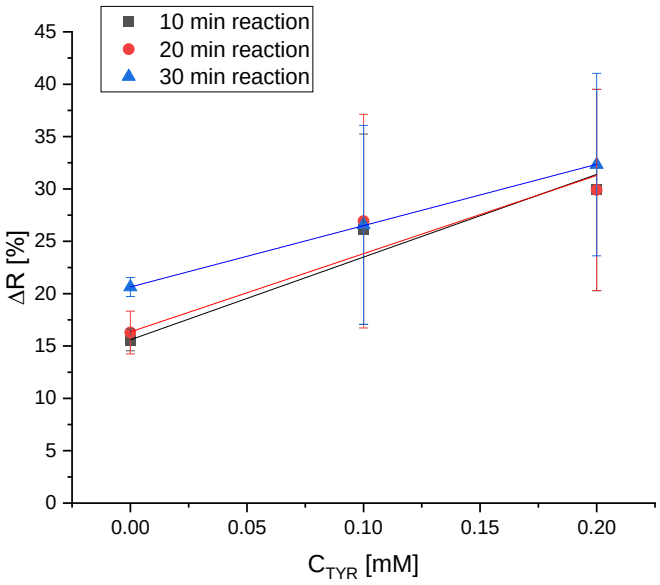

Fig. 9. Calibration plot of reflectance response of microfluidic chips towards TYR developed at 100 ° C for 10, 20, and 30 min, (n=2).

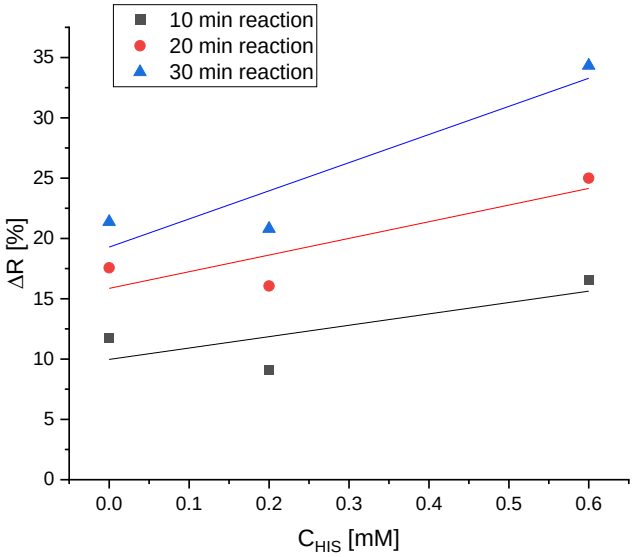

Fig. 10. Calibration of response of microfluidic chips towards HIS at 100 ° C for 10, 20 and 30 min (n=2).

5.4 Conclusion and outlook

S0378–CA nanofibers were incorporated into microfluidic chips, successfully. The design of the chip was optimized based on some preliminary experiments. All of the conditions of related to fabrication of the chip was optimized such as the wax melting temperature (175° C) and the volume of BAs applied to the chip (5µL). Finally the reaction temperature and time with tyramine and histamine were optimized for calibration of BAs. Compared to the dipsticks with fiber mats the sample volume to be applied could be reduced and the response time could be significantly shortened. Here, the inherent advantages of microfluidic µ-TAS become obvious and show the validity of the microfluidic approach. Because of the time constraints, calibration of the chips with all relevant BAs and determination of BAs in real samples with the microfluidic chips containing S0378-CA nanofibers could not be finished. Also a comparison of the sensitivity and LOD of the methods using same fibers (S0378-CA) on dipsticks and in the µ-TAS could not be done any more.

5.5 References

1. Ahn C, Choi J-W (2007) Microfluidics and Their Applications to Lab-on-a-Chip. In: Springer Handbook of Nanotechnology. pp 523–548 .
2. Prakash S, Yeom J (2014) Lab-on-a-Chip and Fluid Manipulation Applications. In: Nanofluidics and Microfluidics. pp 171–239 .
3. Zhang JXJ, Hoshino K (2019) Microfluidics and micro total analytical systems. In: Molecular Sensors and Nanodevices. pp 113–179 .
4. Borbely A, Kreider JF, Bejan A, Cundiff JS, Davis LR (2006) MEMS : introduction and fundamentals
5. Ren K, Chen Y, Wu H (2014) New materials for microfluidics in biology.

Curr Opin Biotechnol 25:78–85 . https://doi.org/10.1016/j.copbio.2013.09.004

6. Pandey CM, Augustine S, Kumar S, Kumar S, Nara S, Srivastava S, Malhotra BD (2018) Microfluidics Based Point-of-Care Diagnostics. Biotechnol J 13:1–11 . https://doi.org/10.1002/biot.201700047

7. Ontiveros F, Mcdowell JR (2016) Ultra-thin Microfluidic Devices Built via Thermal Lamination. Biol Fac Publ 28

8. Jafek AR, Harbertson S, Brady H, Samuel R, Gale BK (2018) Instrumentation for xPCR Incorporating qPCR and HRMA. Anal Chem 90:7190–7196 . https://doi.org/10.1021/acs.analchem.7b05176

9. Narayanaswamy R (1993) Optical Chemical Sensors: Transduction and Signal Processing. Analyst 118: 317-322. https://doi.org/10.1039/AN9931800317

10. Gale BK, Jafek AR, Lambert CJ, Goenner BL, Moghimifam H, Nze UC, Kamarapu SK (2018) A review of current methods in microfluidic device fabrication and future commercialization prospects. Inventions 3: 60 https://doi.org/10.3390/inventions3030060

11. Nath P, Fung D, Kunde YA, Zeytun A, Branch B, Goddard G (2010) Rapid prototyping of robust and versatile microfluidic components using adhesive transfer tapes. Lab Chip 10:2286–2291 . https://doi.org/10.1039/c002457k

12. Kinahan, David J, Julius LAN, Schoen C, Dreo T, Ducréeens J (2018) Automated DNA purification and multiplexed lamp assay preparation on a centrifugal microfluidic “Lab-on-a-Disc” platform. IEEE Micro Electro Mechanical Systems (MEMS), Belfast, pp. 1134-1137, doi: 10.1109/MEMSYS.2018.8346761.

13. Walsh DI, Kong DS, Murthy SK, Carr PA (2017) Enabling Microfluidics: from Clean Rooms to Makerspaces. Trends Biotechnol 35:383–392 . https://doi.org/10.1016/j.tibtech.2017.01.001

14. Mahmud MA, Blondeel EJM, Kaddoura M, MacDonald BD (2018) Features in microfluidic paper-based devices made by laser cutting: How small can they be? Micromachines 9:1–12 . https://doi.org/10.3390/mi9050220

15. Serra M, Pereiro I, Yamada A, Viovy JL, Descroix S, Ferraro D (2017) A simple and low-cost chip bonding solution for high pressure, high temperature and biological applications. Lab Chip 17:629–634 . https://doi.org/10.1039/c6lc01319h

16. Focke M, Kosse D, Müller C, Reinecke H, Zengerle R, Von Stetten F (2010) Lab-on-a-Foil: Microfluidics on thin and flexible films. Lab Chip 10:1365–1386 . https://doi.org/10.1039/c001195a

17. FREE H, COLLINS G, FREE A (1960) Triple-test strip for urinary glucose, protein, and pH. Clin Chem 6:352–361 .

18. Martinez AW, Phillips ST, Butte MJ, Whitesides GM (2007) Patterned paper as a platform for inexpensive, low-volume, portable bioassays. Angew Chemie - Int Ed 46:1318–1320 . https://doi.org/10.1002/anie.200603817

19. Cassano CL, Fan ZH (2013) Laminated paper-based analytical devices (LPAD): Fabrication, characterization, and assays. Microfluid Nanofluidics 15:173–181 . https://doi.org/10.1007/s10404-013-1140-x

20. Carrilho E, Martinez AW, Whitesides GM (2009) Understanding wax printing: A simple micropatterning process for paper-based microfluidics. Anal Chem 81:7091–7095 . https://doi.org/10.1021/ac901071p

21. Fu E, Lutz B, Kauffman P, Yager P (2010) Controlled reagent transport in disposable 2D paper networks. Lab Chip 10:918–920 . https://doi.org/10.1039/b919614e

22. Fenton EM, Mascarenas MR, López GP, Sibbett SS (2009) Multiplex lateral-flow test strips fabricated by two-dimensional shaping. ACS Appl Mater Interfaces 1:124–129 . https://doi.org/10.1021/am800043z

23. Guarino V, Ambrosio L (2018) Electrofluidodynamic Technologies (EFDTs) for Biomaterials and Medical Devices: Principles and Advances. Woodhead Publishing

24. Mahmoudifard M, Vossoughi M, Soudi S, Soleimani M (2017) Electrospun polyethersolfone nanofibrous membrane as novel platform for protein immobilization in microfluidic systems. Biomed Mater Res, Part B 1–13 . https://doi.org/10.1002/jbm.b.33923

25. Chip M (2015) Ultra-Sensitive Nanofiber Fluorescence Detection in a Microfluidic Chip. 15:4890–4898 . https://doi.org/10.3390/s150304890

26. Zhang L, Tong L (2017) Microfluidic chip based microfiber / nanofiber sensors. In: international Conference on Optical Fiber Sensors. p 1032335

27. Cho D, Matlock-Colangelo L, Xiang C, Asiello PJ, Baeumner AJ, Frey MW (2011) Electrospun nanofibers for microfluidic analytical systems. Polymer (Guildf) 52:3413–3421 . https://doi.org/10.1016/j.polymer.2011.05.026

6 Conclusion and Future Perspectives

Biogenic amines are formed in protein rich foods as a result of the amino-acid decarboxylation. The action of microorganisms in the high protein products helps in the formation of biogenic amines which is an issue in the meat industry [1]. Biogenic amines, e.g. histamine, can cause food intoxication at high concentrations, whereas medium levels may result in food intolerance. In addition to spoiled foodstuffs, especially fermented foods usually have high content of BAs [2]. Food poisoning can be a result of the intake of large amount of biogenic amines, especially of histamine [3]. Therefore there is a high demand for methods for BA determination. Thin-layer chromatography (TLC), gas chromatography (GC), capillary zone electrophoresis (CZE), and particularly high-performance liquid chromatography (HPLC) have been used for the quantitation of amines [4]. High-performance liquid chromatography is the most common chromatographic method used for analysis of biogenic amines in food [5]. Recently separation techniques like GC, HPLC, or capillary electrophoresis are combined with optical, electrochemical, or mass spectrometric detection [6–10]. Finally, ELISAs [11]were proposed for BA quantitative detection in food, as well. These methods are highly sensitive and selective but need time and well trained staff [12]. Nowadays, fast, sensitive and easy to operate analytical devices like dipsticks or μ-TAS are required for food quality control in market [5].

In this thesis, we are focusing on devices like dipsticks or μ-TAS for determination of BAs in food, especially for concentrations that are not detected by the human nose by using different inexpensive optical detection methods such as fluorescence emission and reflectance measurements. New dipsticks using Py-1-CA electrospun nanofibers for the detection of BAs and semi-quantitative analysis just by the naked eye were introduced. The fibers are made of cellulose acetate polymer doped with the chameleon dye Py-1. This dye is

reactive to primary amines and upon the reaction its color changes from blue to red with the enhancement of fluorescence emission. Thus, the detection of BAs can be carried out successfully based on either colorimetric, reflectance, or fluorescence detection. For further studies, we concentrated on the fluorescence detection since it is more sensitive and allows to go lower with the LOD. Fluorescence detection is generally more selective and sensitive since the measurements are made against black background. After carrying out the reaction between the dipsticks and BAs, the dipsticks were excited using an UV lamp and the readout was done using a digital camera via the intensity ratio of the red versus the blue channel. The R/B intensity ratio was proportional to the biogenic amine concentration. The Py-1-CA dipsticks were found to be selective to primary amines when tested towards tyramine, histamine, cadaverine, spermidine, putrescine, 2-aminoethylmethacrylate, dimethylamine and triethylamine. The sensitivity of the analysis was enhanced when nanofibers were involved because of their loading efficiency. The sensitivity of the dipsticks towards tyramine was higher by one order of magnitude compared to a sensor made of a polymer film. These dipsticks can give yes/no answers to indicate the presence of BAs and can also be used for semi-quantitative analysis by the naked eye using a calibration color scale. S0378-CA nanofibers were prepared by electrospinning. Upon the reaction with BAs the S0378-CA dipsticks change their color from green to blue. The detection of BAs was carried out by reflectometry since it is a simple instrumental readout (in principle: LED, sample, filter, photodiode). BAs such as spermidine, histamine, tyramine, and putrescine were calibrated. S0378-CA nanofibers were found to be selective to primary amines and not to secondary or tertiary amines or thiols. Proteins can cause an interference if present in relatively high concentrations. If both proteins and BAs exist in the reaction medium the reaction with BAs will be favorable because the CA polymer hinders the reaction with proteins due to the steric effect. The method was successfully applied to study the ageing of

shrimp samples at room temperature. Reflectometry was more sensitive than fluorescence which is obvious from the slope of the calibration plots of TYR in both cases. The LOD for tyramine detection was 10 times lower for fluorescence than for reflectometry. Py-1 reacts faster to BAs at room temperature whereas for S0378 heating is required. Determined concentrations of BAs in shrimp samples upon ageing obtained by both methods reflectometry and fluorescence were comparable. As could be expected, the ageing, and with it, the formation of BAs clearly proceeded much faster upon ageing at room temperature. S0378-CA nanofibers were successfully incorporated into microfluidic chips using a plastic sheet as a base and the wax melting technique for bonding the layers. The design of the microfluidic chip was optimized to give the best reflectance response at a small chip size. Conditions for bonding the layers together and reaction conditions with BAs were optimized for calibration of BAs. For the future work, calibration of BAs and determination of BAs in real food samples using the S0378-CA nanofibers-based microfluidic chips should be carried out to compare the results of these chips with the S0378-CA dipsticks results. Other amine-reactive dyes could be tested and incorporated in a suitable polymer matrix that will be spun to form chromogenic and fluorogenic nanofiber mats that can be used in chips for food quality control. Those could be the basis for portable μ-TAS that could be used by untrained users and are safe to be used in food packaging.

6.1 References

1. Lewis J, Zaukuu Z, Bazar G, Gillay Z, Kovacs Z (2019) Emerging trends of advanced sensor based instruments for meat , poultry and fish quality – a review. Crit Rev Food Sci Nutr . https://doi.org/10.1080/10408398.2019.1691972

2. Bodmer S, Imark C, Kneubühl M (1999) Biogenic amines in foods : Histamine and food processing. 48:296–300

3. Visciano P, Schirone M, Tofalo R, Suzzi G (2012) Biogenic amines in raw and processed seafood. Front Microbiol 3:1–10 . https://doi.org/10.3389/fmicb.2012.00188

4. Smělá D, Pechová P, Komprda T, Klejdus B, Kubáň V (2018) Liquid chromatographic determination of biogenic amines in a meat product during fermentation and long-term storage. Czech J Food Sci 21:167–175 . https://doi.org/10.17221/3495-cjfs

5. Lázaro de la Torre CA, Conte-Júnior CA (2014) Chromatographic methods for biogenic amines determination in foods of animal origin. Brazilian J Vet Res Anim Sci 50:430–446 . https://doi.org/10.11606/issn.1678-4456.v50i6p430-446

6. Mohammed GI, Bashammakh AS, Alsibaai AA, Alwael H, El-Shahawi MS (2016) A critical overview on the chemistry, clean-up and recent advances in analysis of biogenic amines in foodstuffs. TrAC - Trends Anal Chem 78:84–94 . https://doi.org/10.1016/j.trac.2016.02.007

7. Önal A (2007) A review: Current analytical methods for the determination of biogenic amines in foods. Food Chem 103:1475–1486 . https://doi.org/10.1016/j.foodchem.2006.08.028

8. Erim FB (2013) Recent analytical approaches to the analysis of biogenic amines in food samples. TrAC - Trends Anal Chem 52:239–247 . https://doi.org/10.1016/j.trac.2013.05.018

9. He L, Xu Z, Hirokawa T, Shen L (2017) Simultaneous determination of aliphatic, aromatic and heterocyclic biogenic amines without derivatization by capillary electrophoresis and application in beer analysis. J Chromatogr A 1482:109–114 . https://doi.org/10.1016/j.chroma.2016.12.067

10. Li DW, Liang JJ, Shi RQ, Wang J, Ma YL, Li XT (2019) Occurrence of biogenic amines in sufu obtained from Chinese market. Food Sci Biotechnol 28:319–327 . https://doi.org/10.1007/s10068-018-0500-4

11. Huisman H, Wynveen P, Nichkova M, Kellermann G (2010) Novel ELISAs for screening of the biogenic amines GABA, glycine, β-phenylethylamine, agmatine, and taurine using one derivatization procedure of whole urine samples. Anal Chem 82:6526–6533 . https://doi.org/10.1021/ac100858u

12. Danchuk AI, Komova NS, Mobarez SN, Doronin SY, Burmistrova NA, Markin A V., Duerkop A (2020) Optical sensors for determination of biogenic amines in food. Anal. Bioanal. Chem. https://doi.org/10.1007/s00216-020-02675-9

7 Summary

Food quality and safety is a topic of great importance. Daily, there are cases of food poisoning. Consumption of adulterated food or food that was stored not properly can cause severe health problems. Controlling the food quality, also over the storage in supermarkets is therefore necessary. This can be done via determination of BAs in foods as those are indictors for food freshness. BAs are primary amines formed by the enzymatic or bacterial decarboxylation of the respective amino acids during the storage of protein rich products and fermented products. BAs within a concentration range of 0.3 - 1 mM in food cannot be recognized by the human nose but represent a health risk, which is why continuous and simple monitoring of BAs in food is very advantageous. Traditional instrumental methods for analysis of BAs are demanding and time consuming, hence nowadays there is a high interest in simple chemosensors for analyses on-site. Therefore, the development of nanofiber-based dipsticks for the detection of BAs in seafood samples was performed in this thesis. Those nanofibers contain an amine-reactive dye which changes its optical properties upon conjugation with primary amines. Two types of cellulose acetate-based chromogenic and fluorogenic nanofibers (Py-1-CA and S0378-CA) were prepared by electrospinning. One contains the pyrilium dye Py-1 and the other the cyanine dye S0378. The electrospinning conditions were optimized for both types of nanofibers. The nanofiber morphology revealed mat thicknesses of 6.9 ± 1.6 µm and 50.7 ± 8.4 µm and pore sizes were 2.8 ± 0.15 µm and 2.6 ± 1.3 µm for Py-1-CA and S0378-CA nanofibers, respectively. The detection of BAs via Py-1-CA dipsticks relies on on the enhancement of the fluorescence emission which can be measured using a digital camera and is evaluated by a photoshop software due to the color change of the fibers from blue to red upon the reaction. The detection of BAs via S0378-CA dipsticks was based on reflectometry making use of the color change of the fibers from green to blue

upon the reaction. Conditions for the reaction between the dipsticks and BAs and optical detection conditions were optimized. Various biogenic amines were successfully calibrated using both detection methods. Both types of dipsticks were selective to primary amines, but not to secondary or tertiary amines since both dyes do not react at all or very slowly with secondary or tertiary amines. The dipsticks have a very similar response towards monoamines and diamines, respectively, which predestines them for determination of total BA contents in foods. The sensitivity of the reflectometric measurements using S0378-CA dipsticks towards tyramine was much higher than for the fluorescence measurements using Py-1-CA dipsticks. The LOD for tyramine determination, however, was 10 times lower for the fluorescent Py-1-CA dipsticks. When comparing the sensitivity and LOD of both detection methods, one has to keep in mind that the dye concentration of S0378 was 3.5-fold higher than that of Py-1 in the spinning dope. Finally, we intended to set up a µ-TAS based on S0378-CA nanofibers by incorporating them into a microfluidic chip. The BA detection should also be performed by reflectometry. The conditions related to the fabrication of the microfluidic chip and the reaction conditions in this new system were optimized since the reaction conditions for S0378-CA dipsticks could not be used any more. The chips showed a nice response to BAs, however their development could not be finished any more due to time constraints. Hence, a considerable progress in providing miniaturized devices for quantitation of BAs could be made by the development of two different types of dipsticks using two different chromogenic dyes in electrospun nanofibers as sensor material and using two different detection methods amenable for miniaturization. The nanofibers using the NIR dye pave the way to the first miniaturized microfluidic setups. This shows that food analysis is a prospective field for introducing innovative optical sensors employing progressive materials to secure consumer health.

8 Zusammenfassung

Lebensmittelqualität und -sicherheit sind ein Thema von großer Bedeutung, weil es täglich Fälle von Lebensmittelvergiftungen gibt. Der Verzehr von verdorbenen oder nicht ordnungsgemäß gelagerten Lebensmitteln kann schwerwiegende gesundheitliche Probleme verursachen. Daher ist eine Kontrolle der Lebensmittelqualität, auch während der Lagerung in Supermärkten erforderlich. Dies kann durch die Bestimmung des Gehalts von biogenen Aminen (BA) in Lebensmitteln erreicht werden. BA sind primäre Amine, die durch die enzymatische oder bakterielle Decarboxylierung bestimmter Aminosäuren während der Lagerung von proteinreichen und fermentierten Produkten gebildet werden. BAs im Konzentrationsbereich von 0,3 - 1 mM in Lebensmitteln können von der menschlichen Nase nicht erfasst werden, stellen aber dennoch ein Gesundheitsrisiko dar. Daher sind neue Geräte zur kontinuierlichen und einfachen Überwachung von BAs in Lebensmitteln sehr wünschenswert. Traditionelle, instrumentelle Analysemethoden sind teuer und zeitaufwändig, weshalb heutzutage ein großes Interesse an einfachen Chemosensoren für die Analytik vor Ort besteht. Deshalb wurden dieser Arbeit Teststreifen mit Nanofaserlagen zum Nachweis von BA in Meeresfrüchten entwickelt. Diese Nanofasern enthalten einen aminreaktiven Farbstoff, der seine optischen Eigenschaften bei Konjugation mit primären Aminen ändert. Es wurden zwei Arten von chromogenen und fluorogenen Nanofasern auf Basis von Celluloseacetat (Py-1-CA und S0378-CA) durch Elektrospinnen hergestellt. Eine Faserart enthält den Pyriliumfarbstoff Py-1 und die andere den Cyaninfarbstoff S0378. Die Bedingungen für das Elektrospinnen wurden für beide Arten von Nanofasern optimiert. Die Untersuchung der Morphologie der Nanofasernetze ergab Dicken von 6,9 ± 1,6 µm und 50,7 ± 8,4 µm und Porengrößen von 2,8 ± 0,15 µm und 2,6 ± 1,3 µm, jeweils für Py-1-CA- bzw. S0378-CA-Nanofasern. Der Nachweis von BAs mit Py-1-CA-Teststreifen nützt

die Verstärkung der Fluoreszenzemission, die während der Farbänderung der Fasern von blau nach rot bei der Reaktion mit BA auftritt. Diese Emission wurde mit einer Digitalkamera erfasst und mit einer Photoshop-Software ausgewertet. Der Nachweis von BA mittels Teststreifen, die S0378-CA enthielten, basierte auf Reflektometrie, wobei die Farbänderung der Fasern von grün nach blau bei der Reaktion genutzt wurde. Die Bedingungen für die Reaktion der Fasern auf den Teststreifen mit den BA und die Detektionsbedingungen wurden optimiert. Kalibrationskurven für verschiedenste biogene Amine wurden mit beiden Teststreifen erfolgreich erstellt. Beide Teststreifen waren selektiv für primäre Amine und sprachen nicht auf sekundäre oder tertiäre Amine an, da beide Farbstoffe überhaupt nicht oder nur sehr langsam mit sekundären oder tertiären Aminen reagieren. Auch sprechen die Teststreifen sehr ähnlich auf Mono- und Diamine an, was die Bestimmung einer Gesamtkonzentration an BA in Lebensmittelproben ermöglicht. Die Empfindlichkeit der reflektometrischen Messungen gegenüber Tyramin war bei Verwendung von S0378-CA-Teststreifen viel höher als die der Fluoreszenzmessungen bei Verwendung von Py-1-CA-Teststreifen. Die Nachweisgrenze für Tyramin war jedoch bei den fluoreszierenden Py-1-CA-Teststreifen zehnmal niedriger. Die unterschiedlichen Empfindlichkeiten und Nachweisgrenzen der beiden Detektionsmethoden sind vor allem darauf zurückzuführen, dass die Farbstoffkonzentration von S0378 in der Spinnlösung 3,5-fach höher war als die von Py-1. Schlussendlich sollte ein mikrofluidisches Totalanalysensystem für BA mit S0378-CA-Nanofasern und reflektometrischem Nachweis entwickelt werden. Die Bedingungen für die Herstellung des mikrofluidischen Chips und die Reaktionsbedingungen in diesem System wurden optimiert, da sich die Reaktionsbedingungen gegenüber denen der S0378-CA-Teststreifen änderten. Auch diese Chips sprachen auf BA an, aber ihre Entwicklung konnte aus Zeitmangel nicht mehr zu Ende geführt werden. Somit wurde dadurch ein beträchtlicher Fortschritt bei der Entwicklung

miniaturisierter Analysensysteme zur Quantifizierung von BA erzielt, dass zwei verschiedene Arten von Teststreifen mit elektrogesponnenen Nanofasern als Sensormaterial hergestellt wurden. Diese nutzen unterschiedliche chromogene Farbstoffe und zwei verschiedene Detektionsmethoden und sind für die Miniaturisierung geeignet. Auch der Weg zu einem mikrofluidischen Totalanalysensystem unter Verwendung der Nanofasern, die den NIR-Farbstoff enthalten, scheint machbar. Dies zeigt, dass innovative optischer Sensoren aus neuen Materialien gewinnbringend in der Lebensmittelanalytik eingesetzt werden können, um die Gesundheit der Verbraucher zu schützen.

Curriculum Vitae

Personal information

Name	Sarah Nagy Ali Mobarez
Adress	15 Khalf el Obor nearby the Infantry house Apt#131, Misr el gededa, 11811 Cairo (Egypt)
E-mail	sarah_nagy_ali@sci.asu.edu.eg
Birth	Cairo, 11/12/1988
Nationality	Egyptian

Work experience

28/03/2010-09/04/2016	Teaching assistant Analytical and Inorganic Chemistry Department, Faculty of Science, Ain Shams University, Cairo (Egypt)
10/04/2016–Present	Assistant Lecturer Faculty of Science, Ain Shams University, Chemistry Department

Education

09/2005–06/2009	Bachelor of Science in Applied Chemistry Excellent degree with honours Faculty of Science, Ain Shams University, Cairo (Egypt)
11/2010–09/2011	Pre-master courses of Analytical and Inorganic Chemistry Excellent degree Faculty of Science, Ain Shams University, Cairo (Egypt)
03/2012– 14/02/2016	Master's Degree of Science in Inorganic and Analytical Chemistry “Photochromism and Spectroscopic studies of some Spiropyran Complexes of some Transition Metal ions Faculty of Science ,Ain Shams University, Cairo (Egypt)
01/04/2017- 09/2020	PhD in Analytical Chemistry “Development of a Micro-total Analysis System for the detection of Biogenic Amines” Institute of Analytical Chemistry, Chemo- and biosensors. Faculty of Chemistry and Pharmacy, Regensburg University, Regensburg (Germany)

Publications

Yurova NS, Danchuk A, Mobarez SN, Wongkaew N, Rusanova T, Baeumner AJ, Duerkop A (2018) Functional electrospun nanofibers for multimodal sensitive detection of biogenic amines in food via a simple dipstick assay. Anal Bioanal Chem 410:1111–1121 . https://doi.org/10.1007/s00216-017-0696-9

Danchuk AI, Komova NS, Mobarez SN, Doronin SY, Burmistrova NA, Markin A V., Duerkop A (2020) Optical sensors for determination of biogenic amines in food. Anal. Bioanal. Chem. https://doi.org/10.1007/s00216-020-02675-9

EIDESSTATTLICHE ERKLÄRUNG

Ich erkläre hiermit an Eides statt, dass ich die vorliegende Arbeit ohne unzulässige Hilfe Dritter und ohne Benutzung anderer als der angegebenen Hilfsmittel angefertigt habe; die aus anderen Quellen direkt oder indirekt übernommenen Daten und Konzepte sind unter Angabe des Literaturzitats gekennzeichnet.

Weitere Personen waren an der inhaltlich-materiellen Herstellung der vorliegenden Arbeit nicht beteiligt. Insbesondere habe ich hierfür nicht die entgeltliche Hilfe eines Promotionsberaters oder anderer Personen in Anspruch genommen. Niemand hat von mir weder unmittelbar noch mittelbar geldwerte Leistungen für Arbeiten erhalten, die im Zusammenhang mit dem Inhalt der vorgelegten Dissertation stehen.

Die Arbeit wurde bisher weder im In- noch im Ausland in gleicher oder ähnlicher Form einer anderen Prüfungsbehörde vorgelegt.

_____

Ort, Datum Unterschrift